Infrared studies of species adsorbed in zeolites

Noaimi, Asia Nasser Al

INFRARED STUDIES OF SPECIES ADSORBED IN ZEOLITES

BY

ASIA NASSER AL NOAIMI

(B.Sc. Qatar University)

A thesis submitted for the degree of Master of Science in the Department of Chemistry University of Durham

1981

Dedicated to my father Nasser Al Noaimi

Declaration

The work described in this thesis was carried out at Durham University and has not been submitted either wholly, or in part, at this or at any other university

Acknowledgements

I would like to express my thanks to Dr.J. Howard for his advice so freely given through out the period of research.

The help of various members of the technical staff is greatly appreciated. May I also thank my friends for their encouragement, and Mrs. R. Hart for typing this thesis.

Finally I would like to express my thanks to the Government of Qatar and Qatar University for their financial support.

ABSTRACT

The work described in this thesis is concerned with the investigation of the infrared study of zeolites and species adsorbed on zeolites.

In the first three chapters there are accounts on the zeolites structure and chemistry as well as the instrumentation and techniques which have been used.

In the fourth chapter a study of the formation of coke on CaY zeolite and the various factors which influence its presence on the zeolite is reported.

Chapter five is concerned with the presence of the hydronium ion formed by adsorbing water vapour on zeolites. Mn 4A zeolite can form the hydronium ion, while Co-4A does not.

Finally, in chapter six, we report a study of cyclopropane gas adsorbed on Mn(II) and Co(II) partially exchanged A zeolites.

Contents

CHAPTER 1

INTRODUCTION

1. Zeolites

Although zeolites are chemically more complex than some other adsorbents they do possess the advantages of high surface area and adsorption sites which are usually well defined. Furthermore, the strength of the zeolite-to-adsorbed molecule interaction can be altered in a variety of ways including ion-exchange and modification of the Si to Al ratio (1). It is possible, therefore, to study the interaction of a given adsorbate with a series of different cations, each held within the same framework as well as with the same cation in a range of frameworks.

Zeolites have strong affinity for polar or polarizable molecules and this property, combined with the internal adsorption characteristics, allows for purifications and separations to be performed using zeolites. In addition, the properties of zeolites can be altered still further by ion-exchange to provide a nearly limitless variety of products and potential uses (2-4).

Zeolites can also form novel chemical complexes like C_3H_6 (cyclopropane) or N_3H_3 bonded to transition metal ions (5). Note that N_3H_3 does not exist in the pure form and has not been observed outside a zeolite cage (6).

Numerous attempts are currently being made to use zeolites to solve,or improve the solution of technological problems. New types of zeolites and variations on existing types are being synthesized at present and many more will undoubtedly be discovered. Hopefully in the future, scientists

will be able to synthesize a zeolite-type material to meet particular applications.

The first applications of zeolites in industry was in separations, but this was followed by important catalytic uses. Recently, they have also been applied in solving environmental problems (3-9).

2. Spectroscopic studies

Spectroscopic techniques can ideally give information about the nature of surfaces and species adsorbed on surfaces. It has generally proved difficult to obtain the Raman spectra of zeolites, and particularly of zeolites containing adsorbed species. Zeolites themselves give rise to very weak Raman scattering and their fluorescence background is often high (9); this fluorescence is due to the presence of transition metal ions or of trace quantities of organic impurities (10). Similarly, great difficulty has been experienced with far-infrared studies (11). Apart from the intrinsic experimental difficulties, the low frequency normal modes of the adsorbed species appear to yield bands which are of very low intensity relative to the vibrations of the framework.

Infrared spectroscopy can give definite information on the structure and surface properties of zeolites and of how these are modified by various treatments. Changes in the spectra of the zeolite itself and of molecules adsorbed on the surface can yield direct information about the surface, the position of adsorbed molecules and the interaction between them (11-18). Infrared spectroscopy is a most sensitive structural technique (3).

The detailed absorption bands of the solid support and of the adsorbed species are not always all observed. Sometimes the absorption bands of prime interest are obscured by strong bands associated with vibrations of the zeolite.

Despite the problems that may arise, infrared spectroscopy remains a powerful method of studying adsorbed species.

References

1. Breck, D.W., Zeolite Molecular Sieves, Wiley, London (1974).

2. Katzer, J.R., Molecular Sieves II, Am.Chem.Soc. Washington D.C. (1977).

3. Rabo, J.A., Zeolite Chemistry and Catalysis, Am.Chem.Soc. Washington D.C. (1976).

4. Meier, W.M., and Uytterhoven, J.B., Molecular Sieves, Am.Chem.Soc. Washington D.C. (1973).

5. Cruz, W.V., Leung, P.C.W., and Seff, K. J.Am.Chem.Soc. 100 (22),6997 (1978).

6. Kim, Y., and Seff, K., J.Am.Chem.Soc. 99, 7057 (1977).

7. Leonard, D.W., British Zeolite Association (1980).

8. Townsend, R.P., Properties and Applications of Zeolites, The Chem.Soc. London (1980).

9. Angell, C.L., J.Phys.Chem., 77,222 (1973).

10. Tam, N.T., Conney, R.P., and Curthoys, G., J.C.S. Faraday I, 72,2577 (1976).

11. Kiselev, A.V., Lygin, V.I., IR spectra of surface compounds, Wiley, New York (1975).

12. Little, L.H., IR spectra of adsorbed species, Academic Press, London (1967).

13. Ward, J.W., Adv.Chem.Ser., 101,381 (1971).

14. Yates, D.J.C., Catalysis Reviews, 2 (1),113 (1968).

15. Rochester, C.H., Powder technology, 13,157 (1976).

16. Sheppard, H., Chenery, D.H., Lesinnas, A., Pentice, J.D., Pearce, H.A., and Primet, M., Mol.Spect.dense phases proc. of 12th European V.Cong. 345 (1975).

17. Zhdanov, S.P.K., Kiselev, A.V., Lygin, V.I., and Totova, T.I., Russ.J.Phys.Chem. 38,1299 (1964).

18. Masao Hino, Bull.Chem.Soc.Jap.50 (3),574 (1977).

CHAPTER 2

THE STRUCTURE AND CHEMISTRY OF ZEOLITES

1. Zeolites structures and properties

a. General structure

Zeolites are framework aluminosilicates based on a three-dimensional network of AlO_4 and SiO_4 tetrahedra linked to each other by corner sharing of oxygens. Since the Al atoms are trivalent, each AlO_4 unit is negatively charged and the charge on these units is balanced by framework cations. In the hydrated zeolite, the cations are usually quite mobile in the channels and therefore can be exchanged, at least to some extent, by other cations (1-9).

Zeolites may be represented by the empirical formula:

$$M_{2/n}O.\ Al_2O_3.\ XSiO_2.\ YH_2O \quad (2,6)$$

Where n is the valence of the cation M and $X \geq 2$ since AlO_4 tetrahedra are assumed to be joined to SiO_4 tetrahedra. A large number of both natural and synthetic zeolites are known. The structures of these belong to distinct groups with common building blocks; zeolites A, X and Y have frameworks consisting of linked truncated octahedra called sodalite units (Fig.1a) which are characteristic of the structure of sodalite. These are composed of 24(Al, Si) ions interconnected with 36 oxygen anions, and contain eight hexagonal and six square faces.

In zeolites X and Y, the framework consists of a tetrahedral arrangement of sodalite units linked by six

bridging oxygen atoms. The structure is very open with 12Å diameter almost spherical cavities (supercages) (Fig. 1b), each of which is surrounded tetrahedrally by four similar cavities separated one from another by constrictions 8-9Å in diameter, formed by distorted "12-rings" of oxygen atoms. The unit cell composition of zeolite X is $Na_{86}.(AlO_2)_{86}.(SiO_2)_{100}.264\ H_2O$.

The basic framework for zeolite Y is the same as that of zeolite X, but the Si/Al ratio is higher, generally ranging from 1.5 to 3.0.

In zeolite A the truncated octahedron is linked to its neighbour by four bridging oxygen ions (10,11); this configuration gives a roughly spherical internal cavity called the α-cage (Fig.1c) 11.4Å in diameter. This may be entered through six approximately circular windows 4.2Å in diameter, the circumferences of which contain eight oxygen atoms and are hence known as "8-rings". A second set of voids (β-cages:6.6Å in diameter) is contained within the sodalite unit themselves. These interconnect with the α-cages through a distorted "6-ring" of oxygen atoms 2.2Å in diameter. There may, therefore, be considered to be two interconnecting pore systems, one of diameter 11.4Å with 4.2Å constrictions, and the other of alternate 11.4Å and 6.6Å cavities separated by 2.2Å constrictions.

b. Cation positions

Cations are usually distributed over a range of different sites within a particular zeolite framework (2). According to X-ray structural analysis, the distribution

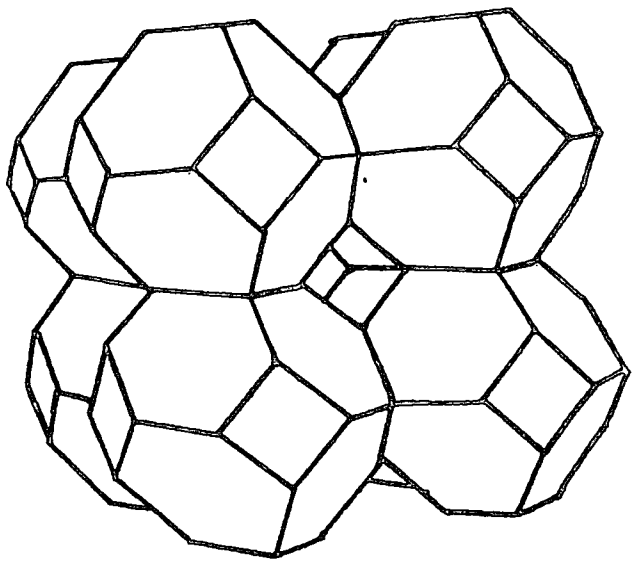

SODALITE

(a)

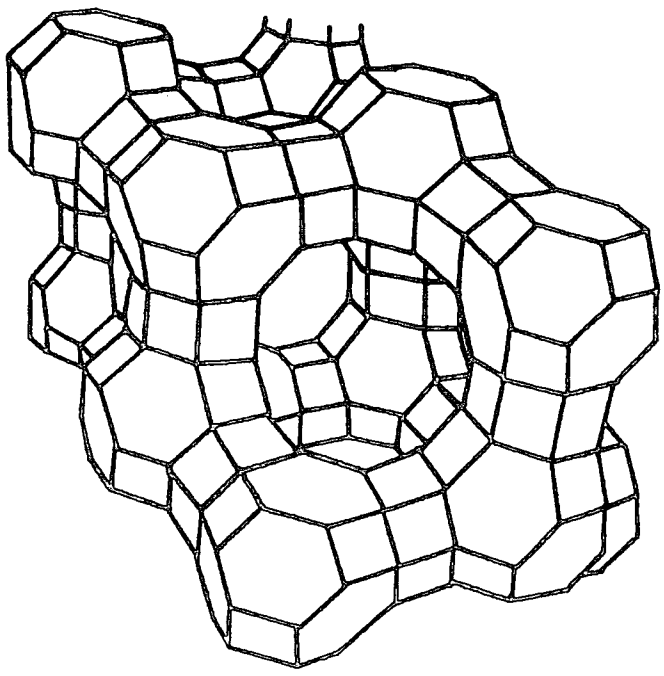

ZEOLITE 13X

(b)

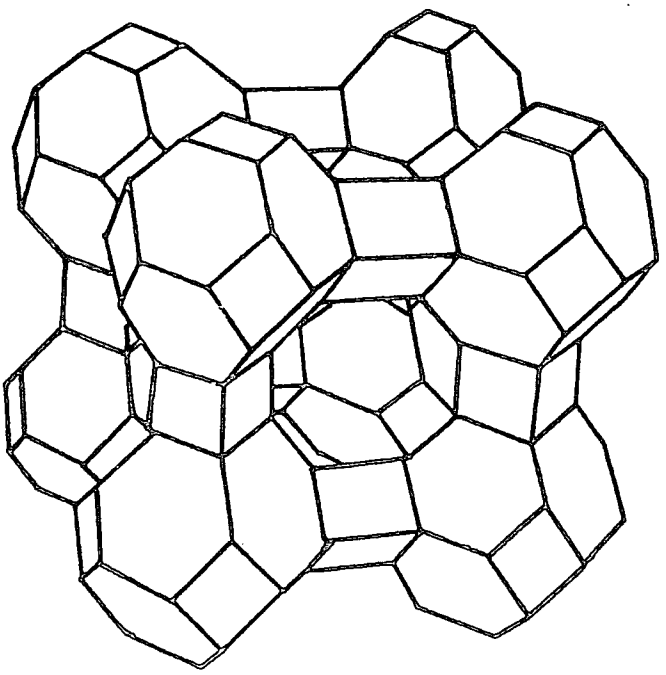

ZEOLITE A

(c)

Fig.1

of cations is altered after the adsorption of water or treatment at different temperatures (13). In general the cations distribute themselves amongst the sites so as to minimise the free-energy and there is usually only partial occupancy of many of the available sites. This distribution is a function of temperature, the cationic species, the state of hydration and the zeolite Si/Al ratio (1).

In the mid-1960s three main types of site were generally recognized, later the number of defined cation sites increased and these are described as follows (Fig.2).

Site I situated in the centre of the hexagonal prism.

Site I' on a triad axis displaced into the sodalite cage from the hexagonal face shared by the sodalite cage and the hexagonal prism.

Site II' on a triad axis displaced into the sodalite cage from the open six membered ring of the sodalite unit.

Site II displaced from the open six membered ring into the supercage.

Site III displaced into the supercage from bridging four membered rings and

SiteIV very nearly at the centre of the twelve membered rings separating the supercages (1-4, 14).

It is reasonable, therefore, that those positions most favourable to the cation under consideration will fill first, and subsequently any remaining cations will occupy sites in order of increasing unsuitability.

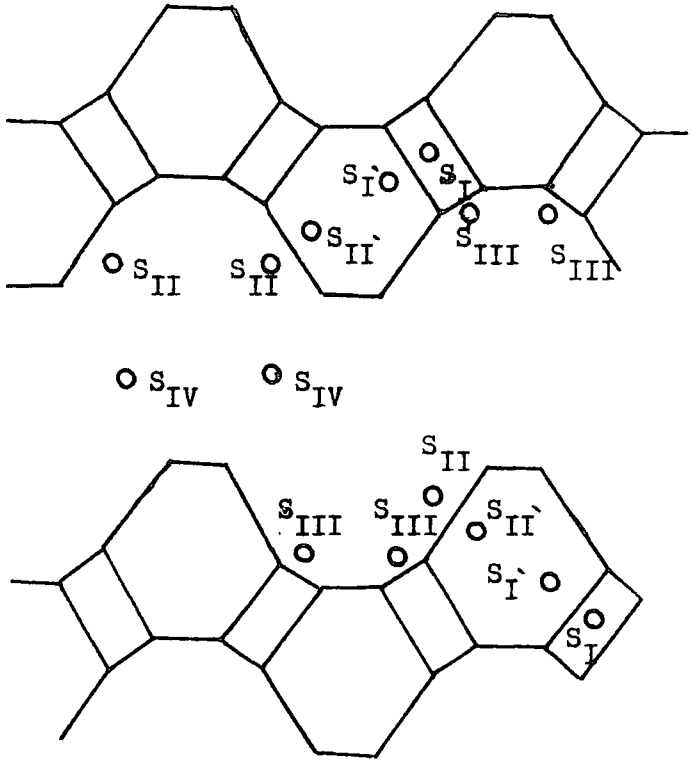

Fig.3

The cation sites in zeolite Y

The lines represent the bonds between the T atoms (Si,Al) and the oxygen atoms. The oxygen atoms are located between the T atoms and are not necessarily on the line joining them.

The possible cation positions within type Y and A zeolite are shown in Tables 1 and 2 respectively.

Table 1: The cation positions in dehydrated NaY zeolites (2)

Types of Sites	Max.available	Site occupancy
I	16	7.5
I'	32	19.5
II'	32	-
II	32	30
U	8	-

c. Ion exchange

Ion exchange in zeolites has been widely studied. Cation selectivities in zeolites, however, do not follow the typical rules (2) that are evidenced by other inorganic and organic ion exchangers. Zeolite structures have unique features which lead to unusual types of cation selectivity and sieving. The cation exchange behaviour of zeolites depends upon the (2,3):

a) Nature of the cation species, the cation size, both anhydrous and hydrated, and cation charge,
b) Temperature,
c) Concentration of the cation species in solution,
d) The anion species associated with the cation in solution,
e) Structure and characteristics of the particular zeolite.

Table 2: Cation Locations in Type NaA zeolite

Position	Designation	Number
In an 8-ring	S1	3 per unit cell
Adjacent to an 8-ring, but displaced into a 26-hedron (α-cage).	S1*	
In a 6-ring	S2	8 per unit cell
Adjacent to a 6-ring, but displaced into a 26-hedron (α-cage).	S2*	
Adjacent to a 6-ring, but displaced into a sodalite β-cage .	S2'	
Against a 4-ring forming one of the ribs of a 26-hedron (α-cage).	S3	12 per unit cell
In the centre of a sodalite β-cage	SU	1 per unit cell
In the centre of a 26-hedron (α-cage).	S4	1 per unit cell

Generally it is easier for a cation to diffuse down a large channel and the temperature at which the exchange is carried out is often of great importance. The ion exchange capacity of zeolites is large and can approach the capacity of the best resin ion exchangers. This ability to undergo reversible cation exchange is one of the most important properties of zeolites, the most striking modification that can be made in this respect is to change the molecular sieve properties. For example, the replacement of Na^+ ions in Linde A by K^+ ions cause a decrease in the O_2 sorption to essentially zero (17). Also, changing the cation for

one of higher charge in a zeolite may effectively enlarge the pore openings by diminishing the cation population and by resiting the cations which are normally located near these openings. In zeolite A, divalent ion exchange opens the aperture to full diameter whereas exchange with a larger univalent ion diminishes the aperture size. Potassium ion exchange in zeolite A reduces the effective adsorption pore size to the point where only small polar molecules are adsorbed (2).

d. Adsorption

In contrast with other molecular sieves, zeolites have pores of uniform size which are uniquely determined by the structure of the crystal. Fig. 3 shows for comparison the pore size distribution for zeolites 4A and 13X, silica gell and activated carbon (10,11,13,14,16-19). The dehydrated crystalline zeolites are the most important molecular sieves (6). These materials have a high internal surface area available for adsorption due to the channels or pores which uniformly penetrate the entire volume of the solid. The external surface of the adsorbent particles contributes only a small amount of the total available surface area. The first experimental observations of the adsorption of gases on zeolites and their behaviour as molecular sieves were conducted on the zeolite minerals.

The adsorbed phase disperses through the internal voids of the crystal without displacing any atoms which make up the permanent crystal structure. There are several factors which influence the rate of adsorption in zeolites such as pressure, temperature, particle size and the conditions of

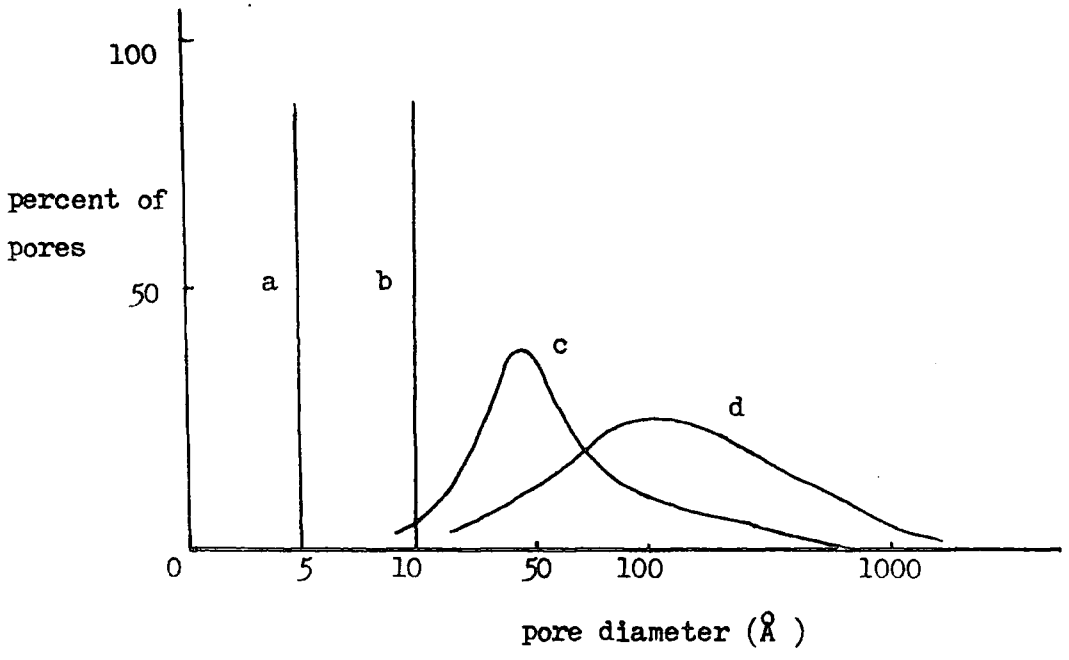

Fig.3 pore size distribution of various molecular sieves

a.type 4A zeolite

b.type 13X zeolite

c.silica gel

d.activited carbon

dehydration. The adsorption of a molecule depends partially upon its polarity and polarizability together with variations in the chemical composition of the zeolite (6).

The main channels by which diffusion occurs in zeolites are formed by cavities connected by apertures, the walls of the channels,which form the internal surface,contain a regular array of cations that bear a charge depending upon the inadequacy of the local coordination or screening by the oxygen ions of the framework. Upon dehydration and removal of water from the channels, the remaining cations are stranded at channel intersections or on channel walls where they inhibit diffusion of other molecules.

e. Catalytic activity

Zeolites offer unique opportunities for studies of heterogeneous catalysis because of their catalytic, structural and ion-exchange properties. These crystalline aluminosilicates, in appropriate ion exchanged forms, can offer sizeable activity enhancements and selectivity alterations for certain reactions (1) when compared with amorphous silica-alumina, although not necessarily for all reactions (20).

The existence of several different zeolite framework structures, each of which can be rationally modified by means of controlled ion-exchange, offer a range of catalytic properties. There are several factors which effect the catalytic activity including (a) the number of active sites, (b) the size and shape of adsorbed molecules, and (c) the rate of diffusion (1). Various guest molecules can also

significantly change the catalytic properties of the zeolites. It is known that the addition of small amounts of water increases the activity of zeolites for carbonium-ion type reactions, cracking alkylation and isomerization (1). The addition of water molecules to X and Y zeolites with monovalent ions increases the isomerization of cyclopropane (21).

2. Applications

The growth of the zeolite industry has been extremely slow considering that it is 25 years since commercially mineable deposits were located (22).

The first application of dehydrated zeolites as molecular sieves was in the separation of gas mixtures. The commercial uses of zeolites in adsorption are summarized in Table 3 .

Table 3 : Adsorption applications (23)

Regenerative

- separations based on sieving
- separations based on selectivity
- purification - bulk separations.

Non-regenerative

- Drying refrigerants.
- cryosorption.

One of the earliest applications in ion exchange was in the removal and purification of caesium and strontium radio-isotopes. Uses of zeolites in ion exchange are listed in Table 4 (23).

Table 4: Ion-exchange application

Removal of NH_4^+ from waste water

Metal separation

Radio-isotope removal and storage

Detergent builder

Artificial kidney dialysate regeneration

Aquaculture - NH_4^+ removal

Ruminant feeding on non-protein nitrogen

Ion-exchange fertilizers.

More zeolites are currently used in catalysis than in any other application, e.g. as cracking catalysts for converting petroleum into lighter fractions including gasoline and fuel oil. Petrochemical feeds have provided the major market for these materials.

Some applications of zeolites in catalysis are given in Table 5 .

Table 5 : Catalysis applications

Hydrocarbon conversion

- Alkylation
- Cracking
- Hydrocracking
- Isomerization

Hydrogenation and dehydrogenation

Hydro-dealkylation

Methanation

Shape-selective reforming

Dehydration

Organic Catalysis

Inorganic reactions

H_2S oxidation

3. Application of infrared spectroscopy to the study of zeolites

Infrared spectroscopy has been of the greatest value in the determination of the structure of molecules. It has been very widely used in research in the field of surface chemistry and in the study of adsorbed species.

a. Infrared studies of zeolite frameworks

Infrared spectroscopy has been extensively used to elucidate the framework structure of zeolites. For instance, Zhdanov et al (24) have applied infrared spectroscopy to the study of the frameworks of a series of X and Y zeolites as a function of Si/Al ratio, cation type and state of hydration. In the region investigated, 400-800 cm^{-1}, they identified two types of vibration : the first due to internal vibrations of the $(Al,Si)O_4$ tetrahedron, which is the primary unit of the structure and which is not sensitive to other structural variation, and the second which may be related to the linkages between tetrahedra. The most detailed study of the framework structures of zeolites and their classification to groups has been made by Flanigen et al (25). The study was made in the 1300-200 cm^{-1} region since this range contains the fundamental vibrations of the $(Si,Al)O_4$ tetrahedra.

A summary of some infrared assignments of framework vibrations are given in Table 6 . This is data for NaY (Fig.5) zeolite and is intended to illustrate the assignment scheme (25). In the spectra shown, the internal

tetrahedral linkages are drawn in full line, and the structure sensitive external vibrations with broken lines (8,10,26,27,28).

Table 6: Infrared assignments of zeolite framework vibrations (25)

Internal tetrahedra		
	- Asym. stretch	1250 - 950
	- Sym. stretch	720 - 650
	- T-O bend	500 - 420
External linkages		
	- Double ring	650 - 500
	- Pore opening	420 - 300
	- Sym. stretch	750 - 820
	- Asym. stretch	1150 -1050 sh

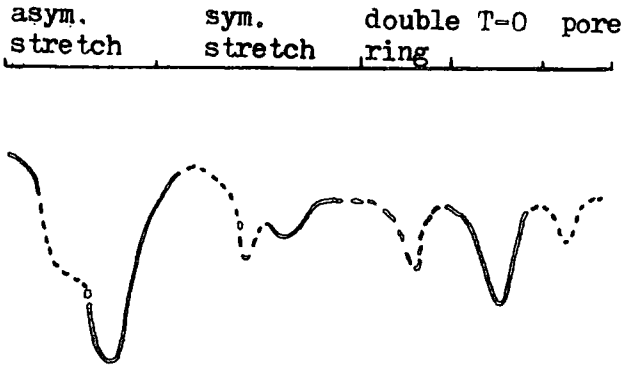

Fig.(5) Infrared assignments illustrated with the spectrum of zeolite Y, Si/Al of 2.5 (25). The full line indicates vibrations due to the internal tetrahedral linkages and the broken line the structure sensitive external vibrations.

The hydroxyl groups in zeolites

The hydroxyl groups have been extensively studied by infrared spectroscopy. Three types of hydroxyl groups were detected by Bertsch and Habgood (39-32). These measurements provide information concerning the location of the hydroxyl groups, their functionality and (28,29,30) information concerning the location of the cations themselves. The bands at 3660 and 3550cm^{-1} are due to the most important hydroxyl groups and are referred to as the high frequency and low frequency bands, respectively.

Infrared provide useful information as to how these surfaces are modified by various treatments.

b. Adsorption of molecules

A large number of studies and reviews have been published of molecules adsorbed on zeolites (5,8,16,32-34). The earliest study was of benzene (33) over Na and CaX zeolites by Kiselev et al. The C-C stretching vibration band at 1486cm^{-1} was very much stronger than the CH stretching band. A detailed study of the adsorption of ethylene has been reported (34). Very large intensity changes, larger than those previously observed with benzene (33) were found. Eberly studied the interaction between olefins and zeolites at high temperatures. The behaviour of adsorbed species at high temperatures is particularly useful in relation to catalysis, which is often conducted under these conditions (35-37). Other applications of infrared spectroscopy to the study of zeolites include:

(1) The SiO_2/Al_2O_3 ratio

The frequency shift of the infrared stretching bands with the variation in Si/Al ratio in the tetrahedral frameworks has been reported (38,39). From infrared spectra of the synthetic sodium zeolites A, X, Y erionite and mordenite, Shikumove et al, drew a quantitative relationship

between the position of the main asymmetric stretch band and zeolite Si/Al ratio, Flanigen and Grose (40 used mid-infrared spectroscopy to characterize the framework composition of phosphate zeolites and establish proof of phosphorous substitution in the framework. The observation and assignment of Infrared frequencies can generally be applied to prove that framework substitution has occurred.

(2) Cation type and cation sites

The nature and crystallographic sites of cations in zeolites have been reported to be reflected in the infrared spectra. Zhdanov et al (24) showed the strong sensitivity of framework infrared vibrations to cation type and charge for a series of Na, Sr and Ca ion-exchanged forms of zeolite X. Flanigen et al (25) noted that dehydration of the synthetic forms of zeolites A, X, Y, L and Ω, all containing alkali metal cations, showed only minor spectral changes; however, they reported significant changes in spectra of dehydrated zeolites in polyvalent cation forms, such as CaY, as shown in Fig.6. The spectral changes were interpreted as due to cation movement or resiting of cations as a result of dehydration, dehydroxylation and rehydration reactions, and it shows the migration of Ca^{2+} cations from inside of the sodalite unit into a position near the centre of the D-6 ring (site I).

Brodskii, Zhdanov and Starevich (41,42) studied the effect of dehydration on a series of alkali-metal cation exchanged forms of zeolite X and Y with varying Si/Al ratios. Their spectral data shows that spectral changes are sensitive to the nature of the substituting cation and

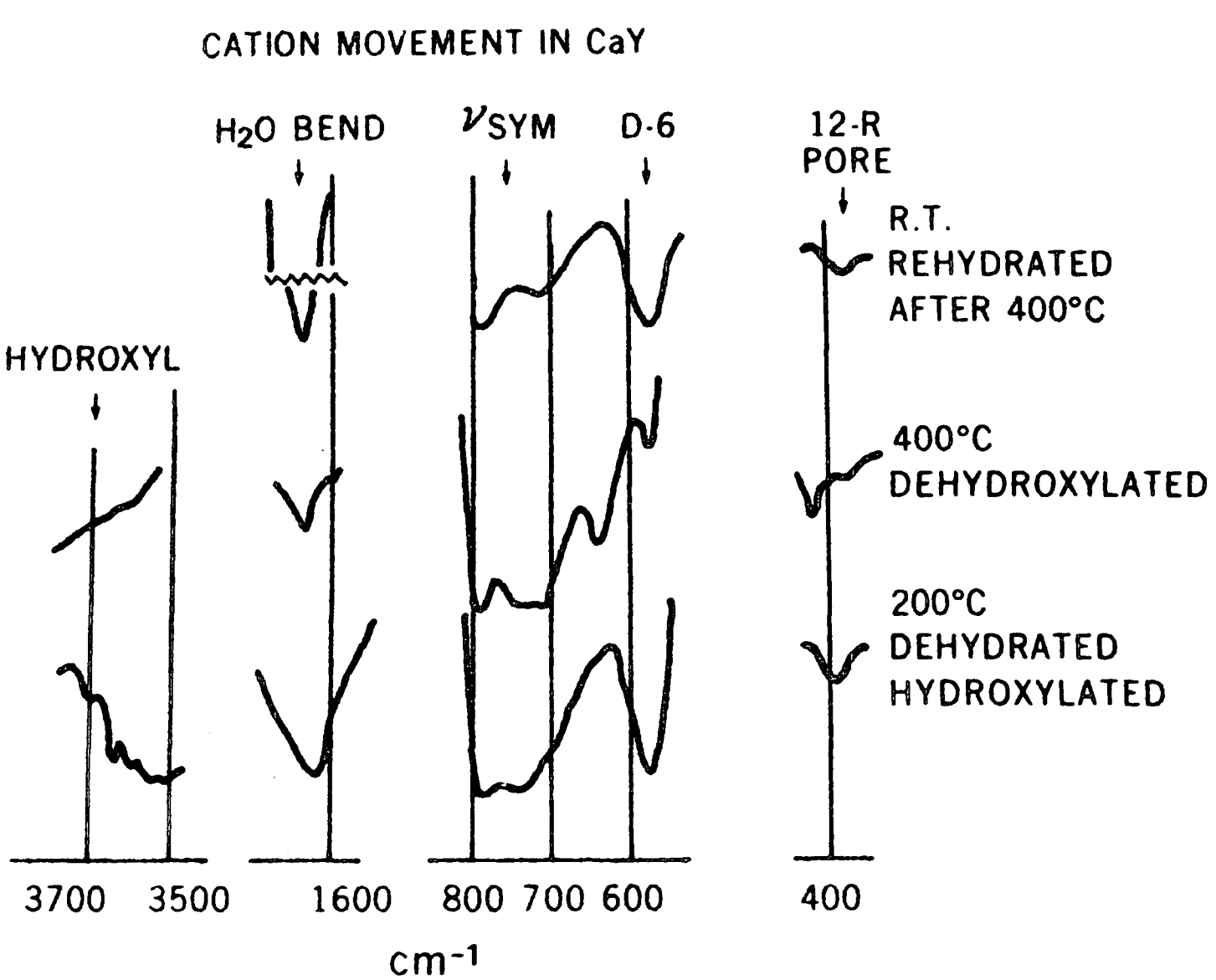

Fig.6 Infrared spectra of CaY zeolite (Si/Al of 2.5) after dehydration, dehydroxylation and rehydration

the cation site. They also showed that the framework frequency is proportional to $m^{-\frac{1}{2}} R^{-3/2}$ where m is cation mass and R is cation radius (42).

(3) Zeolite synthesis mechanism

Infrared spectroscopy can also apply to investigations of the mechanism of crystallization of zeolites from hydrous aluminosilicate gels or other aluminosilicate systems, such as the crystallisation sequence for NaY zeolite from a sodium aluminosilicate gel (2).

(4) Catalytic system

The application of infrared spectroscopy to the catalytic aspects of zeolites has been in two major areas.

a. the elucidation of the structural groups in zeolites and their properties as they pertain to catalytic centres, and

b. the observation of catalytic reactions on zeolites while the reactions are actually occurring on the zeolite surface. The surface of decationated Y zeolite was studied during cumene cracking on the zeolite (43), and it was found that the 3550 cm^{-1} band is not influenced by the cumene while the 3640cm^{-1} band decreased in intensity with time. As the temperature was raised to over 325^{o}C, however, the 3550 cm^{-1} band intensity also decreased. This indicated that no interaction of the cumene with the species responsible for this band occurs below 325^{o}C and that these sites are probably not active catalytic centres. The species producing the 3640 cm^{-1} band are the active sites.

Although many studies have been reported on catalytic reactions over zeolites, the particular sites responsible

for reaction still remain uncertain in all but a few cases.

References

1. Venuto, P.B. and Landies, Advance Catalysis, 18,259(1968).

2. Breck, D.W. Zeolite molecular sieves, Wiley, New York, (1974).

3. Rees, L.V.C., Annual Reports Chem.Soc. A, 67, 191 (1970).

4. Leach, H.F., Annual Reports Chem.Soc. A, 68,195 (1971).

5. Kiselev, A.V. and Lygin, IR spectra of surface compounds (1975).

6. Rees, L.V.C., Solid electrolytes, 417 (1978).

7. Carla, Heitner-Wirgava, Ion exchange solvent ext. 7,88 (1977).

8. Rabo, J.A., Zeolite Chemistry and Catalysis, 1976.

9. Meier, W.M. and Uytterhoeven, J.B., Molecular Sieves (1973).

10. Breck, D.W., Eversole, W.G., Milton, R.M., Reed, T.B., and Thomas, T.L., J.Am.Chem.Soc. 78,5963 (1956).

11. Reed, T.B., and Breck, D.W., J.Am.Chem.Soc. 78,5972 (1956).

12. Yanagida, K.Y., Vance, T.B., and Seff, K., Inorg.Chem. 13, 723 (1974).

13. Rubio, J.A., and Soria, J., J.Colloid Interface, Sci., 73 (2),312 (1980).

14. Stone, F.S., Acta-cient-veuz supl. 33,(1974).

15. Riely, P.E., and Seff, K., J.C.S.Chem.Comm. 1287 (1972).

16. Little, L.J., IR spectra of adsorbed species, Academic Press, London (1967).

17. Sherry, H.S., Adv.Chem.Ser. 101,350 (1971).

18. Katzer, J.R., Molecular Sieve II, Am.Chem.Soc. Washington D.C., ACS Symposium (1977).

19. Biswas, M., and Maity, N.C., Advance in polymer science, Series 40, 31,48 (1979).

20. Venuto, P.B., Adv.Chem.Ser. 102,186 (1970).

21. Habgood, H.W., George, Z.M., Molecular Sieves, 130 (1968).

22. Leonard, D.W., British Zeolite Association, (1980).

23. Townsend, R.T., The properties and application of zeolites (1979). the chemical society London.

24. Zhadanov, S.P., Kiselev, A.V., Lygin, R.J. and Titova I.I., Russ.J.Phys.Chem. 38, 1299 (1964).

25. Flanigen, E.M., Khatami, H., and Szymanski, H.A., Adv.Chem.Ser. 101, 201 (1971).

26. Lygin, V.I., Serogina, V.A., and Gryazrova, Z.V., Vestu.Mosk.Univ.ser Zkhim, 20 (3) 281, (1979).

27. Kondratov, V.K., Lipatova, L.F., and Vythristu, K.V.G., Russ.J.Phys.Chem. 53 (12), 1796 (1979).

28. Smola, V.I., Novgorodova, E.Z., and Mikhailov, A.S., Russ.J.Phys.Chem. 53 (7), 1031 (1979).

29. Bertsh, L., and Habgood, H.W., J.phys.chem. 67, 1621 (1963).

30. Ward, J.W., J.Phys.Chem., 72 (12), 4211 (1968).

31. Angell, C.L., Schaffer, P.C., J.Phys.Chem. 69 (10), 3463 (1965).

32. Yates, D.J.C., Catalysis Reviews 2 (1), 113 (1968).

33. Kiselev, A.V., Abramov, V.N., and Lygin, V.I., Zh.Fiz.Khim. 37, 1156 (1963).

34. Carter, J.L., Yates, D.J.C., Lucchesi, D.J., Elliott, J.J., and Kevorkian, V., J.Phys.Chem. 70, 1126 (1966).

35. Eberly, P.E., J.Phys.Chem. 71, 1717 (1967).

36. Liengme and Hall, W.K., Trans. Faraday Soc. 62, 3229 (1966).

37. Hughes, T.R., and White, H.M., J.Phys.Chem., 71, 2192 (1967).

38. Milkey, R.G., Amer. Mineralogist, 45, 990 (1960).

39. Shikunov, B.I., Lafer, L.I., Yakerson, V.I., Mishin, I.V., Rubinshtein, A.M. Acad. Sci.USSR. Bull.Div.Chem.Sci. 21, 201 (1972).

40. Flanigen, E.M., Grose, R.W., Adv.Chem.Ser. 101, 76 (1971).

41. Brodskii, I.A., Zhdanov, S.P., Stanevich, A.E., Optics Spectr. 30, 30 (1971).

42. Brodskii, I.A., Zhdanov, S.P., Stanevich, A.E., Sov.Phys.Solid state, 15, 1771 (1974).

43. Ward, J.W., J. Catal,11,259 (1968).

CHAPTER 3

TECHNIQUES AND INSTRUMENTATION

1. Infrared Spectrophotometer:

A Perkin-Elmer 580B infrared spectrophotometer was used. It is a double beam, ratio recording instrument, which provides a continuous record of the transmission of a sample as a function of frequency. (1) The source is a ceramic tube, it is heated to 1200^{o}C and produces a continuous spectrum of electromagnetic radiation.

The radiation from the source is focused on a baffle by a toroid mirror, the baffle ensures that radiation from only a limited surface area of the source is admitted to the optical system thus minimizing sample heating. The baffle image is focused on to the first chopper mirror which rotates, dividing the source energy into sample and reference beams. The two beams are focused into the sample compartment. After the sample compartment the alternate pulses of radiation from the two beams are combined by the action of a second chopper, which has reflective first and third quadrants. During the first and second quadrants the second chopper receives energy via the sample and reference beams respectively. During the third and fourth quadrants chopper 1 cuts off the source energy so that any energy appearing at the second chopper is due to re-radiation effects from the sample compartment, then the two beams are combined into a single beam of alternating segments (1). When the beams are of equal intensity, the instrument is at an optical null. The recording pen is then at 100% T when no sample is present (2-4). The beam is then focused on the monochromator entrance slit. The slit restricts

the radiation passing through it to a narrow wavenumber band the mean of which corresponds to the wavenumber at which the measurement is being made. The effective bandwidth varies with the wave number setting of the instrument since the slit width is programmed to maintain approximately constant energy at the detector over most of the wavenumber range.

The detector consists of a thermocouple within an evacuated housing at the focus of an on-axis ellipsoid mirror, the radiant energy leaving the exit slit is therefore focused by the ellipsoid as an image of the slit reduced in linear dimensions by a factor of eight. A caesium iodide lens on the thermocouple assembly further reduces the dimensions of the slit image falling on the target.

The alternating signal from the detector is amplified and then demodulated by the signal processing electronics to give separate sample and reference beam signals, which are compensated for the effects of thermal re-radiation from the sample compartment. The ratiometer produces the ratio of the two signals, which corresponds to the transmittance value of the sample. The ratio signal is then filtered to reduce the noise level, and baseline adjustment, offsetting and scaling operations are performed on the signal in the ordinate functions unit. The signal is then supplied to the recorder.

A brief outline of the operation of the PE 580 infrared spectrophotometer is shown in the block diagram in Fig (1).

2. Infrared data station:

The Perkin-Elmer infrared data station is designed for use with 580 B infrared spectrophotometers and other models.

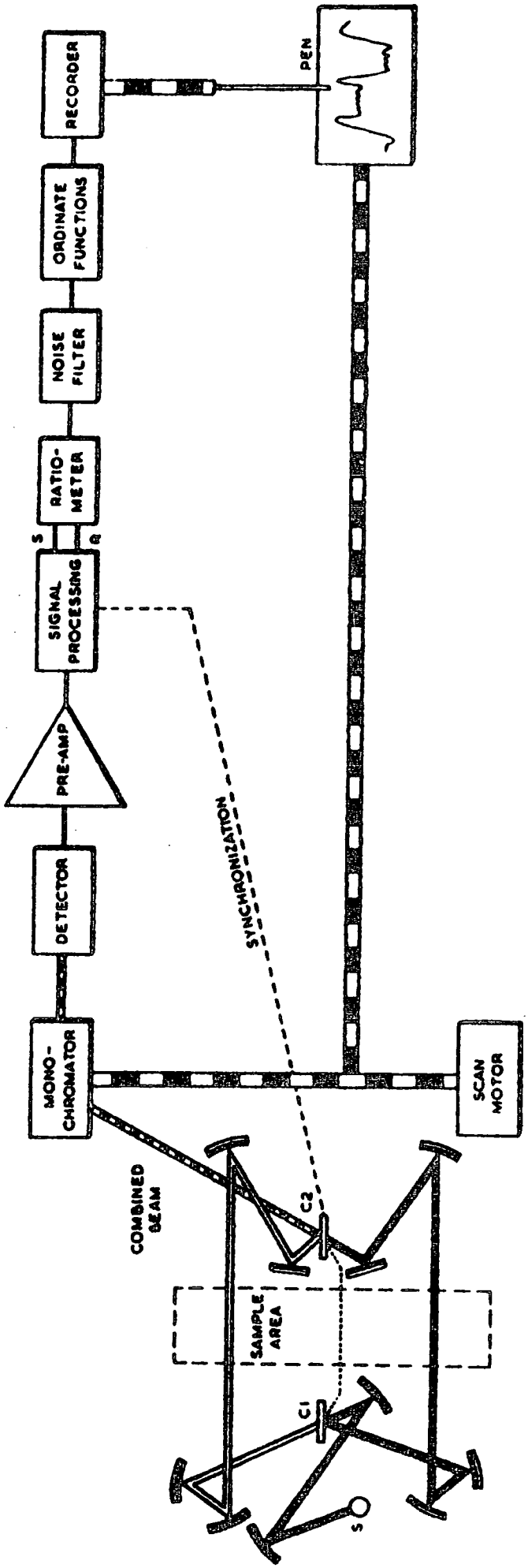

Fig.1 A block diagram of PE 580.

The data station is provided in three modules, (a) the visual display unit, which is used to display a spectra, (b) the keyboard, which is used to enter system commands, and (c) the data processing module which houses the system electronics and two micro-floppy disc drives.

When the data station is connected to the spectrophotometer an integrated infrared data system results, while independent use of the spectrophotometer is possible.

A block diagram of the system is shown in Fig (2) the system software provides the step-by-step instructions to the data station which in turn controls the spectrometer. The data processing module sorts the instructions to the instrument and accepts data from it while the working memory in the data processing module stores the spectral data for manipulation and modification by the applications programme routines. The data then may be saved on a bulk storage disc.

The PE 580 applications programme is provided on one of the microfloppy discs supplied with the system. This programme permits acquisition of spectra from the spectrophotometers, display of the spectra on the visual display unit, and subsequent storage of the spectra on disc.

There are twenty-four special function keys provided at the top of the keyboard module. One of the most important keys, which is often used, is the ABEX command. This command is equivalent to running a second spectrum with a sample of increased or decreased concentration. It is generally used by us to expand spectra of highly absorbing samples and the expansion factor may be entered as any value > 1. If the spectrum is stored in transmission (T%) each point is converted

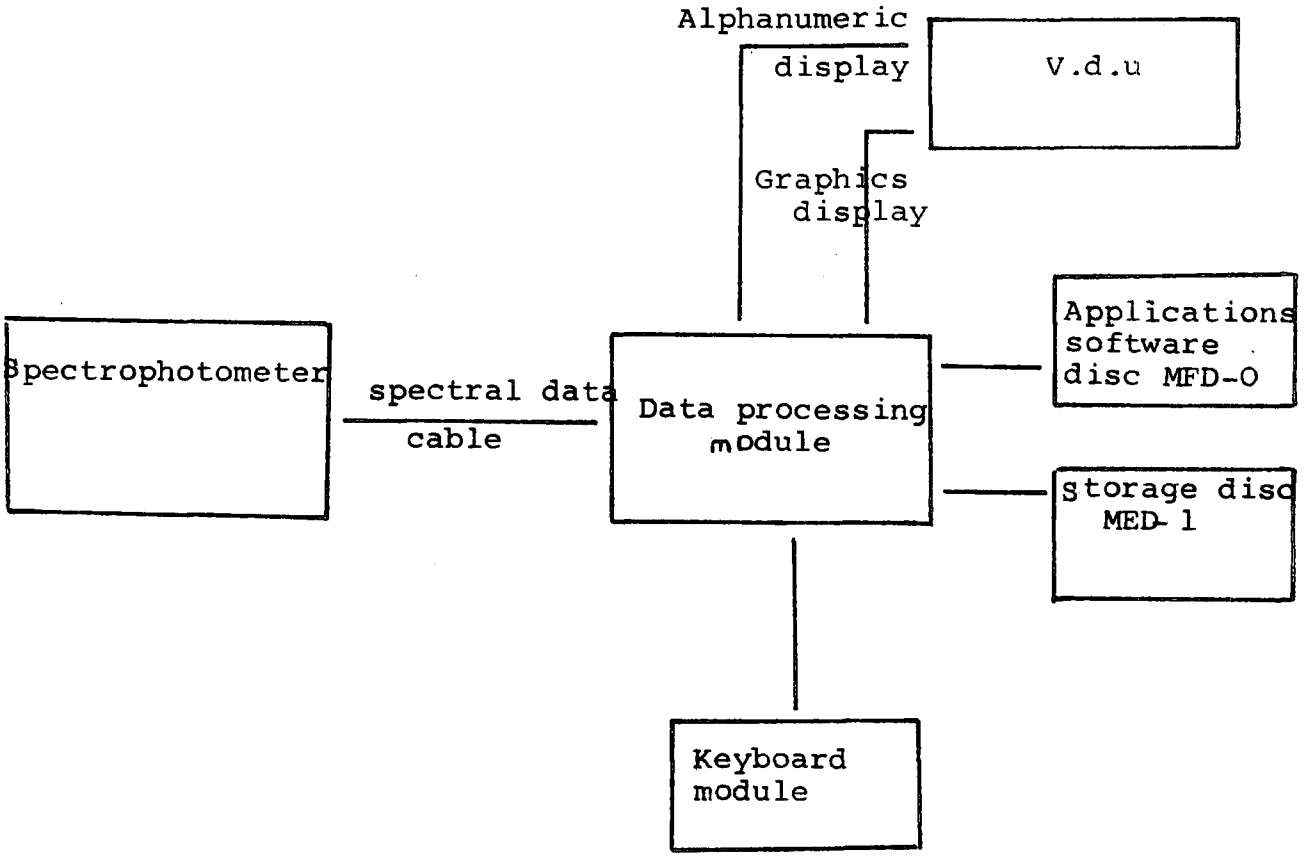

Fig.2 system block diagram

to its corresponding absorbance value and the expansion is preformed on the spectrum and then reconverted to T%. If the spectrum has previously been converted to absorbance (A), it is adjusted to 0.0A and multiplied by the factor.

Reference (5) gives the detailed information about the function keys.

3. Thermogravometric analysis:

Thermogravometric analysis, (TGA) has been carried out using a TGA 750 to detect the changes of zeolite weight as a function of temperature. TGA provides the analyst with a quantitative measurement of any weight change associated with temperature. Changes in weight are a result of the rupture or formation of various physical and chemical bonds at elevated temperatures which lead to the evolution of volatile products. TGA curves are characteristic for a given compound because of the unique sequence of the reactions (6).

In this study, TGA has been used mainly to detect the loss of water molecules from zeolites as a function of temperature.

4. X-ray powder photography:

This method has been used to distinguish between the structure of X and Y zeolites in the powder form, and to test for sample decomposition. Table (1) contains a comparison of the literature data (7) on X and Y zeolite, compared with my values for the same zeolites. Cu K_{α} was used as the source of radiation(7).

$$K_{\alpha} = \frac{2K_{\alpha 1} + K_{\alpha 2}}{3}$$

For the copper target.

$$CuK_{\alpha} = 1.54178\ \text{Å}$$

Table 1 - X-ray data (d,Å) for X and Y zeolites

NaX zeolite ref (7) d(Å)	NaY zeolite ref (7) d(Å)	NaX zeolite our data d(Å)	NaY zeolite our data d(Å)
14.46	14.29	13.53	14.02
8.84	8.75	8.82	8.57
7.53	7.46	7.49	7.35
5.73	5.68	5.72	5.52
4.81	4.76	-	4.69
4.41	4.38	4.37	4.30
4.22	-	-	-
3.94	3.91	-	3.84
3.80	3.77	-	3.79
3.76	-	3.76	-
3.60	3.57	-	3.69
3.50	3.46	-	-
3.33	3.30	3.32	3.39
3.25	3.22	-	3.24
3.05	3.02	-	-
2.94	2.91	-	2.94
2.88	2.85	2.86	2.86

5. Infrared cell:

A purpose built infrared cell was used for studying the infrared spectra of the adsorbed gases. A diagram of this cell is shown in Figs. 3a, 3b. The cell was made from stainless steel and was connected to a transformer which controls the temperature of the disc holder. The cell is also connected to outlets, for admission gases and for evacuations at (a).The head of the cell is a "Vacuum Generator" electral lead through with 70mm UHV flange.

Full details of the dimensions of the cell are shown in Figs. 3a and 3b.

Gases are admitted to the cell using a valve in the vacuum system and the pressure of the gas is measured using a pirani gauge. For liquids a flask with two rotaflows were used to join between the cell and the valve of the vacuum line.

The cell can be heated in situ to 400^{o}C, by using molybdenum wire, as the heating element. The spectra of the sample in this cell could therefore be recorded at any temperature between ambient and 400^{o}C. A water jacket is shown at (b) through which water is circulated to prevent the windows from getting too hot.

KRS-5 (ThI, ThBr) windows were used, since these have high transmission in the near infrared region (20,000 - 250 cm^{-1}).

6. Vacuum systems:

The vacuum line used was metal made of stainless steel except for the gas handling part (which was of glass). Obvious requirements include a pirani and hot cathode ionization gauges. The pumps include the mechanical rotary

Fig.3a side view of the cell

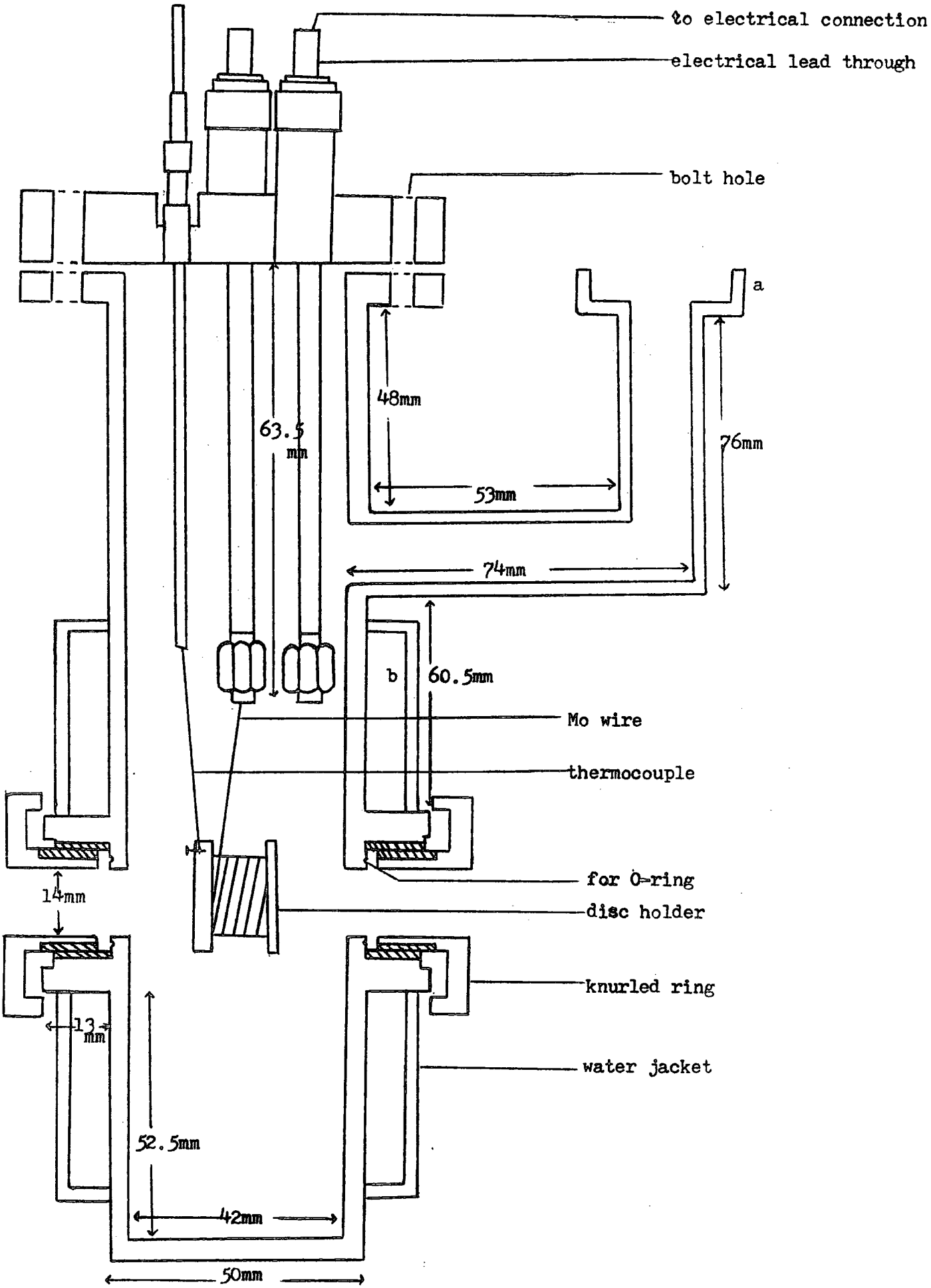

Fig.3b front view of the cell

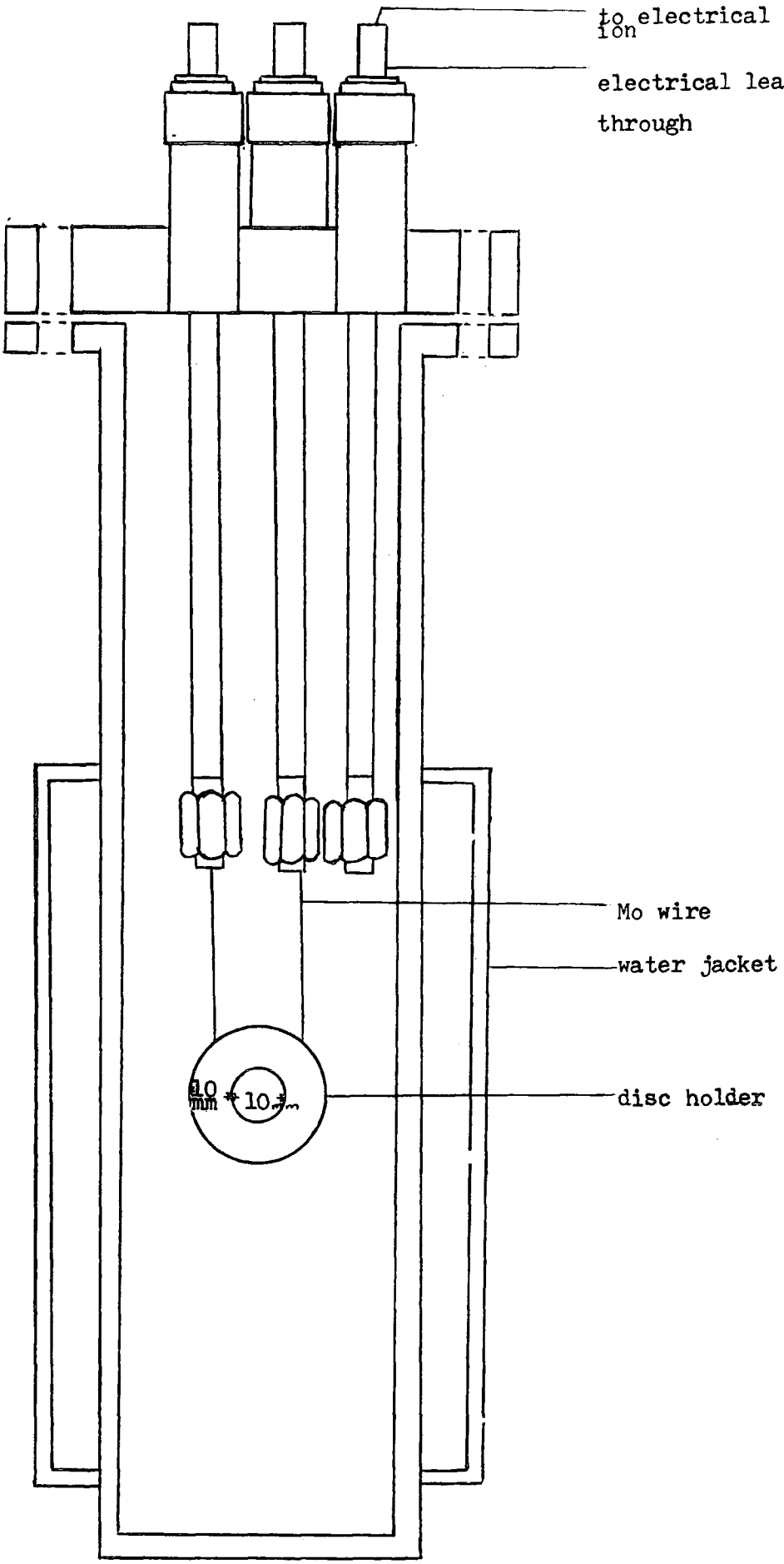

oil pump which can give a vacuum down to 10^{-3} torr, and a turbo-molecular pump which goes to 10^{-7} torr or lower.

A block diagram which shows the whole system is shown in Fig.4

7. Sample preparations:

Gases:

The infrared spectra of the gases were obtained at a range of pressures in the metal cell without the zeolite disc.

Liquids:

These may be examined directly in very thin layers. KBr windows were used to obtain the spectra of the liquids.

Solids:

Transparent discs were made by compressing the zeolite with KBr or as a self-supporting disc 10 mg of the zeolite were pressed in the die which has a diameter of 12mm.

After forming a self-supporting disc of the zeolite the sample was then inserted in the cell and left to evacuate until the pressure reaches 10^{-5} torr or less. The sample was then heated slowly until most of the water bands were removed. During heating the pressure increases initially but after the pressure decreased to 10^{-5} torr, the sample was cooled to the desired temperature, and the relevant adsorbate admitted.

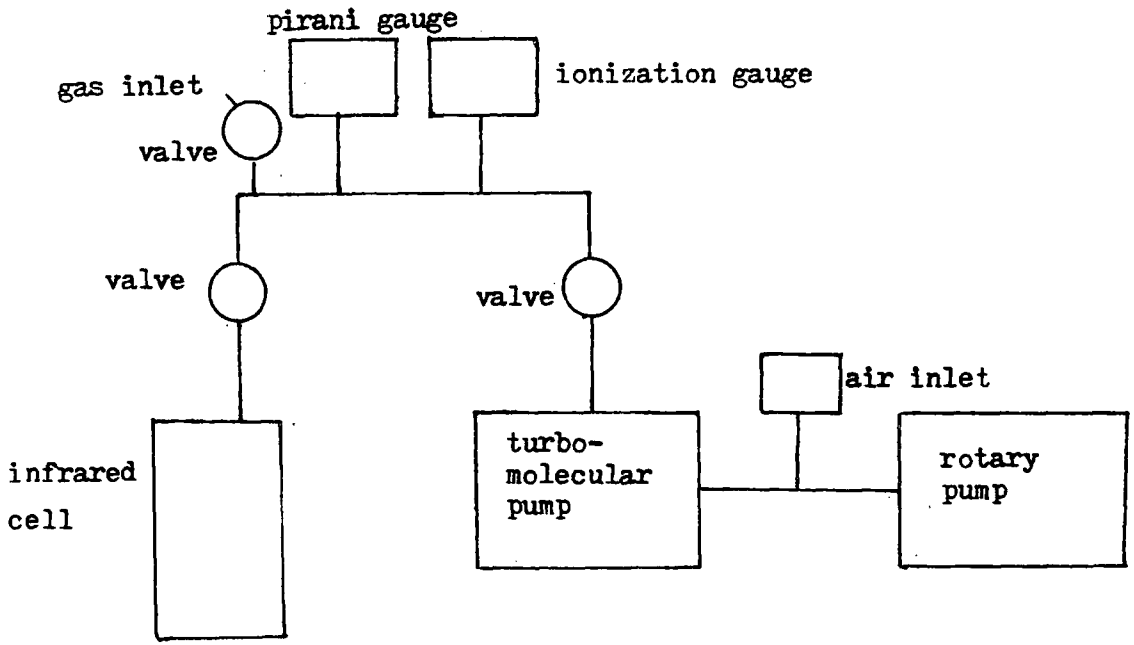

Fig.4 block diagram of the vacuum system

References

1. Model 580 infrared spectrophotometer instructions manual, England, 1977 Perkin-Elmer Ltd.

2. M. Dondrow, Instrumental methods in analytical chemistry, 1967.

3. Silverstein, R.M., Barsler, C.G., and Morril, T.G., Spectrometric identification of organic compounds, Wiley, London 1974.

4. Wright, H.G., Infrared techniques, 1973.

5. Instructions, Perkin-Elmer infrared data station pE 580 application programme, 1980. perkin-Elmer ltd

6. Willard, H.H., Merritt, L.L., J.R., Dean, J.A., Instrumental methods of analysis, 1979.

7. Breck, D.W., Zeolite molecular sieves, Wiley, New York (1974).

8. Donald Bloss, Crystallography and crystal chemistry, 1971.

CHAPTER 4

INFRARED SPECTROSCOPIC INVESTIGATION RELATING TO COKE FORMATION ON ZEOLITES: ADSORPTION OF HEXENE-1 AND N-HEXANE

1. Introduction

Eisenbach and Gallei (1) studied the adsorption of hexene-1 and n-hexane on to Y type zeolites (calcium and ammonium exchanged) in order to elucidate the interaction of the functional hydroxyl groups on both the internal and external surfaces of the zeolite with these hydrocarbons.

By heating the CaY and NH_4Y zeolites with the hydrocarbons, they observed the formation of coke which lowered the activity of the catalyst due to the poisoning of the active catalytic centres. As the coke band increased in intensity, some of the hydroxyl bands decreased. As a result the authors correlated the active sites for coke formation with these hydroxyl groups. The identification of a particular site responsible for coking makes the work both interesting and industrially relevant and represent a new application of infrared spectroscopy.

Many studies of coke formation in zeolite e.g. kinetics, mechanism and the effect on the properties of catalyst have been made by a number of workers (2-9). Some of the work (10) was concerned with catalyst poisoning, which occurs when the hydrocarbon converts over the zeolite and gradually deposits coke on the surface.

None of these studies however elucidate the correlation

of coking activity with a particular site in the catalyst. In contrast with earlier work, this paper of Gallei and Eisenbach (1) links the interaction of the hydrocarbons with particular hydroxyl groups in the zeolite catalyst.

Coke formation involves condensation-hydrogen elimination reactions in which the H/C ratio of the coke and its degree of unsaturation decrease as the time spent by the catalyst particle in the reaction increases. Simultaneously with the deposit of coke on the catalyst the surface area decreased which indicates blocking of pores and active sites. This shortens the life of the catalyst. Deposits of coke at the pores lying on the outer surface of the catalyst prevent entry of reactants to the zeolites framework. In some cases regeneration is possible by blowing oxygen over the surface to reduce the coke.

In this chapter there will be a comparison between our results and those of Eisenbach and Gallei for hexene-1 and n-hexane adsorbed on calcium exchanged Y zeolite.

2. Experimental:

Materials

CaY and NH_4Y zeolites were prepared from NaY zeolite (Union Carbide Corporation) by ion-exchange with 0.1 and 0.3N solutions of analytical grade $CaCl_2 \cdot 2H_2O$, NH_4NO_3 (Analar) and $Ca(NO_3)_2$ (Hopkins and Williams). The ion-exchanges were carried out at ambient temperature, and the zeolites were analysed for Na, Al and either Ca or NH_4, as appropriate, using atomic absorption techniques.

Eisenbach and Gallei presented their results as percentages of the oxides (Al_2O_3, Na_2O, CaO) and NH_4^+ and

so, to compare their results with ours, we have represented our data in the same way. Gallei et.al. also assumed that their samples had zero water content. Since the zeolites were not dehydrated before analysis the percentage figures that they present cannot represent the true compositions of the zeolites. For more details see the analysis of the zeolites in Table 1. Analytical grade hexene-1 and n-hexane were used after distillation and storage over molecular sieve 4A.

Procedures

10mg of the CaY zeolite was pressed in the die (12mm diameter). As the disc was degassed by heating and pumping, spectra were obtained at a range of temperatures. Spectra of CaY zeolite were recorded at ambient temperature, 493 and 623K. The zeolite sample was then cooled to room temperature, the spectrum recorded, the hydrocarbon added and the spectrum obtained once more. The sample was then evacuated for 10 minutes, and the spectrum recorded. The zeolite was then exposed to the hydrocarbon once more at ambient temperature and the sample heated slowly to 473-573K and spectra recorded at a variety of temperatures.

3. Results and discussions

a. Ion exchange

As explained earlier, Eisenbach and Gallei assumed that their samples have zero water content but this is invalid because the zeolite was not dehydrated before analysis. In order to compare our data with theirs, we have calculated the ratios Al_2O_3/Na_2O, Al_2O_3/CaO and Al_2O_3/NH_4, since these are not affected by the presence of water.

Table 1

Analytical data for the Y type zeolites used in this work

Sample number		N[b]	Al_2O_3	Na_2O	CaO	NH_4^+		Days in contact with solution	Al_2O_3/Na_2O	Al_2O_3/CaO	Al_2O_3/NH_4^+
	NaY[(a)]		102.0	62.0	-	-		-	1.65		
1	NaY		29.505	18.303	-	-		-	1.6	-	-
2	CaY	0.1	28.378	7.305	5.404	-	exact amount	25	3.88	5.25	-
3	CaY	0.1	29.429	6.946	6.33	-	excess	25	4.26	4.66	-
4	CaY	0.3	31.58	5.93	6.72	-	excess	35	5.32	4.69	-
5	NH_4Y	0.1	29.31	8.922	-	2.25	exact amount	25	3.29	-	13.02
6	NH_4Y	0.1	33.242	7.477	-	3.342	excess	25	4.44	-	9.95
7	NH_4Y	0.3	29.84	6.613	-	3.6	excess	35	4.51	-	8.28

(a) Calculated from the standard formula, $Na_{56}(AlO_2)_{56}(SiO_2)_{136} \cdot 250\ H_2O$

b. normality

Eisenbach and Gallei (1) prepared their zeolites from the Na form of faujasite by ion exchange with 0.1N solutions of NH_4NO_3 and $Ca(NO_3)_2$ and their analysis data is given in Table 2. By comparing Tables 1 and 2, it can be seen that the two sets of results are very different. It should be noted that the samples were prepared by the same methods, except that we do not have any information on how long Eisenbach and Gallei left their ion exchange to take place. From Table 1, one can see that 0.1N solution gives a lower degree of ion exchange than that of Eisenbach and Gallei. In view of this, we carried out ion exchange in 0.3N solutions to try to reach the same degree of ion exchange that they reached. In both cases, however, the degree of exchange we obtained is less than that of Eisenbach and Gallei although they used only 0.1N solutions. In fact, the published analytical data of Eisenbach and Gallei is incorrect, and they have sent us a new table containing correct values (Table 3). Unfortunately this data does not agree with ours either.

Eisenbach et al (11) suggest that the zeolite which we used in our experiments is not Y zeolite but X. By obtaining the X-ray powder photograph of the sample, we have shown that the zeolite is indeed of type Y and not X (Table 4).

Several papers (13-16) show a range of values of the degree of ion exchange of CaY zeolite, when prepared by different methods. None of these results agree with ours or those of Eisenbach et al (1).

Table 2: Analysis of Zeolites by Eisenbach and Gallei (1)

Sample	SiO_2 Wt %	Al_2O_3 Wt %	Na_2O Wt %	CaO Wt %	NH_4^+ Wt %	Al_2O_3/Na_2O	Al_2O_3/CaO	Al_2O_3/NH_4
NaY	64.3	21.9	13.8	-	-	1.58	-	-
CaY	65.0	22.1	3.5	9.4	-	6.3	2.35	-
NH_4Y	64.8	22.2	3.8	-	9.2	5.84	-	2.41

Table 3: The chemical analysis of zeolite CaY and NH_4Y by Eisenbach and Gallei (11): (correct version)

Sample	SiO_2	Al_2O_3	Na_2O	CaO	NH_4^+	Al_2O_3/Na_2O	Al_2O_3/CaO	Al_2O_3/NH_4
CaY	66.8	22.7	3.6	6.8	-	6.3	3.33	-
NH_4Y	68.2	23.2	4.0	-	4.6	5.8	-	3.04

Table 4: X-ray data (d,Å) for X and Y Zeolite

NaX (Å) our data	NaY (Å) our data	Nax (Å) ref 12	Nay (Å) ref 12
13.53	14.02	14.46	14.29
8.82	8.57	8.84	8.75
7.49	7.35	7.53	7.46
5.72	5.52	5.73	5.68
-	4.69	4.81	4.76
4.37	4.30	4.41	4.38
-	-	4.22	-
-	3.842	3.94	3.91
-	3.79	3.80	3.77
3.76	-	3.76	-
-	3.69	3.60	3.57
-	-	3.50	3.46
3.32	3.39	3.33	3.30
-	3.24	3.25	3.22
-	-	3.05	3.02
-	2.94	2.94	2.91
2.86	2.86	2.88	2.85
-	2.72	2.79	2.76

There are several possible reasons for the difference between our results and those of Eisenbach and Gallei.

1. The ion exchanges were not carried out in exactly the same way. Possible differences include length of time in solution and temperature, neither of which were specified by Eisenbach and Gallei.
2. Errors in analysis.
3. Zeolites from different sources.
4. Eisenbach and Gallei may have used repeated exchange.

Of these, the most likely are 1 and 4. Despite the difference in degree of ion exchange we felt it worthwhile repeating the experiments carried out by Eisenbach and Gallei in order to determine the influence of the degree of ion exchange on the results. For our experiments we have chosen to use the sample which had the highest degree of exchange (sample 4 of Table 1).

b. The Adsorption:

1. The hydroxyl groups

Fig.1 shows our spectra of CaY zeolite obtained at ambient temperature, 493, 623 and 303 K. A band which occurs at 3690cm^{-1} at room temperature (RT) apparently changes its position on heating the sample (493K) to 3640cm^{-1}, and a broad band at 3560-3100cm^{-1} (RT) which gives on heating to 493K a band at 3560-3440cm^{-1}. The broadness of the band at RT (Fig.1a) probably arises because it consists of two components, a band due to a hydroxyl group (ca.3540cm^{-1}) and one due to H_2O (ca.3400cm^{-1}). The latter is mostly removed on heating the sample so that in the higher temperature spectrum (Fig.1b) the band due to the hydroxyl group dominates.

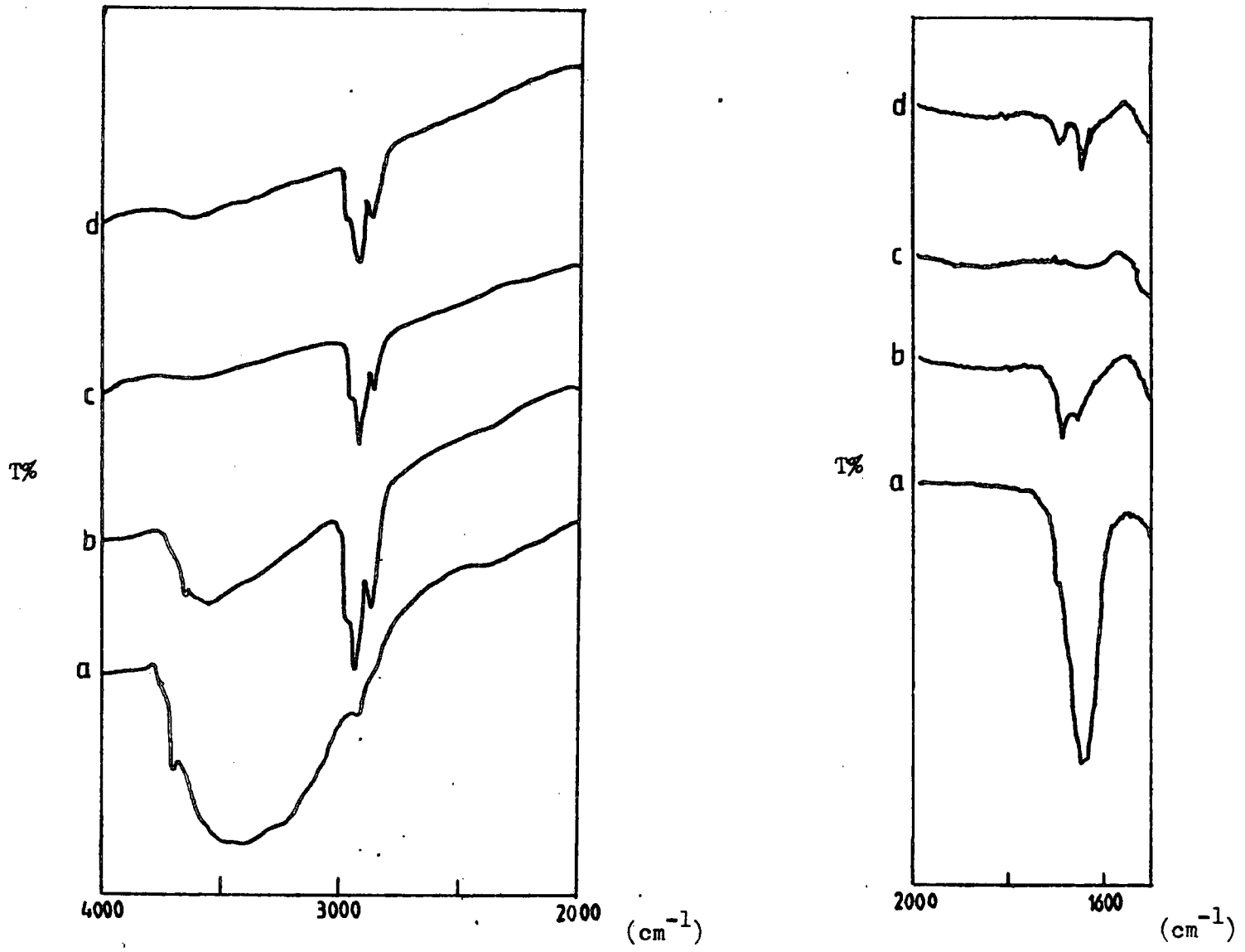

Fig.1 CaY zeolite at a.ambient temperature b.493K
c.623K d.303K

Also there is a strong band (Fig.1a) in the deformation region (1650cm^{-1}) due to water molecules, which disappears on heating (Fig.1b) and reappears on cooling. After cooling to RT we observe a band at 1695cm^{-1} which we assign to the ν_4 normal mode of a hydronium ion (Fig.1d). A detailed discussion of the vibrations of the hydronium ion will be given in chapter 5. Eisenbach et al did not report the change in position of the band around 3600cm^{-1} on heating. Also, on comparing the intensities (i.e. comparing the heights of the bands not their integrated intensities) of the two corresponding bands in Eisenbachs paper (Fig.2) and in ours (Fig.1), we can see that the band at 3640cm^{-1} is more intense than that at 3540cm^{-1} (RT) in Eisenbach et al's paper, and becomes stronger on heating to 575K. In our spectra, however, the bands at 3560-3440cm^{-1} are more intense than that at 3640cm^{-1} at room temperature (Fig.1b), but they all disappear on heating to 623K (Fig.1c). In our sample, therefore, all the bands due to the hydroxyl groups disappear on heating to 623K. This did not happen in the work of Eisenbach and Gallei. The difference in behaviour must stem from the different degree of ion exchange.

The band at 3640cm^{-1} (493K, Fig.1b) has previously been assigned to the hydroxyl stretching vibration in the supercages (17,18) and the band at 3540cm^{-1} to the hydroxyl groups in the cubooctahedra (15-19).

Eisenbach and Gallei found two other bands at, 3750 and 3585cm^{-1}, as shown in Fig.2a and 2b, which they assign to hydroxyl groups located on the external zeolite crystal surface, and the hydroxyl-stretching vibration of $Ca(OH)^+$

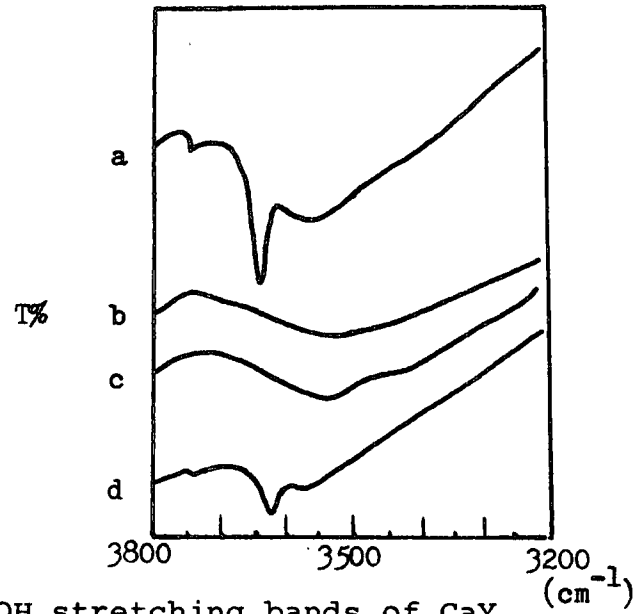

Fig.2a

OH stretching bands of CaY
a. before adsorption of hexene-1
b. after adsorption of hexene-1 in the presence of the gas phase
c. after pumping off the gas phase
d. after pumping off and heating to 570K (ref.1)

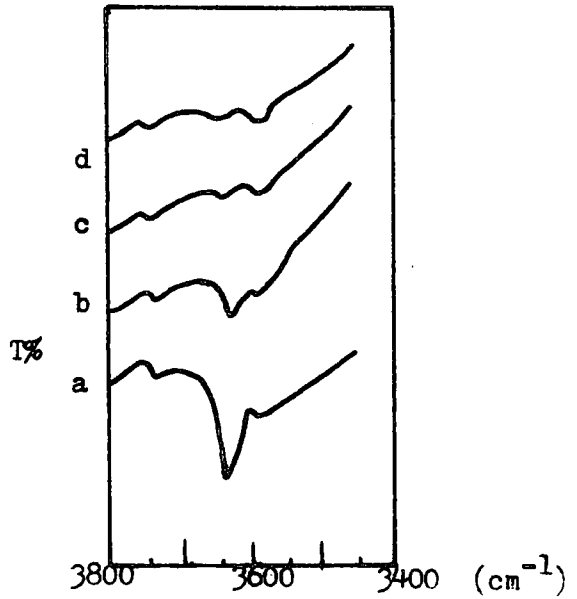

Fig.2b

OH stretching bands of Pt/CaY
a. before adsorption
b. after adsorption of n-hexane and 10 min. of reaction time
c. 22 hr. of reaction time
d. after 22 hr of reaction time followed by evacuation (ref.1)

groups, which are formed by a reaction between adsorbed water molecules and Ca^{2+} ions, respectively. Table 5 summarises our data together with that of Eisenbach et al. Also shown in Table 5, are the assignments of the observed bands (15,16).

Table 5: Infrared data (cm^{-1}) of the OH groups observed by Eisenbach et al, and by us

Eisenbach et al (1)	This work[a]		assignment (15,16)
	RT	493K	
3740	-	-	external
3640	3640	3640	supercages
3585	-	-	$Ca(OH)^+$
3540		3540	cubo-octahedra
	3560-3100		H_2O str.

a. at 623k all of the bands disappear

Several papers (15-19) have reported these four hydroxyl groups on elevated temperature for CaY zeolite and after dehydration at 743K the bands at 3738, 3640, 3585 and 3540cm^{-1} are still there. Some studies have also reported more than four bands due to OH groups. For NaY zeolite, three bands at 3735, 3635 and 3544cm^{-1} are observed (17). We have been unable to observe the bands assigned by Eisenbach and Gallei to OH groups on the surface of the zeolite and to $Ca(OH)^+$. This could be due to the concentration of these species being very low in our sample.

Eisenbach et al described the importance of each OH group in forming coke. The influence of the external hydroxyl groups ($3740cm^{-1}$) on coke formation is very low, below 773K and the $Ca(OH)^{+}$ ($3585cm^{-1}$) groups do not participate at all in the coking reaction. They observed that the highest activity for coking is associated with the hydroxyl groups in the supercages ($3640cm^{-1}$). This band decreases in intensity with increasing intensity of the band at $1585cm^{-1}$ which is due to coke. On the other hand, the band at $3540cm^{-1}$ (cubooctahedra OH) is much less changed in intensity.

In our experiment, it was not pssible to see the hydroxyl groups at 3740 and $3585cm^{-1}$ which Eisenbach et al saw at room temperature and on heating the sample, so it is impossible to predict the relation between the hydrocarbon molecules and these hydroxyl groups. These observations may be due to the difference in the degree of ion exchange.

2. Adsorption of the hydrocarbons on CaY zeolite at room temperature

On adsorbing hexene-1 and n-hexane separately on to different discs of CaY zeolite and evacuating for 10 minutes at room temperature several new bands are observed (Figs. 3 and 4). Tables 6 and 7 summarise the frequencies of the bands due to each adsorbed species and the frequencies of the bands in the spectra of the pure zeolite. Three of the bands due to adsorbed n-hexane occur at 2960, 2925 and $2865cm^{-1}$ and hexene-1 at 2956, 2925 and $2850cm^{-1}$ (Tables 6 and 7) which may be assigned to antisymmetric CH_3-, CH_2-stretching vibration and symmetric C-H vibrations respectively (19). The bands at 1465 and $1380cm^{-1}$ for n-hexane and

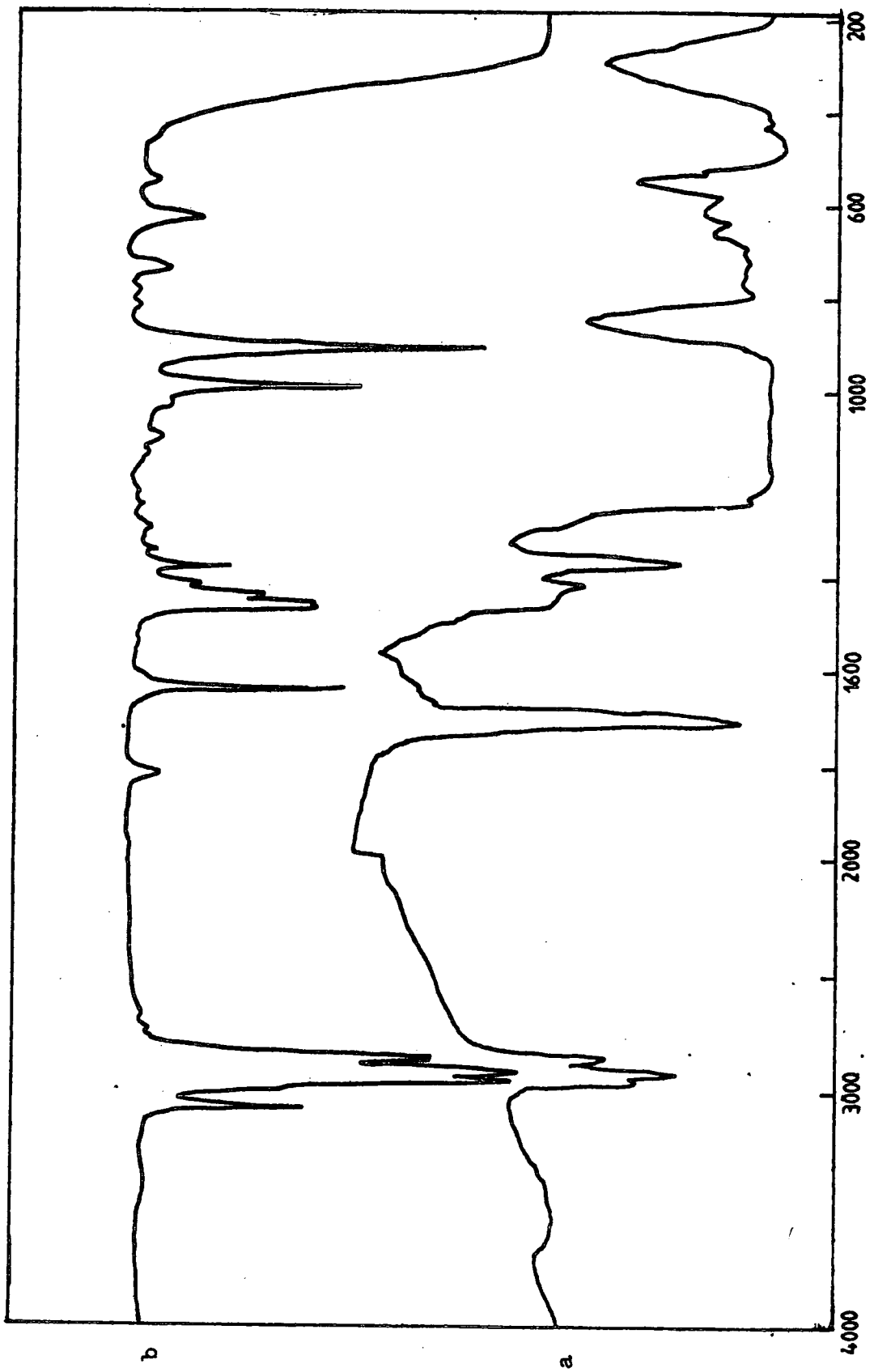

Fig-3 a.hexene-1 adsorbed on CaY zeolite at 293 K

b.hexene-1 liquid

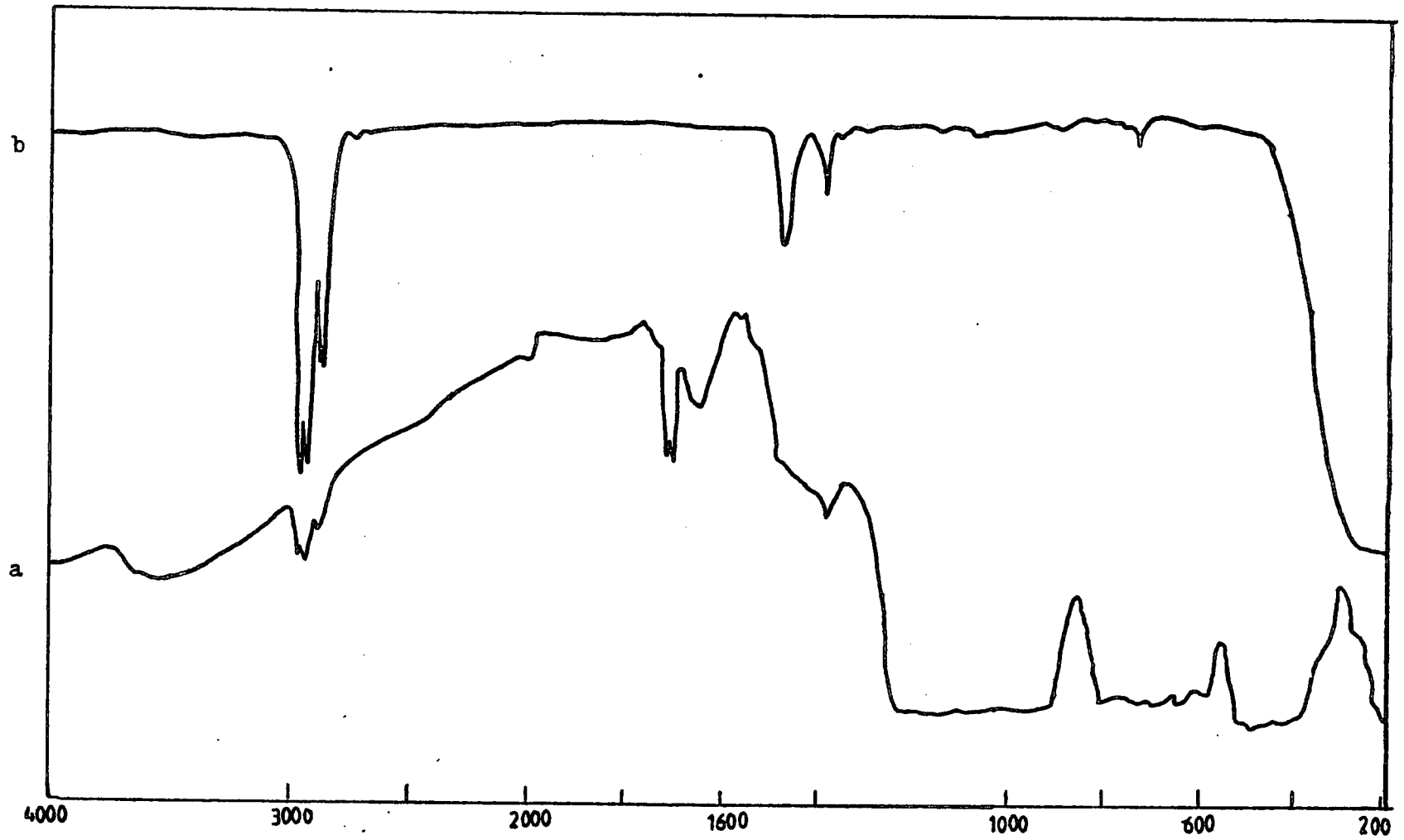

Fig -4 a.n-hexane adsorbed on CaY zeolite at 293 K
b.n-hexane liquid

Table 6: Infrared data for dehydrated CaY zeolite, CaY - n-hexane and n-hexane liquid (cm^{-1}) in the range 4000-1000cm^{-1} (this work).

CaY After baking at 573K	CaY n-hexane 10 mins evacuation	n-hexane	assignment
	2960	2955 s	$\nu_{as}(CH_3)$ (20)
	2925 s	2925 s	$\nu_{as}(CH_2)$ (20)
2910 s	-	-	instrument background
	2865 s	2870,2855 s	$\nu_s(CH)$ (20)
2825 m		-	instrument background
1685 m	1710,1695 s	-	$\nu_4(H_3O)^+$
1650 w		-	$\nu_2(H_2O)$
1470-1380 b	1470 Sh	-	zeolite structure
-	1430 w	1465 m	δ (CH_3) (20)
-	1380 m	1380 m	δ (CH_2) (20)

Table 7: Infrared data for dehydrated CaY zeolite, CaY-hexene-1, and hexene-1 Liquid (cm^{-1}) in the range 4000-1000cm^{-1} (this work).

CaY after baking at 573K	CaY-hexene-1 10 mins evacuation	hexene-1	assignment
-	-	3080 s	ν(H-C=C) (20)
-	2956 w	2960 s	$\nu_{as}(CH_3)$ (20)
-	2925 s	2925 s	$\nu_{as}(CH_2)$ (20)
2910 s	-	-	instrument background
-	2850 m	2880,2860 s	ν_s(CH) (20)
2825 m	-	-	instrument background
1685 m	1710 s	-	$\nu_4(H_3O^+)$
1650 w	-	-	$\nu_2(H_2O)$
-	-	1642 s	ν(C=C) (20)
1470-1380 b	1470 sh		zeolite structure
-	1450 w	1467,1458 s	$\delta(CH_3)$ (20)
-	-	1440,1415 m	$\delta(CH_2)$ (20)
-	1370 m	1380 m	$\delta(CH_2)$ (20)
-	1235 w	-	$\nu_2(H_3O^+)$

1450 and 1370cm^{-1} for hexene-1 are due to the CH_3 and CH_2 deformation modes (20). No absorption bands from olefinic species at 3080 and 1642cm^{-1} of hexene-1 adsorbed on to CaY were detected after 10 minutes evacuation (Table 7). This is in agreement with the data of Eisenbach and Gallei, who explained this by proposing a linear adsorbed hydrocarbon species formed by interaction of the strong acidic hydroxyl groups with the π electrons of hexene-1 according to the equation:

$$\nearrow O\text{-}H + CH_2 = CH(CH_2)_3\text{-}CH_3 \rightleftharpoons \nearrow O^{\ominus} + CH_2^{\oplus}\text{-}(CH_2)_4\text{-}CH_3 \quad (1)$$

In addition to the above results, we can see from Tables 6 and 7 that there are two bands at 1710 and 1240cm^{-1} which were not found in the work of Eisenbach and Gallei. A band at 1710cm^{-1} was observed with both hexene-1 and n-hexane but the band at 1240cm^{-1} was observed only for hexene-1 (Fig.3). The 1240cm^{-1} band could not be seen with n-hexane and this may be because:

1. There is a very intense absorption due to the framework in the region 1250-900cm^{-1} which may conceal the band expected at ca 1240cm^{-1} for n-hexane, or
2. If the bands at ca 1710 and 1240cm^{-1} are due to the same species then since the 1240cm^{-1} band is very much less intense than that at 1710, it will be more difficult to observe in the spectrum of adsorbed n-hexane than hexene-1, since the intensity of the 1710cm^{-1} band is very much less in the former (Fig.4) than in the latter case (Fig.3).

These two bands can be assigned to the hydronium ion which is present because there are some water molecules in the zeolite as was seen on cooling the sample (Fig.1d). In the case of hexene-1 these water molecules could interact with the proton released in the formation of the adsorbed species (equation 1), to form the hydronium ion. The band in the region of 3100-2800cm^{-1}, which is due to the hydronium ion, could not be seen because of the presence of three bands due to the instrument background in the same region. The presence of the hydronium ion in zeolites will be discussed in more detail later (chapter 5).

3. The effect of temperature on adsorbed hydrocarbons

The adsorption of the hydrocarbons on CaY zeolite at room temperature followed by heating to higher temperature in the presence of the gas phase causes dramatic changes to be observed in the infrared spectra as a function of temperature. Since excess hexene-1 is present, the spectra shown in Fig.5 are a mixture of gas phase and adsorbed species. Fig.5 shows that as the temperature is increased hexene-1 loses its double bond character as evidenced by the absence of an absorption band near 3080cm^{-1} due to ν (H-$\overset{H}{\overset{|}{C}}$ = C). The spectra show that the gas phase hexene is reacting with the zeolite and being consumed. New bands at 1580 and 1340cm^{-1} appear at high temperature. These two bands become more intense as the band due to ν(H-$\overset{H}{\overset{|}{C}}$ = C) decreases in intensity and as the temperature is increased (Fig.5). The band at 1340cm^{-1} is assigned to a vibration of tertiary C-H groups (20).

4. Coke formation

When either hexene-1 or n-hexane is added to CaY zeolite at room temperature and the sample heated, a new band appears at 1580cm^{-1}. From Figs. 5 and 6 we can see that the intensity of this band increases with increasing temperature.

Infrared studies by Unger and Gallei (21) of activated carbon and soot samples show a band at 1585cm^{-1} which was assigned to the C=C stretching vibration of microcrystalline graphatic carbon structures, which are present in polycyclic aromatic compounds.

The coke formation at higher temperatures can be seen only if the gas phase is present over the zeolite surface. Also coke formation will be effected by the type of hydrocarbon which is in contact with the zeolite surface. When we compare the two hydrocarbons, hexene-1 and n-hexane it can be seen that hexene-1 can form coke faster than n-hexane (Fig.6), and confirms the observations of Eisenbach and Gallei. The band due to coke is very much stronger in the case of hexene-1 than for n-hexane (Fig.6), indicating that coke is formed much more easily from the unsaturated hydrocarbon. Radioactive tracer studies conducted by Hightower and Emmett (22) have indicated that the olefins have the highest ability to form coke. Also it was found (2) that the saturated hydrocarbons are very much less reactive than their corresponding olefins.

Eisenbach and Gallei have assumed that the hydroxyl groups react with adsorbed hydrocarbon species producing coke and thereby are consumed irreversibly. We can see,

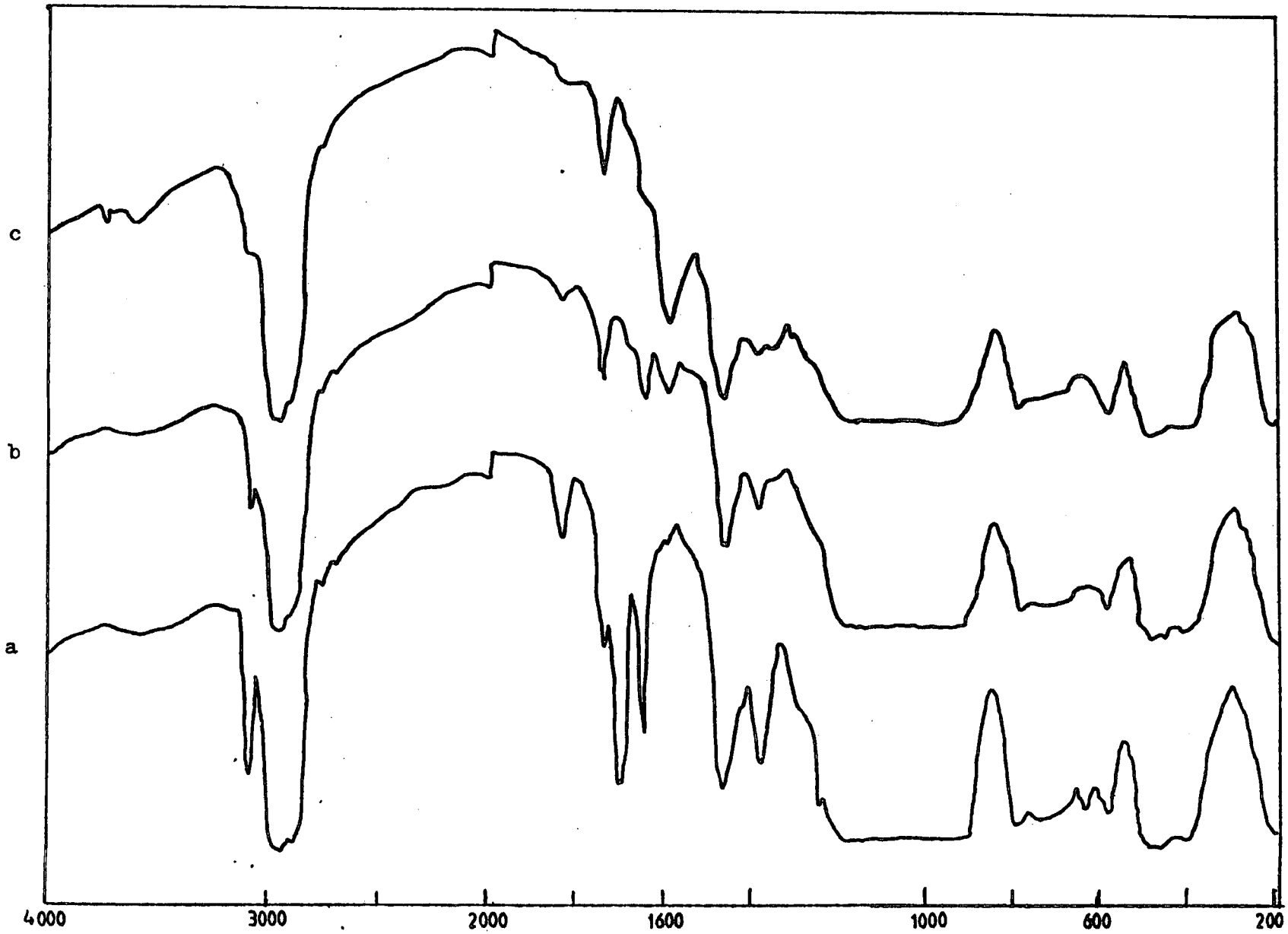

Fig-5 CaY zeolite-hexene-1 a.at 293 K
b.at 453 K
c.at 573 K

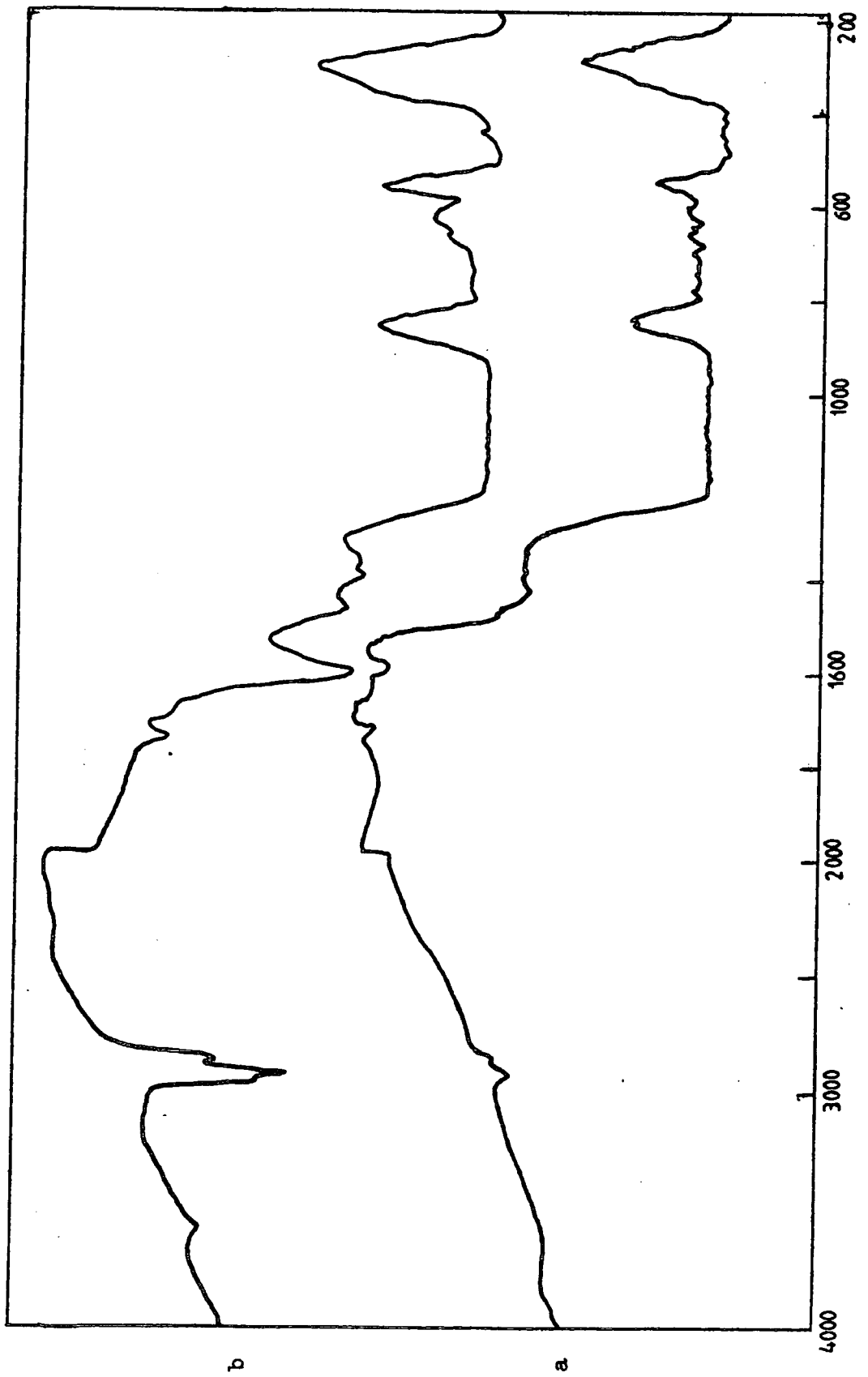

Fig -6 a. n-hexane adsorbed on CaY zeolite at 573 K

b. hexene-1 adsorbed on CaY zeolite at 573 K

(Fig. 5) that we have observed two new bands at 3740 and 3600cm^{-1} which appeared when CaY zeolite was heated with hexene-1 at 550K. Since these hydroxyl groups appear to be formed only on the breakdown of the hexene-1 the group giving a band at 3740cm^{-1} is unlikely to be the same as that observed by Eisenbach and Gallei at room temperature at the same frequency.

c. Conclusion

Several of our observations are in agreement with those of Eisenbach and Gallei:

1. The appearance of a "coke-band" for both hexene-1 and n-hexane adsorbed on CaY zeolite.
2. The unsaturated hydrocarbon forms coke more readily than the saturated one.
3. There are several bands due to the species adsorbed at room temperature.
4. In the case of hexene-1 the adsorbed species does not have any olefinic character.
5. We observe bands due to O-H groups at 3640 and 3540cm^{-1}.

In some ways, however, our results differ from theirs:

1. We observe bands due only to two types of hydroxyl groups while Eisenbach and Gallei observe four at RT.
2. At high temperature we could not observe any bands due to hydroxyl groups and so could not correlate coking activity with a particular hydroxyl site as Eisenbach and Gallei were able to do.
3. Two new hydroxyl bands appear at high temperature in the case of hexene-1.

References

1. Eisenbach,D. and Gallei,E., J.Catal. 56, 377 (1979).

2. Montes, A., Perot-Gand Guisret, React.Kinet.Catal. lett. 13(1), 77 (1980).

3. Levinter, M.E., Panchenkov, G.M., and Tanatrov, M.A., International Chem.Eng. 7(1), 23 (1967).

4. Butt, J.B., Delgado-Diaz, S., Muno, W.E. J.Catal. 37, 158 (1975).

5. Gupta, K., Kunzru, D., and Saraf, D.W., J.Chem. Eng. data, 25, 14 (1980).

6. Zhavoronkov, M.N., Neft Khimiya, 20(1), 146 (1980).

7. Bulow, M., Struve, P., Finger, G., Redszns, C., Ehrtard, E., and Schimer, W., J.C.S. Faraday I, 76, 597 (1980).

8. Butt, J.B., Advan.Chem.Ser., 109,259 (1972).

9. Karmarkar, K.H., and Natu, G.N., Spectrochimica.Acta, 30A, 547 (1974).

10. Appleby, W.G., Gibson, J.W., and Good, G.M., Ind. Eng. Chem.Process Des.Develop., 1, 102 (1962).

11. Gallei, E. Privet communication

12. Breck, D.W., Zeolite molecular Sieves, Wiley, London, (1974).

13. Uytterhoven, J.B., Christner, L., and Keith, H.W., J.Phys.Chem., 69 (6), 2117 (1965).

14. Ward, J.W., J.Phys.Chem., 72 (12), 4211 (1968).

15. Angell, C.L., and Schaffer, P.C., J.Phys.Chem. 69, 10 (1965).

16. Gallei, E., and Eisenbach, D., J.Catal, 37, 474 (1975).

17. Datka, J., J.C.S. Faraday I, 76, 705 (1980).

18. Jacobs, P.A., and Uytterhoven, J.B., J.C.S.Chem. Commun. 373 (1972).

19. Rabo, J.A., Zeolite Chem. and Catal. No.171, Amer.Chem.Soc., Washington, D.C. (1976).

20. Silverstein, R.M., Bassler, C.G., and Morril, T.C., Spectrometric identification of organic compounds, Wiley, London (1974).

21. Unger, K., and Gallei, E., Erdel Kohle. Erdgas petrochem. 29 (9),409 (1976).

22. Hightower, J.W., and Emmett, P.H., J.Am.Chem.Soc. 87 (5),939 (1965).

CHAPTER 5

INFRARED STUDIES OF WATER ADSORBED ON PARTIALLY MANGANESE OR COBALT EXCHANGED ZEOLITES

1. Introduction

Most spectroscopic studies of adsorption on zeolites so far reported discuss the spectra of water molecules and hydroxyl groups (1-22). The infrared spectra of water adsorbed on several synthetic zeolites has been studied by a number of experimentalists (19-23). Of particular relevance to this work the influence of dehydration and adsorption of water on

1. the coordination of the cations,
2. the state of the adsorbed water,
3. the stretching vibrations of the water molecule,

in CoNaA and NaA zeolite has been investigated by means of electronic and infrared spectroscopy (16).

The presence of the hydronium ions which compensate for cation deficiencies in zeolites has been discussed (24) and the bands corresponding to the normal modes of the hydronium ion reported (25). The existence of the hydronium ion as a discrete chemical entity has been known since the early 1920s. From nuclear magnetic resonance studies Richards and Smith (25) were able to measure H-H separations ($\sim 1.72\text{Å}$) in the hydronium ion in $H_3O^+ClO_4^-$. They concluded that the hydronium ion was a nearly flat pyramidal species with O-H bond lengths of $\sim 1.02\text{Å}$ and H-O-H angles of 115^o

(26-30). Neutron diffraction studies indicated a pyramidal C_{3v} symmetry for the hydronium ions with O-H bond length of $\sim$0.98Å and H-O-H angle of 111°. A spectroscopic study and normal coordinate analysis of the H_3O^+ and D_3O^+ species in solid $H_3O^+CH_3C_6H_4SO_3^-$ were made (30).

In Chapter 2, a general account of the structure of A type zeolites was given. A more detailed account of the Mn-4A and Co-4A zeolites structures will be given in this chapter.

a. Structure of partially exchanged Mn-4A zeolite.

1. Dehydrated

An X-ray study of dehydrated partially Mn-exchanged A zeolite (31-33) revealed a total of 4.5 Mn(II) and 3 Na^+ ions per supercage and these were located near the centres of 6-rings. The Mn(II) ions are recessed 0.108Å into the sodalite unit from the plane of three oxygens O(3) (Fig.1a,b). The Na^+ ions are 0.46Å from the corresponding plane but are recessed into the large cavity. Both Mn(II) and Na^+ ions are trigonally coordinated to respective sets of three framework O(3)'s at 2.11 and 2.16Å respectively.

2. Hydrated

In hydrated MnA, each of the 4.5 Mn(II) ions lies in a 6-ring where the two Mn(II)-OH_2 distance are 2.03 and 2.06Å for $H_2O(1)$ and $H_2O(2)$ (Fig.2a,b). The three symmetry-equivalent Mn(II) to framework O(3) distances are 2.28Å. These complete a slightly distorted bipyramid with Mn displaced 0.2Å into the larger cage from the plane of the O(3) ions.

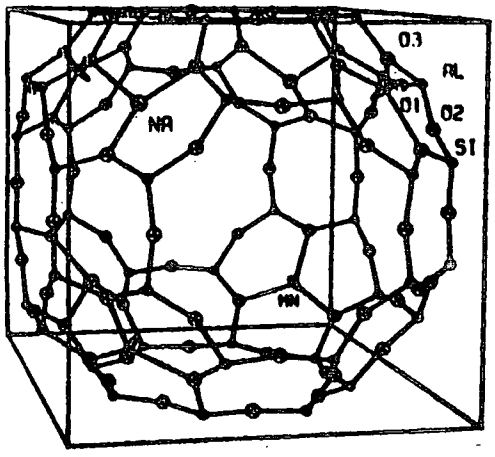

DEHYDRATED $MN_{4.5}NA_3$-ZEOLITE A

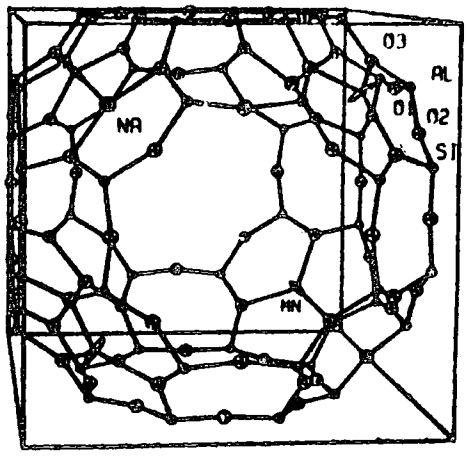

DEHYDRATED $MN_{4.5}NA_3$-ZEOLITE A

Fig.1a

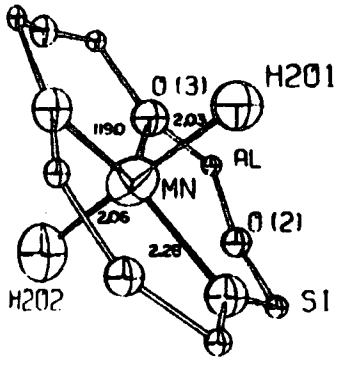

Fig.2a

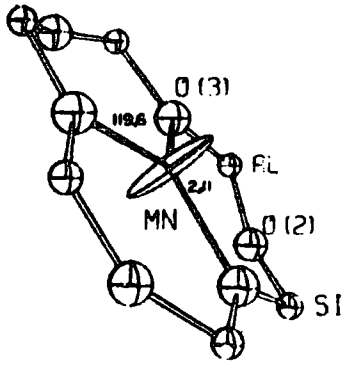

Fig.1b

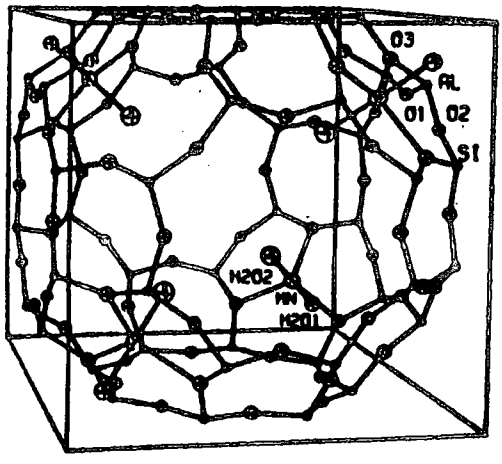

HYDRATED $MN_{4.5}NA_3$-ZEOLITE A

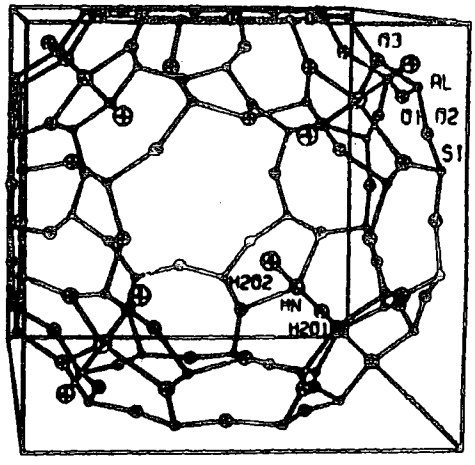

HYDRATED $MN_{4.5}NA_3$-ZEOLITE A

Fig.2b

b. Structure of partially exchanged Co-A zeolite

1. Dehydrated

Dehydrated partially Co-exchanged A zeolite (34,35) has a structure similar to the manganese form with the Co(II) ions occupying threefold axis sites near the 6-ring oxygen windows, but recessed by 0.16Å into the sodalite cavity (Fig.3). Each Co(II) is 2.08Å from three equivalent O(3) ions arranged trigonally in the six-oxygen ring, and 4 Na^+ ions are at 2.12Å from the O(3) ions.

2. Hydrated

Amaro et al (35) have reported data for hydrated Co_4-Na_4-A zeolite. One Co(II) ion lies at the centre of the sodalite cage where it is surrounded by 6 water molecules (Co-OH_2=2.11Å) each hydrogen-bonded to two framework oxygens. Three Co(II) ions lie on or near a triad axis displaced 1.6Å into the larger cage from the plane of a 6-ring (Fig.4). The distance to the nearest framework oxygens is 2.7Å. Each Co(II) is tetrahedrally coordinated to one $H_2O(2)$ and three oxygens (36).

2. Experimental

Materials

Partially exchanged Mn-4A and Co-4A zeolites were prepared from NaA zeolite (BDH Chemicals Ltd) by ion exchange with 0.1N $MnSO_4$ and $Co(NO_3)_2$ (BDH analar grade) solutions respectively following the method described by Seff (37). Two additional different Mn concentrations were used to obtain different degrees of ion exchange as shown in Table 1.

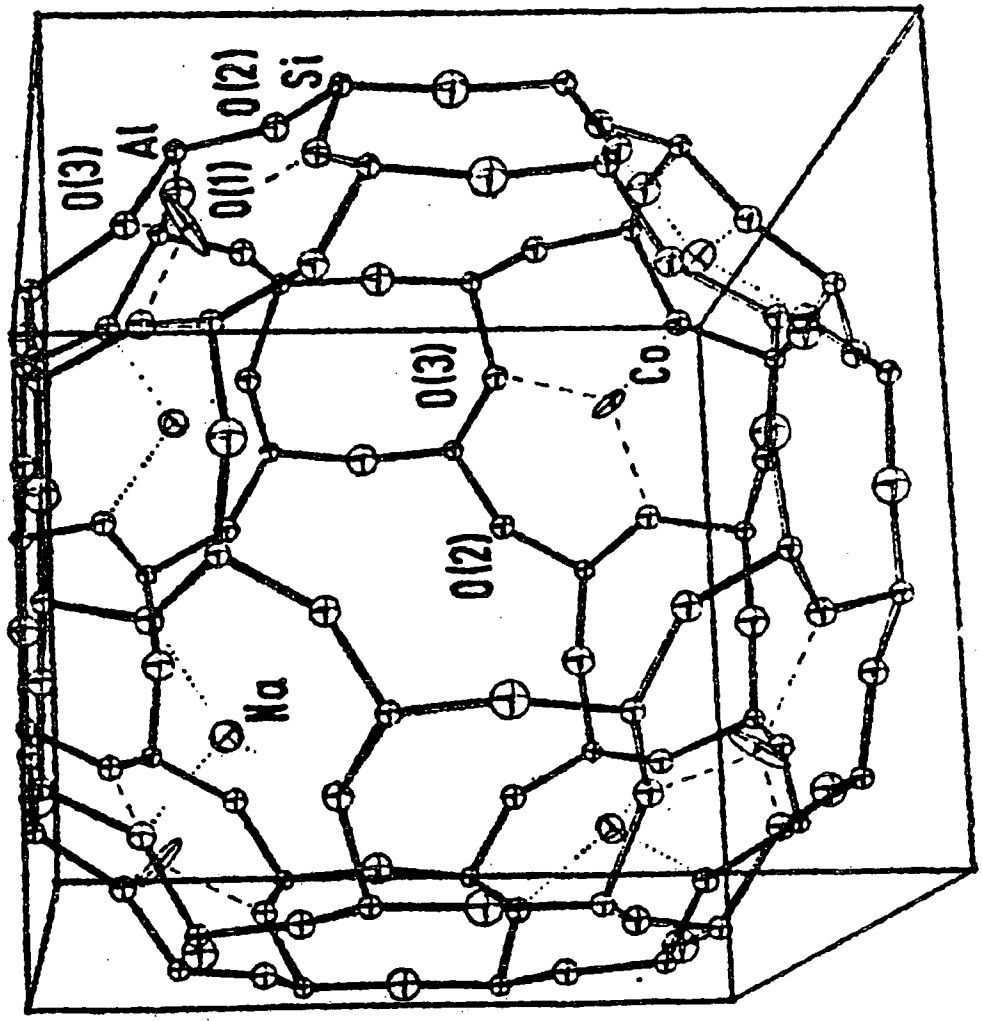

Fig.3 Co-A zeolite fully dehydrated

Thermogravometric analysis of each Mn-4A and Co-4A zeolites were obtained.

Procedure

Self supporting discs were evacuated in the infrared cell, then heated under vacuum to 533K and cooled to the desired temperature. Water was admitted to the cell, the sample cooled to room temperature and evacuated then heated to 533K. Spectra were obtained at all stages.

The exchange of D_2O for H_2O

Exchange of D_2O for H_2O in Mn-4A zeolite (which had previously been dried at 323K for one day) was attempted using several different methods.

1.2g of Mn-4A zeolite was dispersed in 10 mls of D_2O and stirred at room temperature for one week. The sample was dried under vacuum. A similar procedure was used involving 30 ml of D_2O with 1g of Mn-4A zeolite but in this case the temperature of the sample was increased to 363K in a nitrogen atmosphere for 5 days.

2. In the second method 1g of Mn-4A zeolite was heated under vacuum over a period of 17 hours, to 673K. The sample was then cooled slowly to 573K when D_2O was admitted and the sample cooled to room temperature.

3. In the third method a Carius tube was used with 20 ml of D_2O and 1g of Mn-4A zeolite. The tube was evacuated and sealed then left in a furnace for two days at 473K, the sample was dried under vacuum.

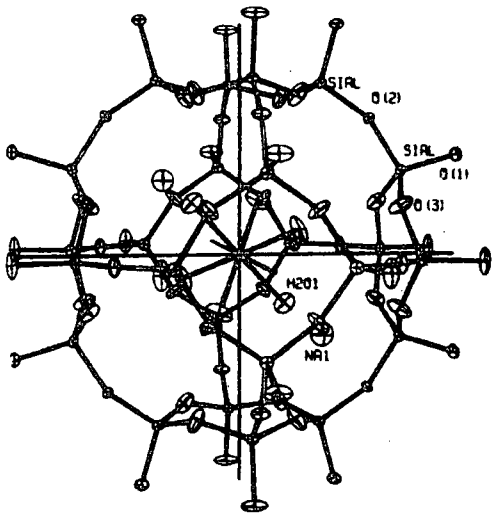

HEXAAQUO CO(II) SODALITE CAGE

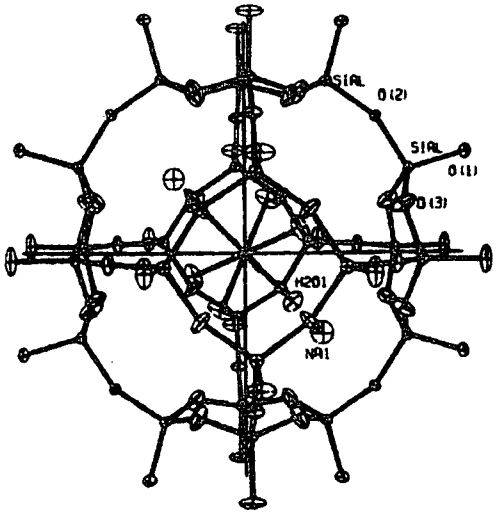

HEXAAQUO CO(II) SODALITE CAGE

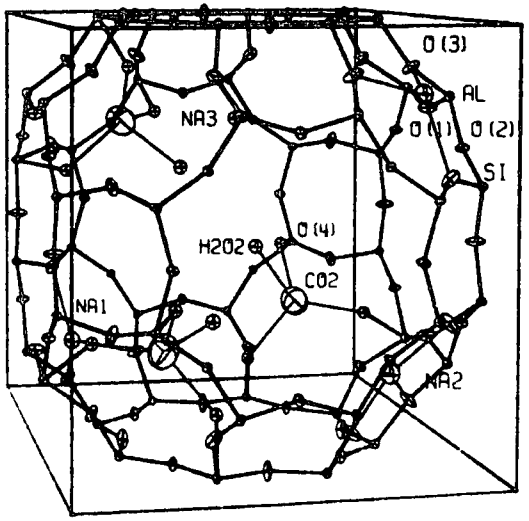

$(CO)_4$-A (HYDRATED) LARGE CAGE

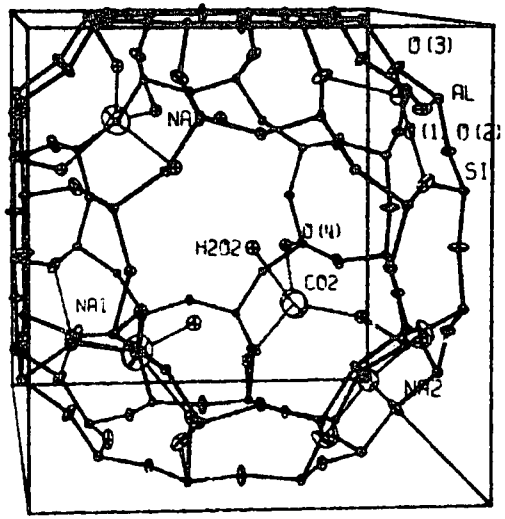

$(CO)_4$-A (HYDRATED) LARGE CAGE

Fig.4

Table 1: Chemical analysis of the Mn-4A and Co-4A zeolites (% by weight)

	N[a]	Al	Na	Mn	Co	Ion ratios	
						Mn(II)/Na(I)	Co(II)Na(I)
Mn-4A	0.03	12.6	6.65	2.95	-	1.061	-
Mn-4A	0.07	14.79	4.37	7.71	-	4.219	-
Mn-4A	0.1	12.77	3.44	7.41	-	5.151	-
Co-4A	0.1	12.9	0.75	-	15.55	-	53.185

a.normality

4. A disc of ~10mg of Mn-4A zeolite was inserted in an infrared cell then heated under vacuum to 553K. The sample was cooled to 473K and D_2O inserted, then it was cooled to room temperature. Spectra were obtained at all stages.

3. Results and discussion:

The spectrum of Mn-4A zeolite (Mn(II)/Na^+ ratio = 5.15) before heating (Fig.5) shows a band at 1355cm^{-1}. This band disappears on heating (Fig.5c). To determine whether or not this band was associated with the water molecules, it was decided to exchange D_2O for H_2O since if the band was due to water it should shift to lower frequency on adsorption of D_2O.

a. Ion and molecular exchange

(1) D_2O exchange

From Fig.6 we can see that it is difficult to exchange the H_2O molecules inside the zeolite. None of the first three methods gave any sign of the presence of D_2O exchange except for a small band which occurred after using the Carius tube method (Fig.6b). The spectra do not show any sign of the bands (2600 and 1210cm^{-1}) which are characteristic of D_2O. In the spectrum of Mn-4A-H_2O we can see that there are two bands which can be easily assigned to vibrations of the H_2O molecules. The first at 3500cm^{-1} which is very broad, and the second is at 1650cm^{-1}. On exchanging D_2O for H_2O it is expected that these two bands will shift to lower frequency and occur at ~ 2600 and

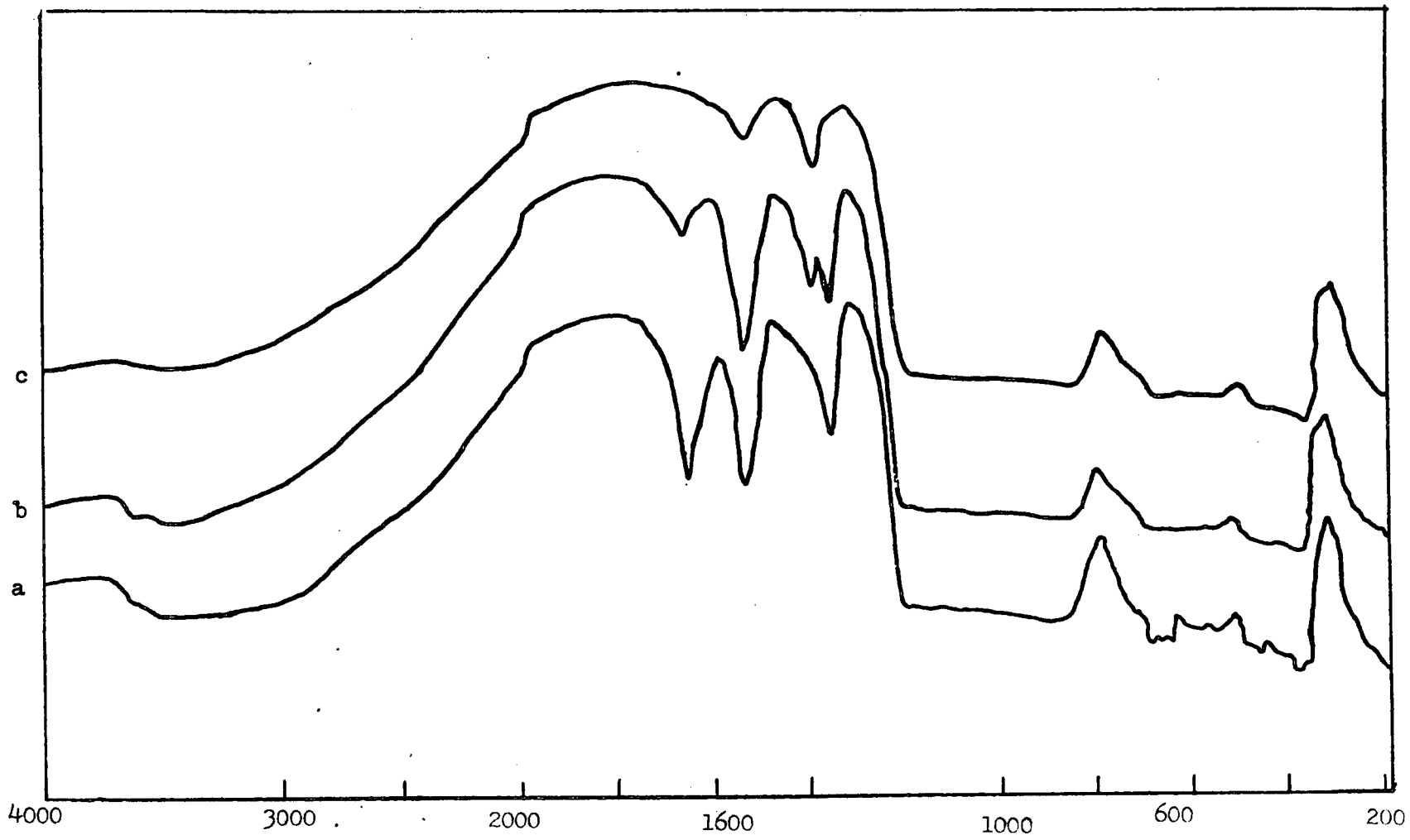

Fig.5 Mn-4A zeolite at a.293 K
b.348 K
c.473 K

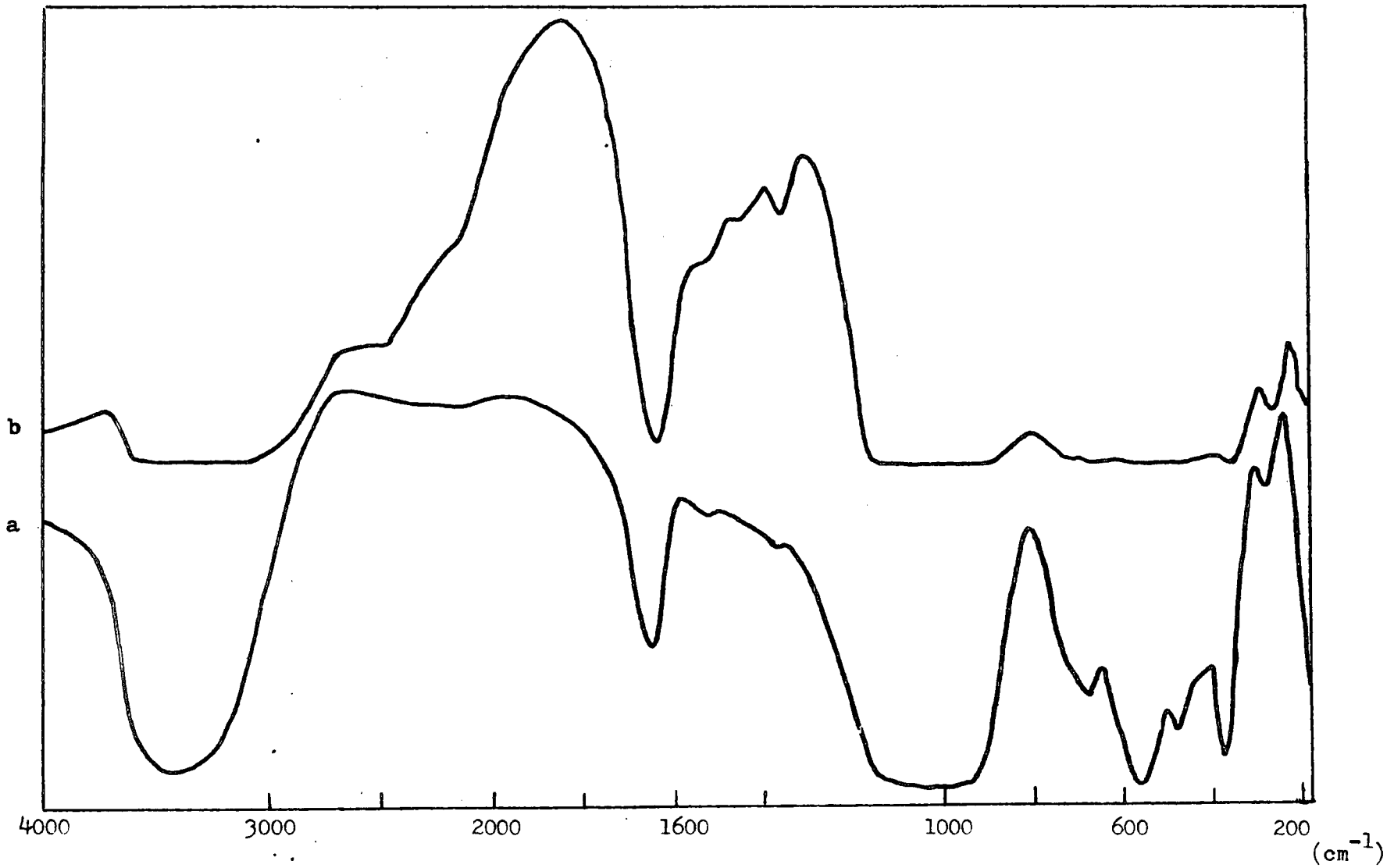

Fig.6 Mn-4A zeolite-D_2O a.with KBr.
b.self supported disc

1210cm^{-1} respectively. In Fig.6a, however, we can see only those bands due to H_2O molecules and there is no sign of the bands one would expect if D_2O had been exchanged for H_2O in the cages. In Fig.6b, while the bands due to H_2O dominate the spectrum there is a weak band at 2600cm^{-1} which is due to D_2O. Therefore even under the stringent conditions of the Carius tube experiment, only a small degree of exchange has occurred. These results are indicative of the difficulties of exchanging H_2O for D_2O.

When the experiments were first attempted, it was expected that the replacement of H_2O by D_2O molecules would be relatively easy because the water molecules are regarded as being mobile within the framework. Several studies (20,21) on D_2O exchange in zeolite, by adsorption of D_2O on a dehydrated zeolite disc which gives bands due to the D_2O molecules have been reported. Our experiments using this technique were also successful (see later discussion).

This difficulty of exchanging the H_2O molecules inside the zeolite is rather surprising, and it may mean that the D_2O is not able to enter the same sites as the H_2O in a hydrated framework. It was found (22) that surface OH groups in Na and NH_4 X zeolite do not exchange rapidly with the physically sorbed deuterium oxide. So Lynch et al (22) saturated the zeolite with the heavy water and both the OH and OD frequencies were observed. No further experimental details were given.

Since type A zeolites have smaller pores than X zeolites, it will be expected that if zeolite X does not exchange rapidly with deuterium oxide (22), we can expect that A zeolite be even more difficult.

(2) Ion exchange

We will discuss here the spectral region 1600-1300cm^{-1}. This region contains at low degree of exchange (Mn(II)/Na^+ ratio = 1.06) one broad band at 1440-1350cm^{-1} (Fig.7a) at room temperature. This band does not change its position on heating. On comparing this spectrum with that of NaA zeolite, we can see that there is a band at 1425cm^{-1} (Table 2) in the later case. Table 2 shows also that there is a band at 1355cm^{-1} which is present in zeolites which have a high degree of Mn exchange (Mn(II)/Na^+ratio = 5.15) and could be due to the presence of Mn ions. From these two observations there is no alternative but to assign the broad band at 1440-1350cm^{-1} observed in the sample with low degree of exchange, to two vibrations associated with the presence of two types of cations (Mn(II) and Na^+).

Table 2: Infrared data (cm^{-1}) of Mn-4A zeolite at different degree of exchange and of NaA zeolite (1600-1300cm^{-1})

temperature (K)	Mn-4A zeolite Mn(II)/Na^+ ratio = 1.06	Mn-4A zeolite Mn(II)/Na^+ ratio = 5.15			NaA zeolite	
R.T.	1440-1350s-b	1355 s	1395 w-sh	1540 s	1375 m	1595-1565 w-b
573	1440-1350s-b		1395 s	1540 s	1425 w	1590-1550 w-b

s-stronge
b-broad
m.medium
w.weak

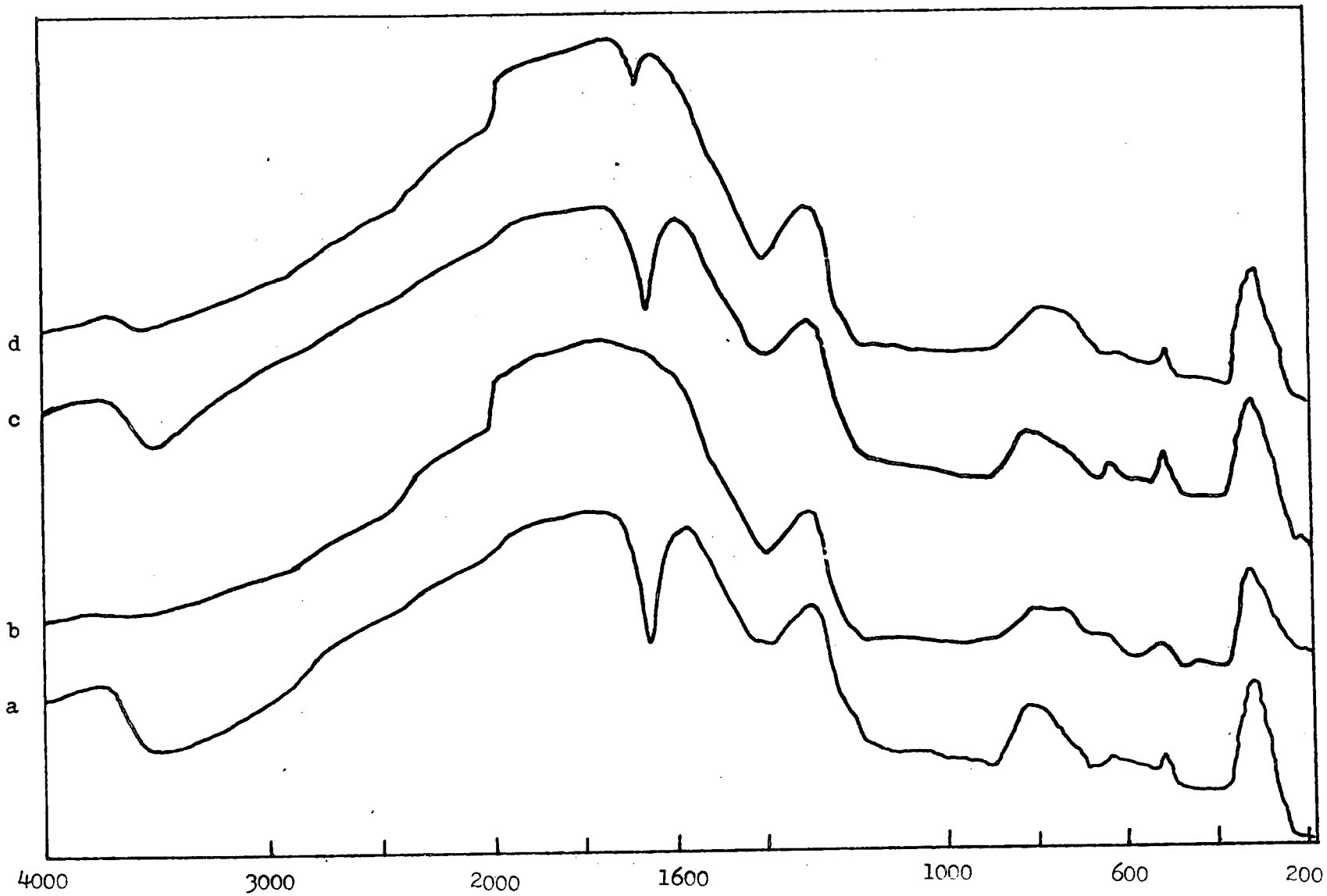

Fig.7 $Mn_{1.06}$-4A zeolite. a.at 293K
b.at 573K
c.after adding H_2O at 473K
d.after adding H_2O at 573K

Riley and Seff (32,33 and 38) have suggested that dehydrating Mn-4A zeolite ($Mn(II)/Na^+$ ratio = 1.5) causes the Mn ions to move from a position slightly inside the sodalite unit to one slightly inside the large cage. They therefore found two sites, one site present on the hydrated form and the other on the dehydrated. In our spectra, however, we could not see any change in the position of the band at 1440-1350cm^{-1} on heating.

At higher degree of Mn-exchange ($Mn(II)/Na^+$ ratio = 5.15) it can be seen that a strong band appears at 1355cm^{-1} immediately after recording the spectrum (Fig.5a); also a weak band at 1395cm^{-1} appears after evacuation for one night. This implies that the Mn ions occupy a site at room temperature which is associated with the presence of the strong band at 1355cm^{-1}. At the same time if we look to the spectra we can see that with NaA zeolite there is a band at 1425cm^{-1} which is due to the presence of Na ions. MnA zeolite with low degree of exchange shows a broad band at 1440-1350cm^{-1} which is assigned to two vibrations, each one associated with the presence of the Na^+ ions, and Mn ions. The MnA zeolite spectrum of the high degree of exchange sample has a strong band at 1355cm^{-1} assigned to vibration associated with the presence of Mn ions and a weak band at 1395cm^{-1} associated with the presence of Na ions. The observed change in relative intensity of the bands associated with the Na^+ and Mn(II) ions is in agreement with the alteration in the degree of exchange. This can be explained by the movement of Mn(II) ions from one site to a different one. The Mn ions, when they move coincidentially, have the same frequency as that associated

with the Na ions ($1395cm^{-1}$). This band will therefore coincide with the small band which is due to the presence of Na^+ ions. From these facts one can assign the two bands at 1355 and $1395cm^{-1}$ to the Mn ions in different sites which are present at different temperatures.

A band at $1535cm^{-1}$ has been observed at room temperature with high Mn exchange and does not appear with low degree of exchange (Fig.5). This band does not change on heating which implies that a totally different site has been occupied with Mn ions when a high degree of Mn has been exchanged.

From the above one can conclude that at high degree of exchange the Mn ions will occupy two sites at room temperature and two sites at high temperature.

b. The hydroxyl groups

Bands at 3740 and $3640cm^{-1}$ were observed in the spectra of Co-4A and Mn-4A(Mn(II)/Na^+ ratio = 5.15) zeolites (Figs. 5 and 8) respectively. The weak band at $3740cm^{-1}$ observed at 348K in Co-4A zeolite is still present at 548K while the band observed at $3640cm^{-1}$ in Mn-4A zeolite disappears at 423K. . These two bands have been observed in several studies (39-41), with a variety of cations in A, X and Y zeolites. The band at $3740cm^{-1}$ has been assigned to the Si-OH groups which terminate the external surface and this corresponds with the observations for CaY zeolite (40). The band at $3640cm^{-1}$ has been assigned to interaction of the hydroxyl groups with the cations, since this band has been observed to shift with different cations (39).

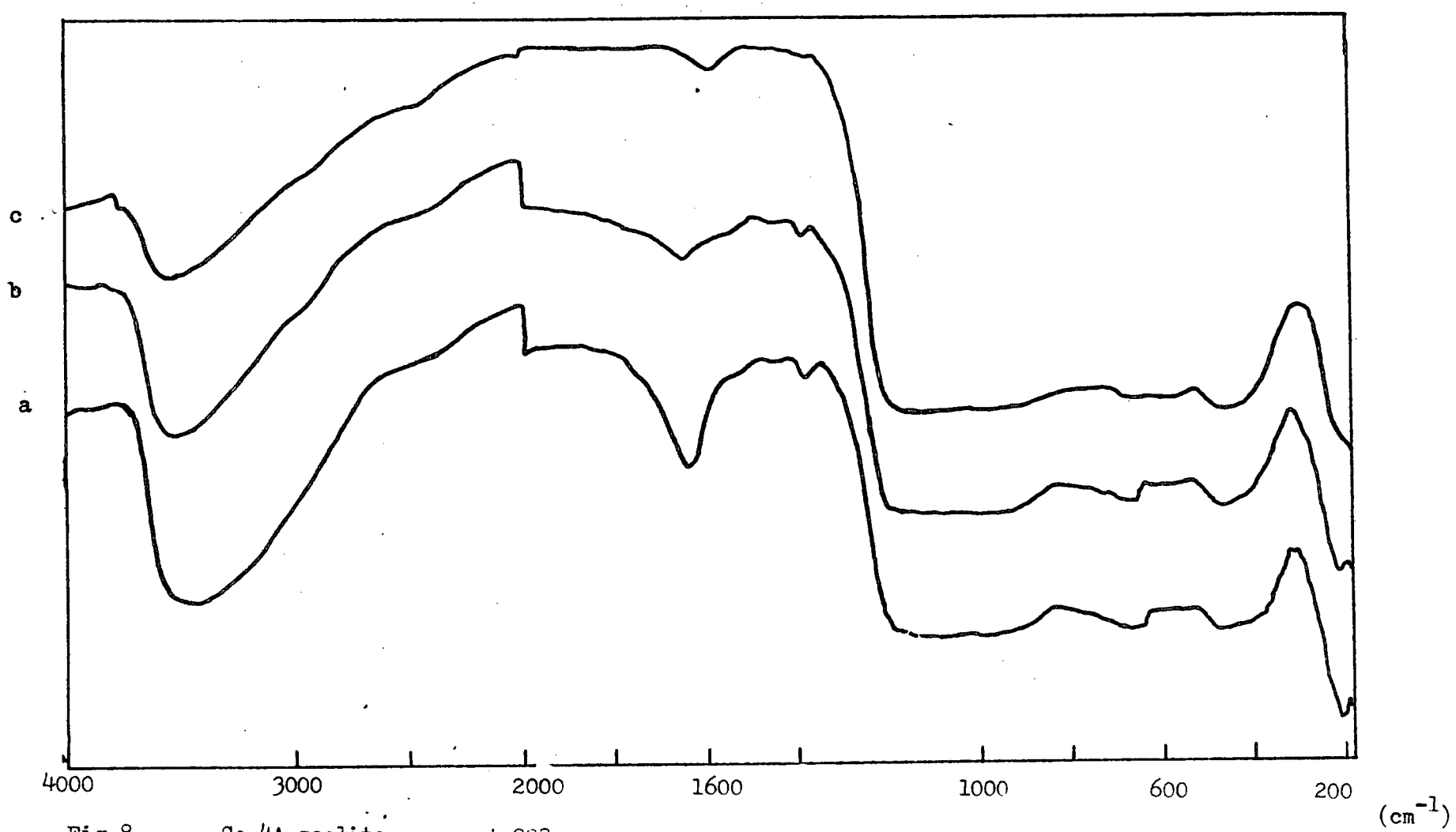

Fig.8 Co-4A zeolite a.at 293K
b.at463K
c.at 548K

The broad band at 3700-3300cm^{-1} (Fig.8) can be assigned to water molecules which might form a hydrogen bond with a lattice oxygen and this may be the reason for the non-disappearance of this band even when heated to 558K. From the TGA (Fig.9) of Mn-4A zeolite (Mn(II)/Na^+ ratio = 5.15) and Co-4A zeolite, there is a big step at around 413K which is due to the loss of water molecules. With increasing temperature there is a continuous loss of the water molecules until 673K. The water being lost is that which gives rise to the band at 3600-3300cm^{-1}.

Strong absorption bands at 1655 and 1645cm^{-1} were observed in the spectra of Mn-4A and Co-4A zeolites respectively (Figs.5a and 8) and these are completely removed after evacuation of these zeolites at approximately 473K. These bands are due to deformation vibrations of the water molecules (39,40); and arise from those molecules which do not form a hydrogen bond and which are therefore probably interacting with the cation via the oxygen atom.

c. <u>The presence of the hydronium ion</u>

On adding water to the Mn-4A zeolite (Mn(II)/Na^+ ratio = 5.15) at approximately 403K and then cooling, a broad band at 3700-3000cm^{-1} was observed (Fig.10). This is due to the presence of excess water molecules. As expected from this, the band at 1655cm^{-1} can also be observed. These observations correspond with those already reported for adsorbed water (40). There is however a new band at 1685cm^{-1} (Fig.10) which only appears when water vapour is admitted to a hot zeolite. Table 3 summarises our results for Mn-4A zeolite

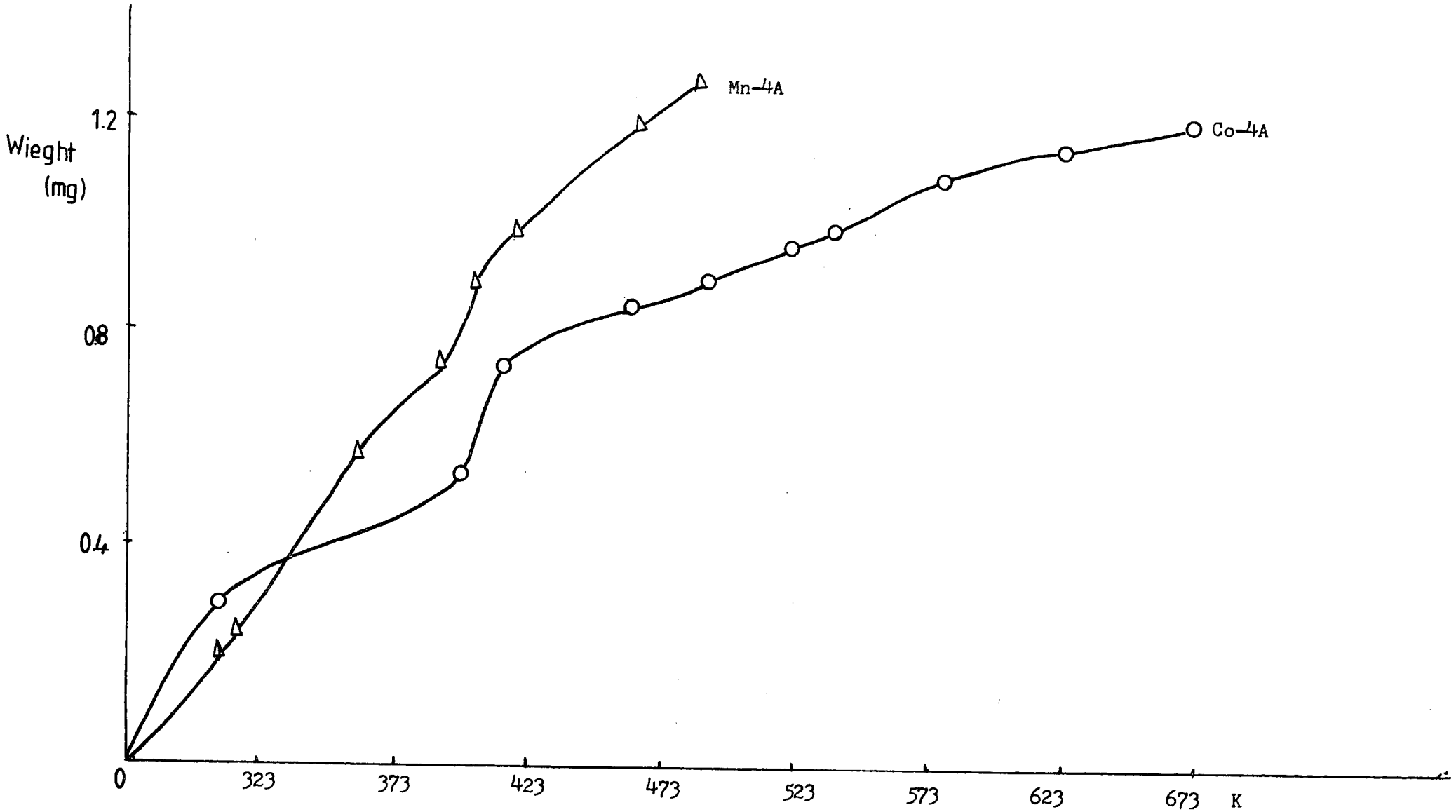

Fig.9 thermogravometric analysis of Co-4A and Mn-4A zeolite

before and after adding water vapour.

Table 3: Infrared data (cm^{-1}) for Mn-4A (Mn(II)/Na+ ratio = 5.15) zeolite and of adsorbed water in the range 4000-1000cm^{-1}.

before adding water		after adding water at 403K		assignment
293K	533K	403K	293K	
3700-3000b-m	3600-3400b-w	3600-3300b-m	3600-2900b-m	ν_1, ν_3 (OH)
-	-	1685 s	1695 s	ν_4 (H_3O^+)
1655 s	-	1655 sh	1645 s	ν_2 (H_2O)
1535 s	1540 s	1555 m	1520 sh	zeolite structure
-	1395 s	1420 sh	1420 sh	zeolite structure
1355 s	-	1365 s	1370 s	zeolite structure
-	-	1245 m	1230 m	ν_2 (H_3O^+)

As the zeolite was heated, the water band at 1655cm^{-1} disappeared while the band at 1685cm^{-1} remained (Fig.11). A band at 1230cm^{-1} also appeared upon adding water vapour to the hot zeolite and became more intense at room temperature (Fig.10). On heating the sample to 573K the band at 1230cm^{-1} slowly disappeared also (Fig.11). At the same time the sharp band at 1685cm^{-1} decreases slightly in its intensity. When we compare these spectra (Figs.11a,b) with the spectrum of liquid water (Fig.11c) [see also ref.(26,42-45)], we can deduce that the bands in the region 1300-1200cm^{-1} cannot be due to the water molecules. The bands found in the

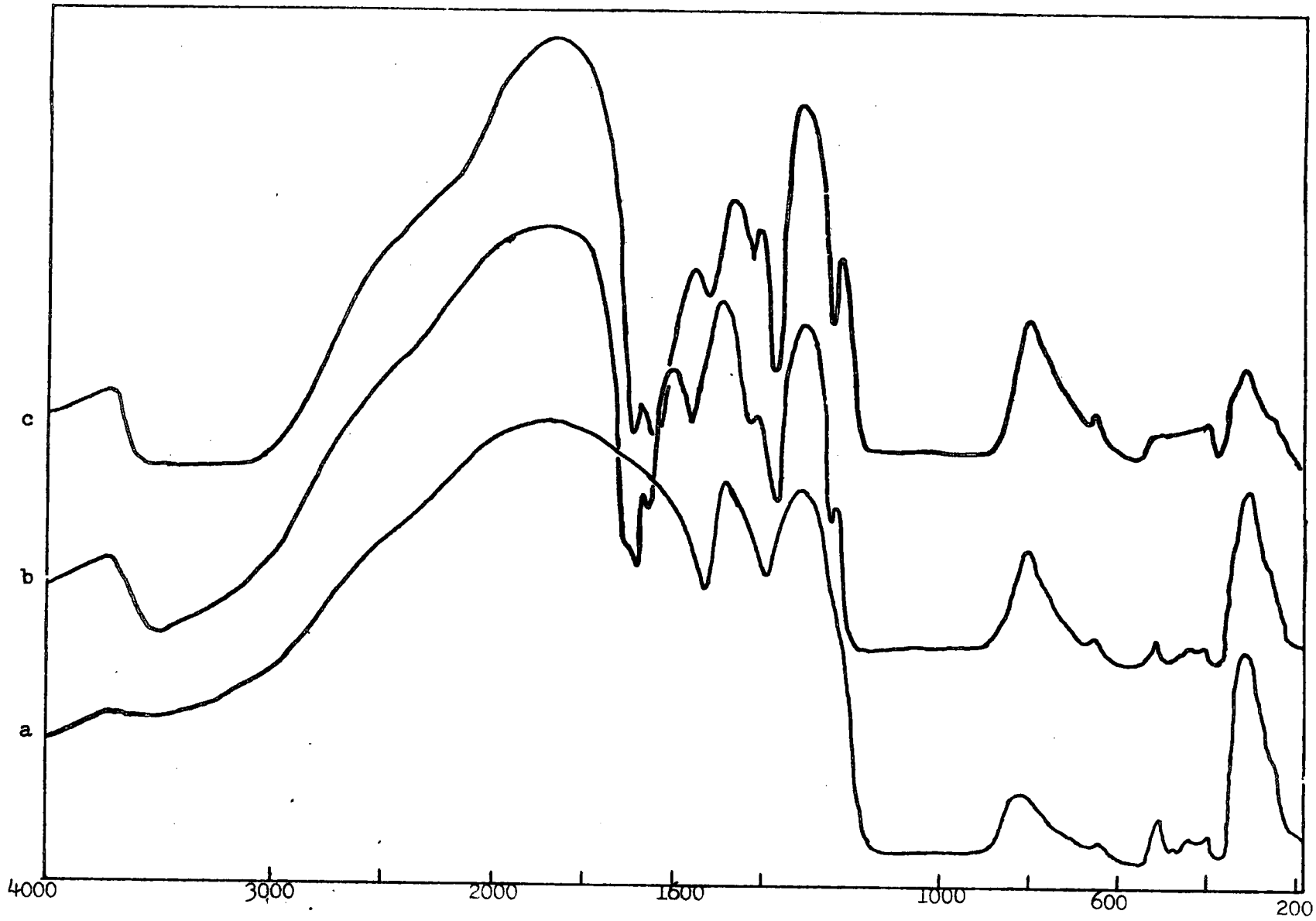

Fig. 10 Mn-4A zeolite a.at 533 K before adsorping H_2O
b.at 403 K after adding H_2O
c.at 293 K

spectrum of the zeolite at 1685 and 1230cm^{-1} must therefore be due to other species. The species most likely to be present is the hydronium ion. From the infrared spectrum of the hydronium ion in crystals (26,46) we find that the vibrational frequencies of the H_3O^+ and D_3O^+ ions are as shown in Table 4.

Table 4: The infrared data (cm^{-1}) for H_3O^+ and D_3O^+ ions in crystals (26, 46)

H_3O^+ Cl^-	D_3O^+ Cl^-	assignment
1150	785	ν_2
1700	1255	ν_4
2540-3235	2000-2445	ν_3 , ν_1

The normal modes of vibrations for H_3O^+ are shown in Fig.12.

The hydronium ion in NaX and NH_4X zeolites have been shown to be unstable and to decomposes when the zeolites are heated in vacuo (47). Szymanski et al (21) have also reported bands due to hydronium ion on NaX zeolite at 1700-1750cm^{-1}, at high water concentration.

From the above we can assign the bands at 1685 and 1230cm^{-1} to the hydronium ion. We must also consider the fact that while the band at 1230cm^{-1} disappears at 573K the band at 1685cm^{-1} only decreases slightly in intensity (Fig.11).

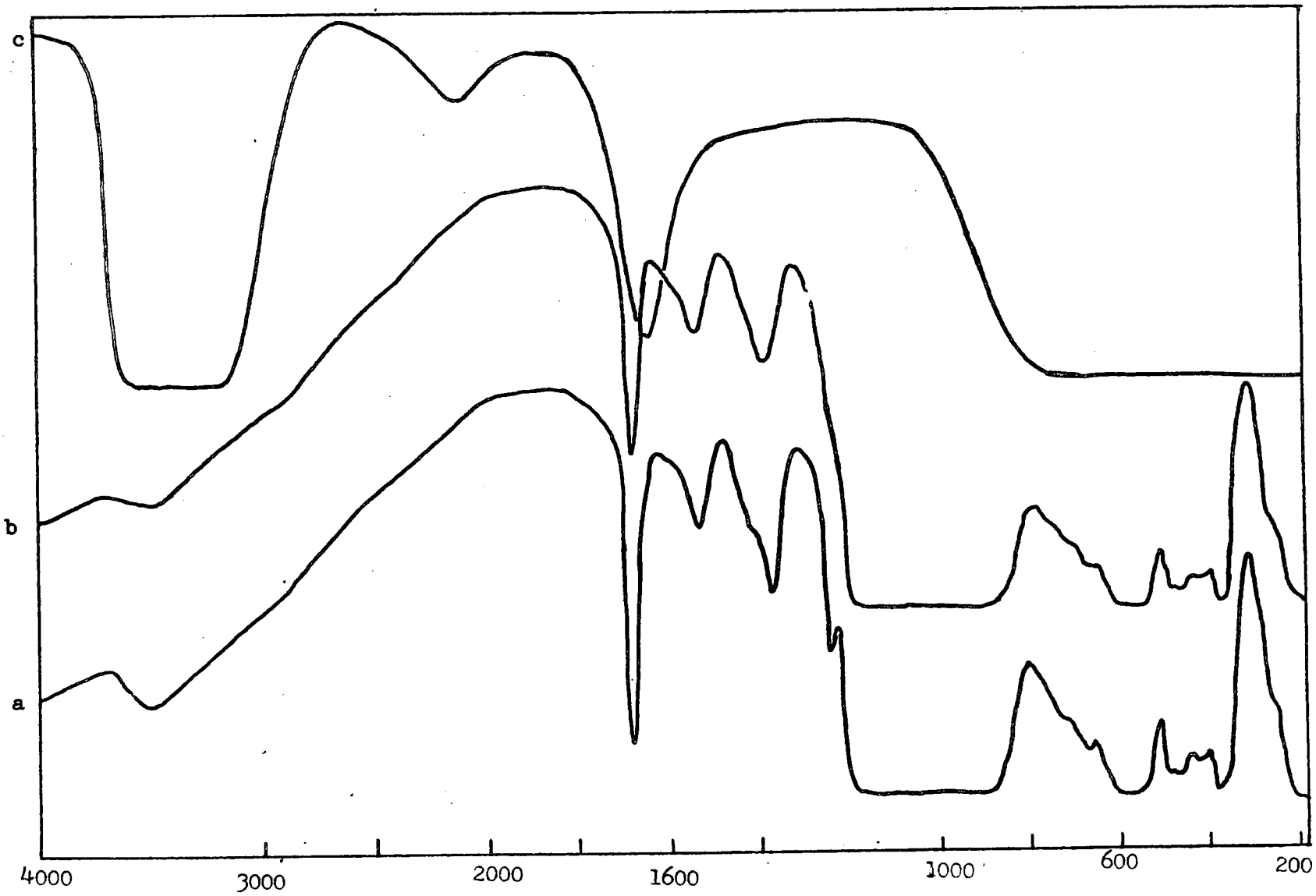

Fig.11 a.Mn-4A zeolite-H_2O at 445K

b.Mn-4A zeolite-H_2O at 573K

c.H_2O

One possible explanation for this is that when the hydronium ion decomposes, the water molecules which are formed, form strong hydrogen bonds with the zeolite framework via the interaction of the framework oxygen atoms with the hydrogen atom of the water molecules (39, 48, 49). This is indicated by the fact that the band at 1685cm^{-1} is not removed even after evacuation at 573K. This band we assign to the HOH bend of the hydrogen bonded water molecules. If this assignment is correct then as we observe the band at 1685cm^{-1} we also expect to observe a band in the O-H stretching region due to the presence of the hydrogen bond. Because the H_2O is strongly hydrogen bonded the O-H stretch should be reduced considerably in frequency relative to the value in liquid water. There is no suitable band in the spectrum and it is possible that it is too weak to observe.

It should be noted that the stretching mode (ν_1, ν_3) of the hydronium ion (observed in $H_3O^+Cl^-$ crystal at2540-3235 cm^{-1}) was also not observed in our spectrum (Fig.10). The stretching mode of the hydronium ion known to be weak and broad relative to ν_2, ν_4 and may explain why it was not observed in our spectra since ν_2 was not itself very intense. It is also possible that the band at

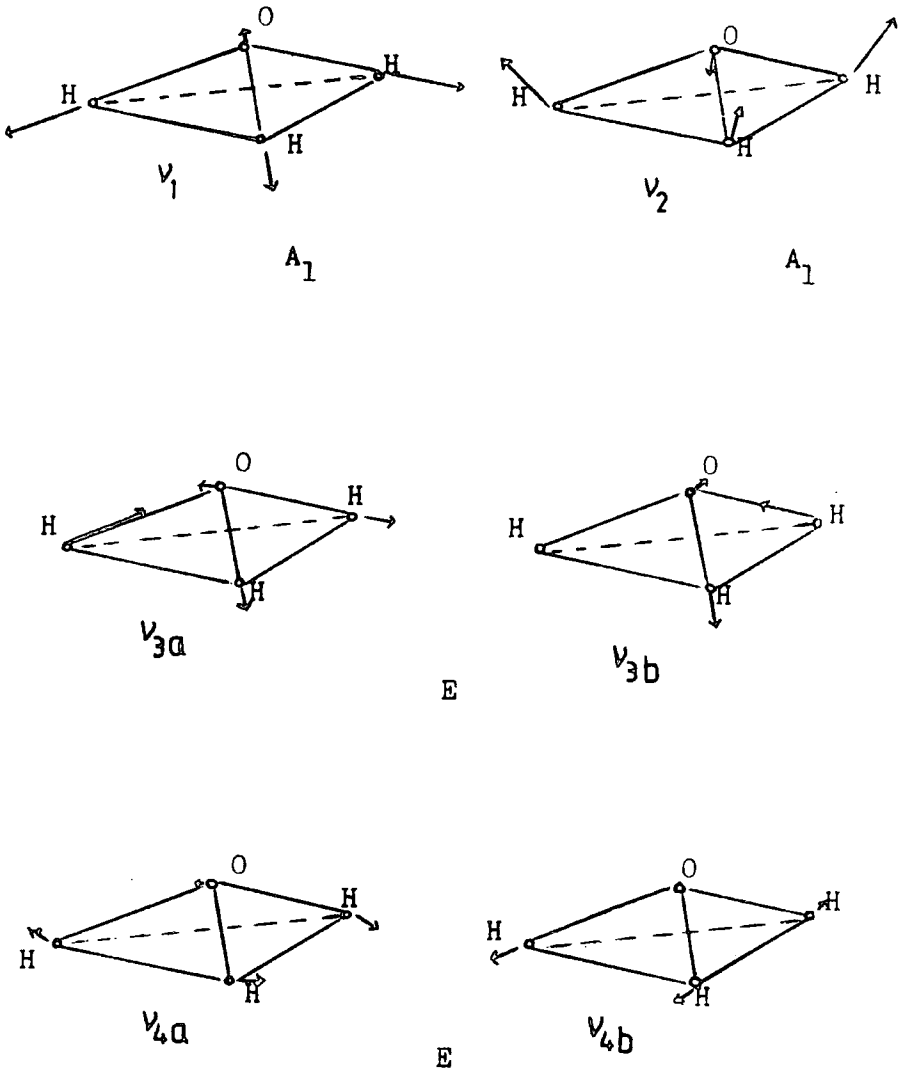

Fig.12 Normal modes of vibration for H_3O^+ (30)

1230cm^{-1} does not disappear on heating but that the broad zeolite absorption (1250-900cm^{-1}) increases in width and the two are not resolved.

When the same procedure was carried out with samples of different degrees of exchange of Mn(II) for Na^+(Table 1), the intensity of the band at 1685cm^{-1}, which we have assigned to the hydronium ion,varies with the degree of ion exchange. From Figs. 7, 10 and 11, it can be seen that the intensity of this band is strong with the zeolite of high Mn content (Mn(II)/Na^+ ratio = 5.15) and is less intense with the Mn(II)/Na^+ ratio = 1.06 (Fig. 7). This suggests that the hydronium ions are bonded to the Mn ions rather than Na^+ ions.

In the case of the Co-4A zeolite, when water vapour is added a broad band occurs at 3700-3000cm^{-1} (Fig.13), which is due to the presence of water, and a band at 1645cm^{-1} due to $\nu_2(H_2O)$. There are no bands at 1685 or 1230cm^{-1}, however, which can be assigned to the hydronium ion. The hydronium ion is therefore not formed in this case. A study (16) on the interaction of CoNaA zeolite with water has been reported in which it was noticed that on hydration and dehydration there was no water dissociation. From their spectrum we can see that hydronium ions were not formed in that case either. From this we can conclude

that the hydronium ion is formed in the Mn-4A zeolite but not in Co-4A zeolite.

When doing the D_2O exchange experiments only the experiment of admitting D_2O vapour to Mn-4A zeolite ($Mn(II)/Na^+$ ratio = 5.15) was successful. The spectrum (Fig.14) shows a broad band at 2700-2100cm^{-1} and this band is due to ν_1 and ν_3 of D_2O molecules. In this case it is difficult to see the bend of the D_2O molecules since it occurs at $\sim$1178cm^{-1} in liquid D_2O and hence is amongst the strong framework absorption below 1250cm^{-1}. For the same reasons, we cannot tell whether D_3O^+ is present since we can see from Table 4 that the two bands corresponding to those we observed for H_3O^+ would occur beneath the strong framework bands (Fig.14). The infrared data for Mn-4A zeolite and D_2O adsorbed at 527K is shown in Table 5.

Table 5: Infrared data (cm^{-1}) of Mn-4A with water adsorbed at 527K (3000-1000-cm^{-1}) the spectra recorded at different temperatures.

527K	289K	513K	assignment
2700-2500 b-w	2700-2300 b-s	2600-2400 b-m	ν_1 ν_3 (D_2O) ν_1(HDO)
1655 w	1645 m	-	ν_2 (H_2O)
1540 s	1540 m	1540 s	zeolite structure
-	1440 m	-	ν_2(HDO)
1395 s	1380 m	1395 s	zeolite structure

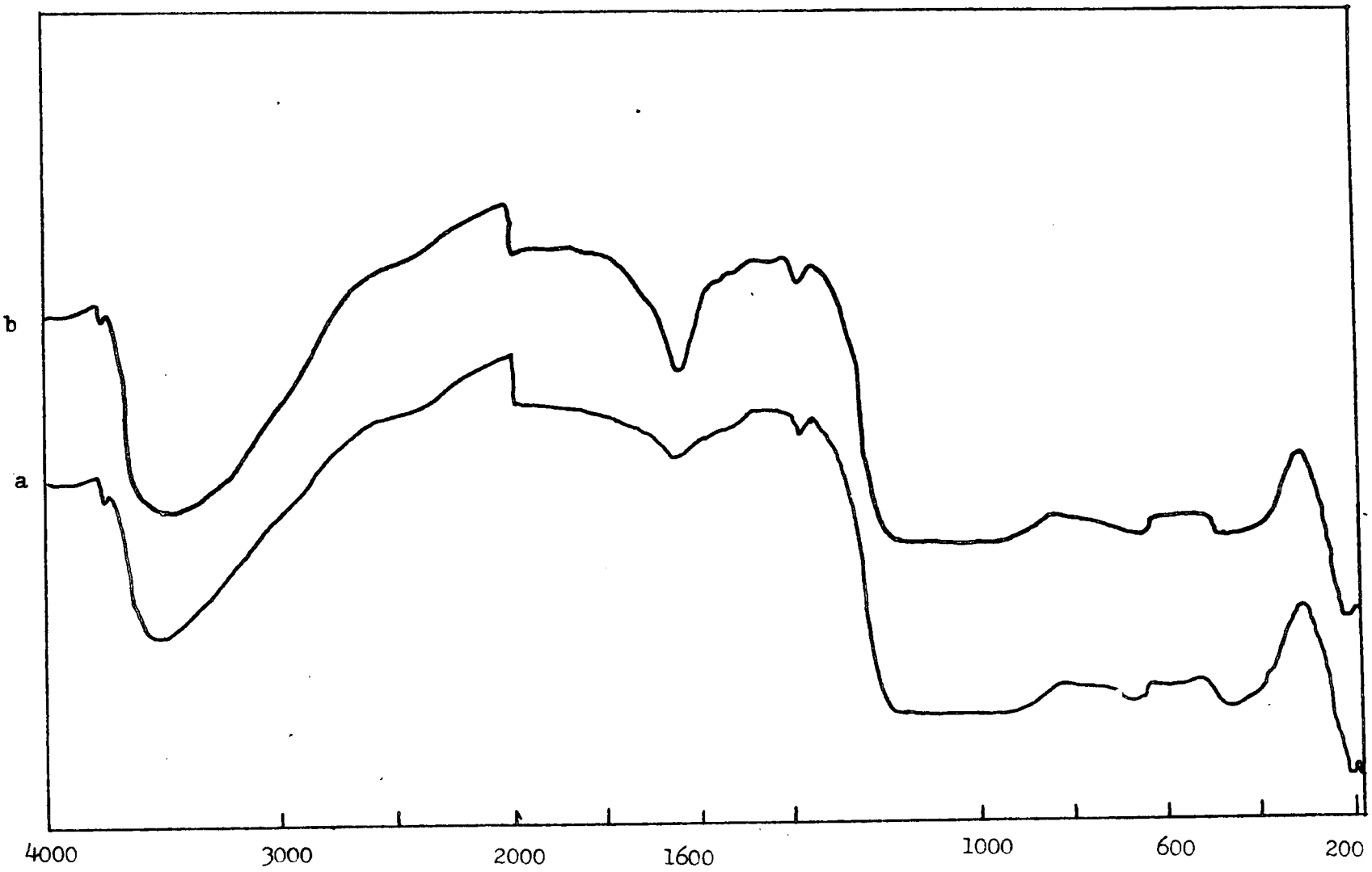

Fig.13 a.Co-4A zeolite after adsorbing H_2O at 463K
b.Co-4 zeolite after adsorbing H_2O at 463K then cooling to 293 K

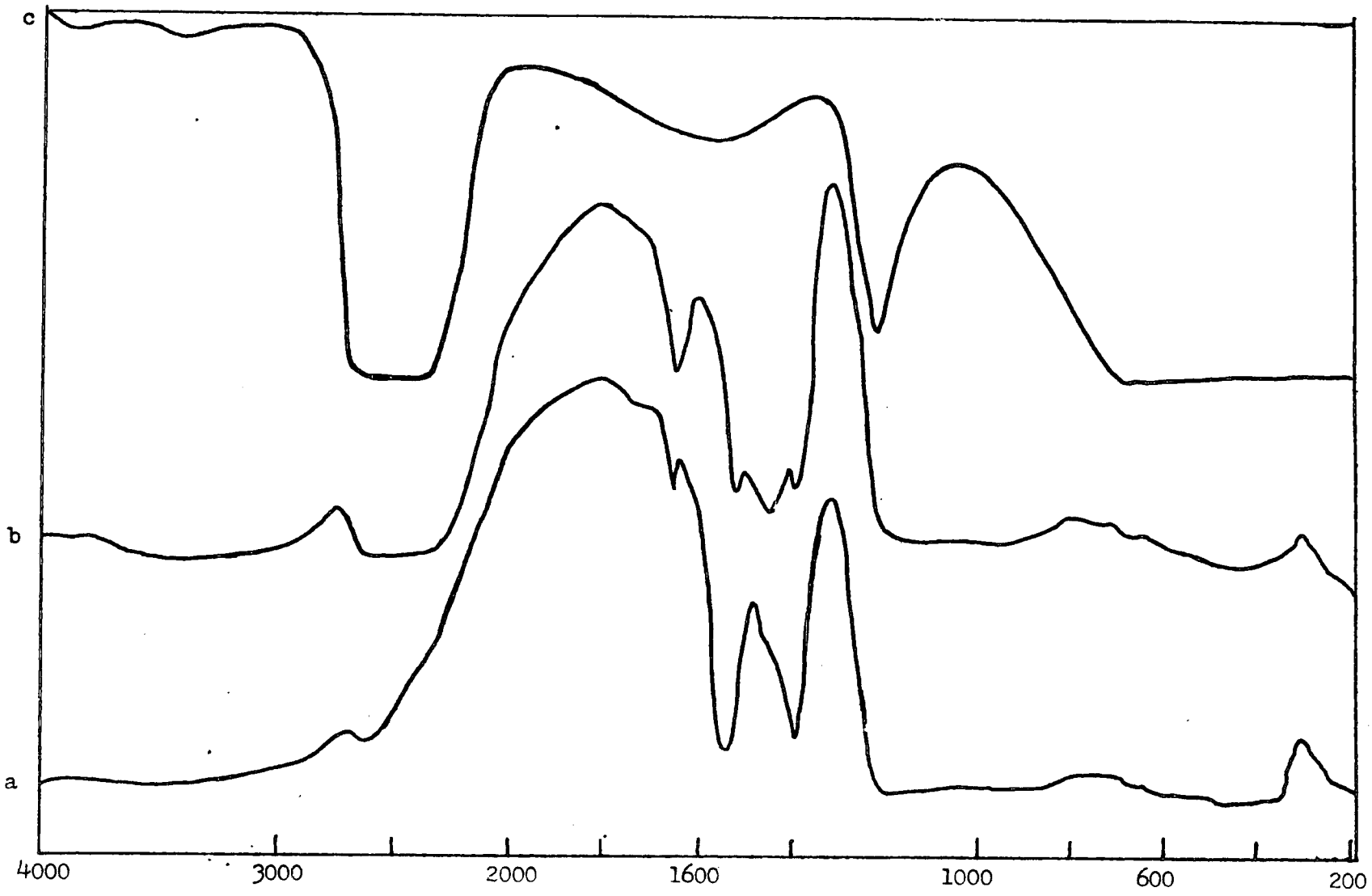

Fig.14 a.Mn-4A zeolite-D_2O at 473K
b.Mn-4A zeolite-D_2O at 320 K
c.D_2O

From Table 5 it can be seen that a band at 1645cm^{-1} appears when D_2O is added which is due to the presence of residual H_2O. Also in the presence of residual H_2O a new band occurs when adding D_2O vapour to a hot zeolite, at 1440cm^{-1} (Fig.14), which can be assigned to HDO (49) as shown in Table 6.

Table 6: Infrared data (cm^{-1}) of the D_2O and HDO vapour and their assignment (49)

HDO	D_2O	assignment
1402	1178	ν_2
2719		ν_1
	2789	ν_3
2809		ν_2

4. Conclusion:

A. The Mn ions occupy two different sites in the presence of high degree of Mn ion exchange. On heating the Mn ions will leave one of these sites and transfer to a different one, which will give a total of three sites which might be occupied by the Mn at different temperatures.

B. Hydronium ions are only formed on adding water to a hot zeolite.

C. The presence of the hydronium ion depends on

(1) The degree of ion exchange, since with high degree of Mn ions a strong band will occur due to the

hydronium ion and at low degree of Mn ions give weak band due to H_3O^+

(2) The cations present, since Co(II) does not give any bands due to the hydronium ions.

D. It has not proved possible to exchange D_2O for H_2O in A zeolite at room temperature.

References

1. Bretsch, L. and Habgood, H.W., J.Phys.Chem. 67, 1621 (1963).

2. Jacobs, P.A., and Uytterhoven, J.C.S.Chem.Commun. 128, (1977).

3. Oleson, D.H., J.Phys.Chem, 72 (4), 1400 (1968).

4. Peterson, D., ACS.Sym.Ser., 135, 107,(1980).

5. Shen, J.H., Zehiemoyer, A.C., and Klier, K., J.Phys.Chem. 84, 1453 (1980).

6. Shikunov., B.I., Dokl.Akad.Nauk.SSSR, 200 (5), 1119, (1971).

7. Praliaud, H., and Coudurier, G., J.C.S.Faraday Trans. 75 (12), 2601 (1979).

8. Sidamonidze, S.L., and Tsitsishvili, Prir.Tseolity Tr. Sov-Bolg.Simp.Issled.Fiz-Khim. Szoisty Prior, T.Seol. Tore, 321 (1979).

9. Belitskii, I., ibid., 63 (1979).

10. Fripiat, J.J., Bull.Mineral, 103, 440 (1980).

11. Selim, M.M., and El-Shobaky, G.A., Surf.Technol. 9(6), 435 (1979).

12. Mikhallova, M.V., Issled adsorption protessav. Adsorb. Tushkent, 132 (1979).

13. Pfeifer, H., and Grneuder, W., Mang.Reson.Relat.Phenom. Proc.Congr.Ampere 20th, 135 (1978).

14. Bhomrah, J.S., Proc.Natt.Symp.Catal.4th, 195 (1978).

15. Ward, J.W., J.Phys.Chem. 72 (12) (1968).

16. Wichterlova, B., Kybelkova, L., and Jiru, P., Collect.Czech.Chem.Commun. 45, 9 (1980).

17. Yates, D.J.C., Catal.Review, 2, 113 (1968).

18. Zhdanov, S.P., Kiselev, A.V., Lygin, V.I., and Titova, T., Russ.J.Phys.Chem.38 (10),1209 (1964).

19. Mirzai, D.I., Geterog.Katal,(2),479 (1979).

20. Hino, M., Bull.Chem.Soc.Jap. 50(3),574 (1977).

21. Hino, M., and Mikami, Y., Bull.Chem.Soc.Jap. 52 (7), 2099 (1979).

22. Szymanski, H.A., Stamires, D.N., and Lynch, G.R., J.Opt.Soc.Am. 50 (12), 1323 (1960).

23. Frohnsdroff, G.J.C., and Kington, G.L., Proc.Roy.Soc. (London) A, 247, 469 (1958).

24. Falk, M., and Giguere, P.A., Can.J.Chem. 35, 1195 (1957).

25. Richards, K.E., and Smith, J.A.S., Trans.Faraday Soc. 47, 1261 (1951).

26. Finholt, J.E., and Williams, J.M., J.Chem.Phys. 59 (9), 5114 (1973).

27. Bishop, D.M., J.Chem.Phys. 43 (12),4453 (1965).

28. Roziere, J., and Potier, J., Inorg.Nucl.Chem. 35, 1179 (1973).

29. Bethell, D.E., and Sheppard, N., J.Chem.Phys. 21, 1421 (1953).

30. Basile, I.J., Laborville, P., Ferraro, J.R., and Williams, J.M., J.Chem.Phys. 60 (5),1981 (1974).

31. Yanagida, R.Y., Vance, T.B.Jr., and Seff, K., Inorg.Chem. 13 (3),723 (1974).

32. Yanagida, R.Y., Vance,T.B.,Jr., and Seff, K., J.C.S.Chem.Comm. 382 (1973).

33. Riley, P.E., and Seff, K., Inorg.Chem. 13, 1355 (1974).

34. Riley, P.E., and Seff, K., J.C.S.Chem.Commun. 1287 (1972).

35. Amaro, A.A., Kovaciny, C.L., Knuz, K.B., Riley, P.E., Vance, T.B. Jr., Yanagida, R.Y., and Seff, K., Molecular Sieves, Leuvan Univ.Press, Belgium (1973).

36. Riley, P.E., and Seff, K., J.Phys.Chem. 79 (15), 1594 (1975).

37. Cruz, W.V., Leung, P.C.W., and Seff, K., J.Am.Chem.Soc. 100 (22),6997 (1978).

38. Riley, P.E., and Seff, K., J.Phys.Chem. 95, 8180 (1973).

39. Carter, J.L., Lucchesi, P.J., and Yates, D.J.C., J.Phys.Chem. 68 (6) 1385 (1964).

40. Habgood, H.W., J.Phys.Chem. 69 (5),1764 (1965).

41. Patzelova, V., and Tvaruzkov , Z., J.Catal. 33 (1) 158 (1974).

42. Jacobs, P.A., and Uytterhoven, J.B., J.C.S.Chem.Commun. 359 (1972).

43. Adams, D.M., J.Chem.Soc. (A) 2801 (1971).

44. Bertie, J.E., and Whalley, E., J.Chem.Phys. 40 (6) 1846 (1964).

45. Bertie, J.E., and Whalley, E., J.Chem.Phys. 40 (6) 1637 (1964).

46. Bosi, P., Tubino, R., and Zerbi, G., J.Chem.Phys. 59 (4) 4578 (1973).

47. Ferriso, C.C., and Hornig, D.F., J.Chem.Phys. 23, 1464 (1955).

48. Kiselev, A.V., and Lygin, V.I., Infrared spectra of Surface Compounds (1975) wiley,New York

49. Herzberg, G., Infrared and Raman Spectra (1945) London.

Chapter 6

An infrared study of cyclopropane adsorbed on Co(II) and Mn(II) partially exchanged A zeolites

1. Introduction

The isomerization of cyclopropane to propylene is a widely used test reaction for the investigation of the performance of catalytic reactors (1) and the activity of acid-type solid catalysts (2). Bassett and Habgood (1) and Habgood and George (3) have studied the isomerization on various cation exchanged forms of zeolite Y at a temperature of 200°C. Bartley et al (4) and George and Habgood (5) in their studies using deuterated zeolite Y have concluded that both exchange and isomerization of cyclopropane proceed via a non-classical protonated cyclic carbonium ion intermediate (6-10).

Infrared spectroscopy was used to study the chemisorption and reactions of cyclopropane over zeolite HY at room temperature by Tam et al (11). Isobutane was the major product. A mechanism for this transformation involving the formation of a non-classical protonated cyclopropane ion intermediate was proposed. Other studies have been made to investigate the skeletal isomerization of cyclopropane over NaY, NaCaY and NaHY zeolites (11-14).

Structure of cyclopropane adsorbed on Mn(II) and Co(II) Exchanged A zeolite

Seff et al (15) determined the crystal structures of the cyclopropane sorption complexes of partially Co(II)-exchanged and partially Mn(II)-exchanged zeolite A (Figs.

1 and 2), the unit cell constants are 12.147 Å for $Co_4Na_4Si_{12}Al_{12}O_{48}.4C_3H_6$ and 12.146Å for $Mn_4Na_4Si_{12}Al_{12}O_{48}.4C_3H_6$.

In each structure transition metal cations are located on three-fold axes inside the large cavity, close to three trigonally arranged framework oxide ions on alternate 6-oxygen rings. The metal to oxygen distances are Co(II)-O = 2.174Å and Mn(II)-O = 2.122Å. There are four cyclopropane molecules per unit cell, each of them is found to complex to a transition metal ion with Co(II)-C=2.81Å and Mn(II)-C=3.09Å. No interaction between Na^+ ions and cyclopropane molecules was observed. The adsorption complexes represent novel chemical species since stable organometallic complexes of C_3H_6 have not been reported in the scientific literature.

2. Experimental

Materials

Mn-Na-4A and Co-Na-4A zeolites were prepared from NaA zeolite (BDH Chemicals Ltd) by ion exchange with 0.1N $MnSO_4$-$4H_2O$ and $Co(NO_3)_2$ (BDH analar grade) solutions respectively ($Mn(II)/Na^+$ ratio = 5.15 and $Co(II)/Na^+$ ratio = 53.18) following the method described by Seff (15). These samples were also used for part of work in the previous chapter (chapter 5). Cyclopropane gas of 99.8% was used without further purification.

Procedure

The self-supporting disc was evacuated in the infrared cell, then heated under vacuum and cooled to room temperature.

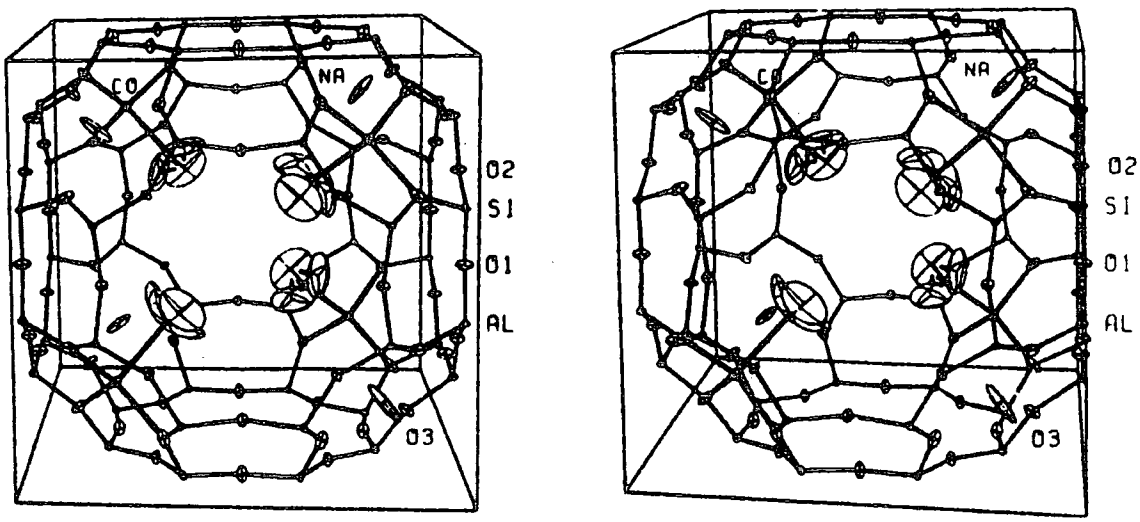

Fig.1a A stereoview of the Co-4A-$4C_3H_6$ unit cell

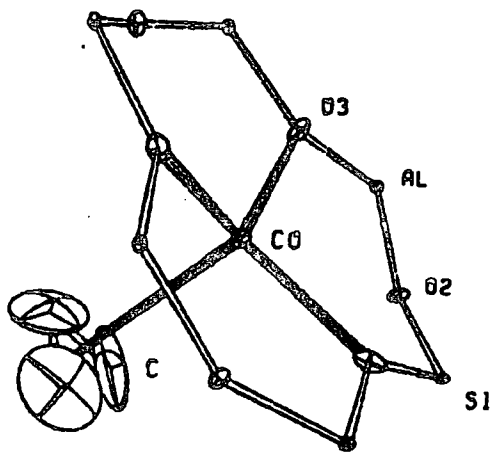

Fig.1b

The coordination environment of the Co(II) ion.

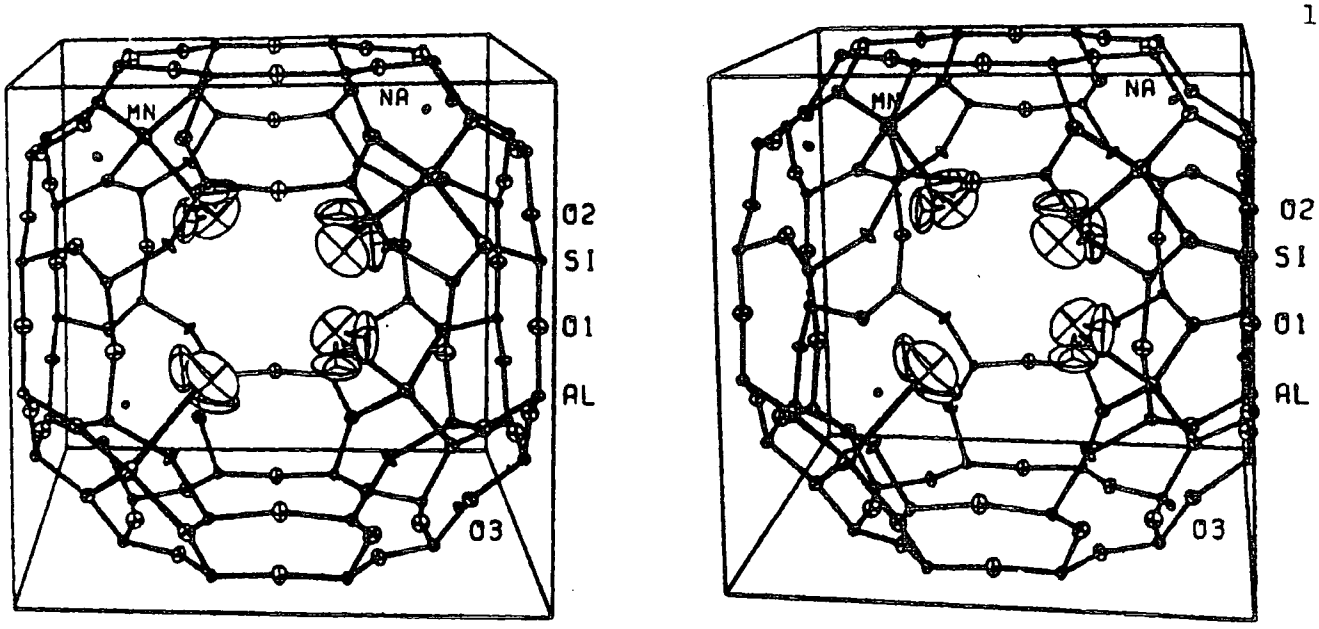

Fig.2a A stereoview of the Mn-4A-4C_3H_6 unit cell

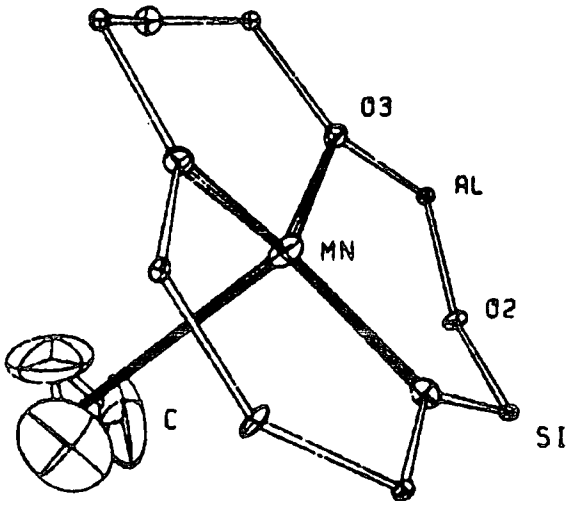

Fig.2b

The coordination environment of the Mn(II) ion.

Cyclopropane gas was admitted to the cell which then was evacuated for 10 minutes before obtaining the spectra. A spectrum of cyclopropane gas was also obtained.

3. Results and discussion

a. The hydroxyl groups

These were discussed in chapter 5.

b. The adsorption of cyclopropane

Figs. 3 and 4 show the spectra of Mn.4A and Co-4A zeolite (after baking and cooling to room temperature) before and after adsorbing cyclopropane. An isolated cyclopropane molecule has D_{3h} symmetry. The activities of the normal modes are summarized in Table 1 together with their symmetry classes (16,17). The spectra of cyclopropane gas is shown in Figs. 3c and 4c.

Table 1: The symmetry classes and selection rules for the internal vibrations of the isolated cyclopropane molecule(16,17).

Symmetry class	No.of fundamental vibrations in classes	Raman	Infrared
A_1'	3	active	inactive
A_2'	1	inactive	inactive
E'	4	active	active
A_1''	1	inactive	inactive
A_2''	2	inactive	active
E''	3	active	inactive

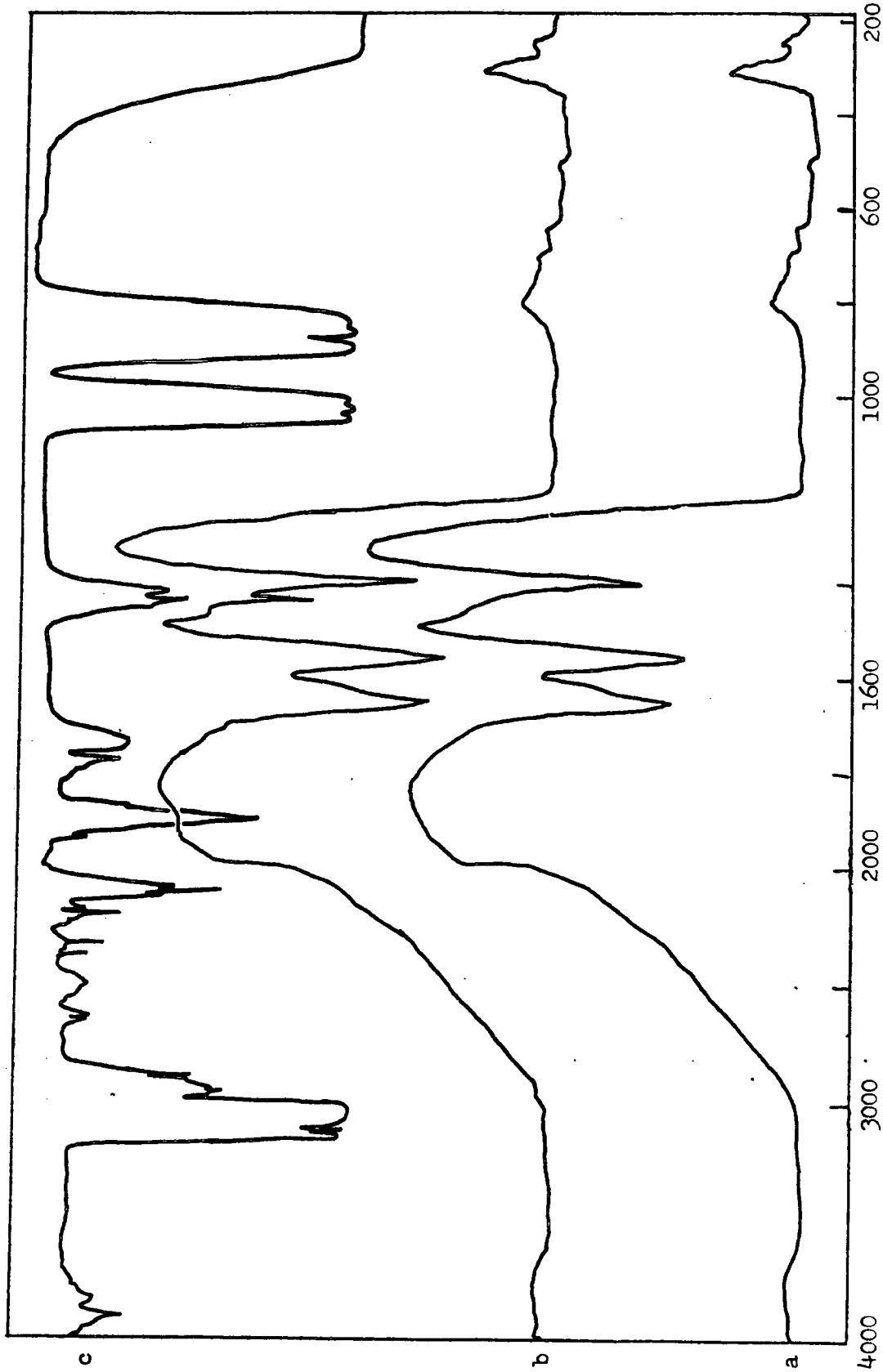

Fig.3 Mn-4A zeolite a.at 293k after baking at 593K
b.with C_3H_6 at 293K
c.C_3H_6 gas

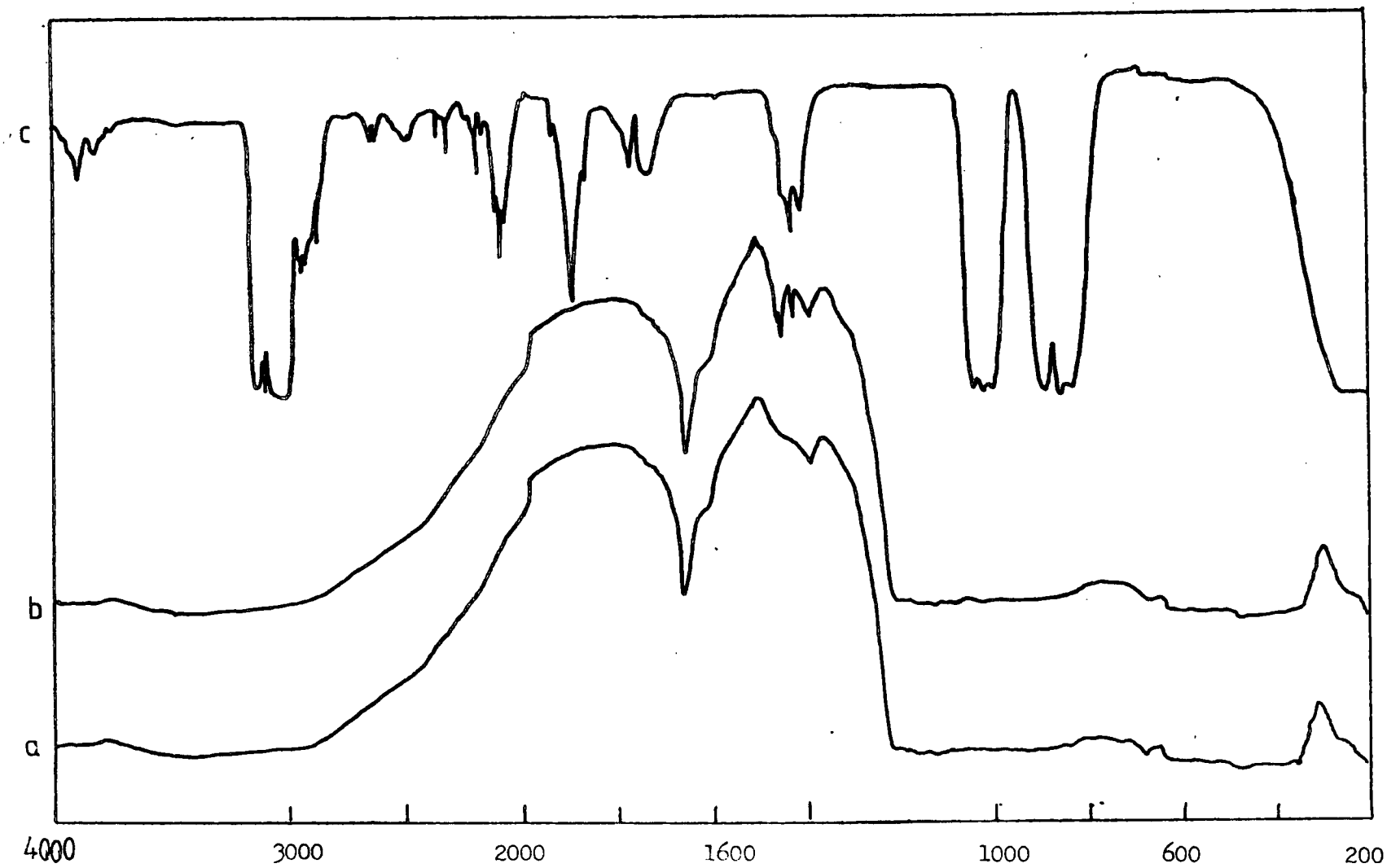

Fig.4 Co-4A zeolite a.at 293k after baking at 593K
b.with C_3H_6 at 293K
c.C_3H_6 gas

Table 2 contains some of the infrared and Raman frequencies of cyclopropane gas, liquid and from the crystals together with their assignments as given by Linnett (16).

Table 2: Infrared and Raman data (cm^{-1}) of cyclopropane gas, liquid and crystals in the range of 3000-1000 cm^{-1} (16,17).

Infrared		Raman		Assignment
-		2952	w	$4\nu_{14}$
-		2854	w	$2\nu_9$ $(A_1'+E')$
2631	w	-		$\nu_3+\ \nu_9(E')$
2493	w	-		$\nu_2+\ \nu_{10}(E')$
				$\nu_5+\ \nu_9(E')$
2330	w	-		$\nu_2+\ \nu_{11}(E')$
2178	w	-		$\nu_9+\ \nu_{14}(A_2'')$
2084	s	-		$\nu_5+\ \nu_{10}(E')$
1888	s	1873	vw	$\nu_{10}+\ \nu_{11}(A_1'+E')$
1779	w	-		$\nu_7+\ \nu_{14}(E')$
1739	m	-		$\nu_4+\ \nu_{14}(E')$
-		1504	w	$\nu_2\ CH_2\ (a_1')$
-		1454	m	$2\ \nu_{14}(A_1'+E')$
1432	s	1435	m	$\nu_9\ \ CH_2\ (e')$
-		1189	v.s	$\nu_3\ \ C_3\ (a_1')$
-		1120		ν_{13} (e'') rocking
1027.6	s	1022	w	ν_{10} (e') bending

After adsorbing cyclopropane gas on each of the dehydrated Co-4A and Mn-4A zeolites at room temperature and evacuating for 10 minutes (Fig.5), new bands were observed in the 1500-1300cm^{-1} region (Table 3). Two bands were observed, at 1456 and 1430cm^{-1}, for Co-4A zeolite and one band at 1435cm^{-1} for Mn-4A zeolite.

Table 3: Infrared data and assignments of Mn-4A and Co-4A zeolites and the adsorbed species (C_3H_6) in the range 1300-1700cm^{-1}

Mn-4A	Mn-4A.C_3H_6	Co-4A	Co-4A.C_3H_6	Assignment
1660 s	1650 s	1650 s	1645 s	$\nu_2(H_2O)$
-	-	1610 w	1610 w	zeolite structure
1535 s	1535 s	-	-	zeolite structure
		1465 w	1465 w	zeolite structure
-	-	-	1456 m	$2\nu_{14}(A_1'+E')$
-	1435 m	-	1430 w	ν_9 (E')
1395 s	1395 s	1390 w	1390 w	zeolite structure

The band at 1456cm^{-1} can be assigned to 2 $\nu_{14}(A_1'+E')$ which is not observed in the infrared spectra with isolated cyclopropane molecules as can be seen from Table 2. This transition is observed because when cyclopropane is adsorbed on the zeolite the symmetry of the molecule is lowered from D_{3h} to C_{3v} (Table 4). Thus A_1 (D_{3h}) correlates with $A_1(C_{3v})$ which is active in the infrared (Table 5).

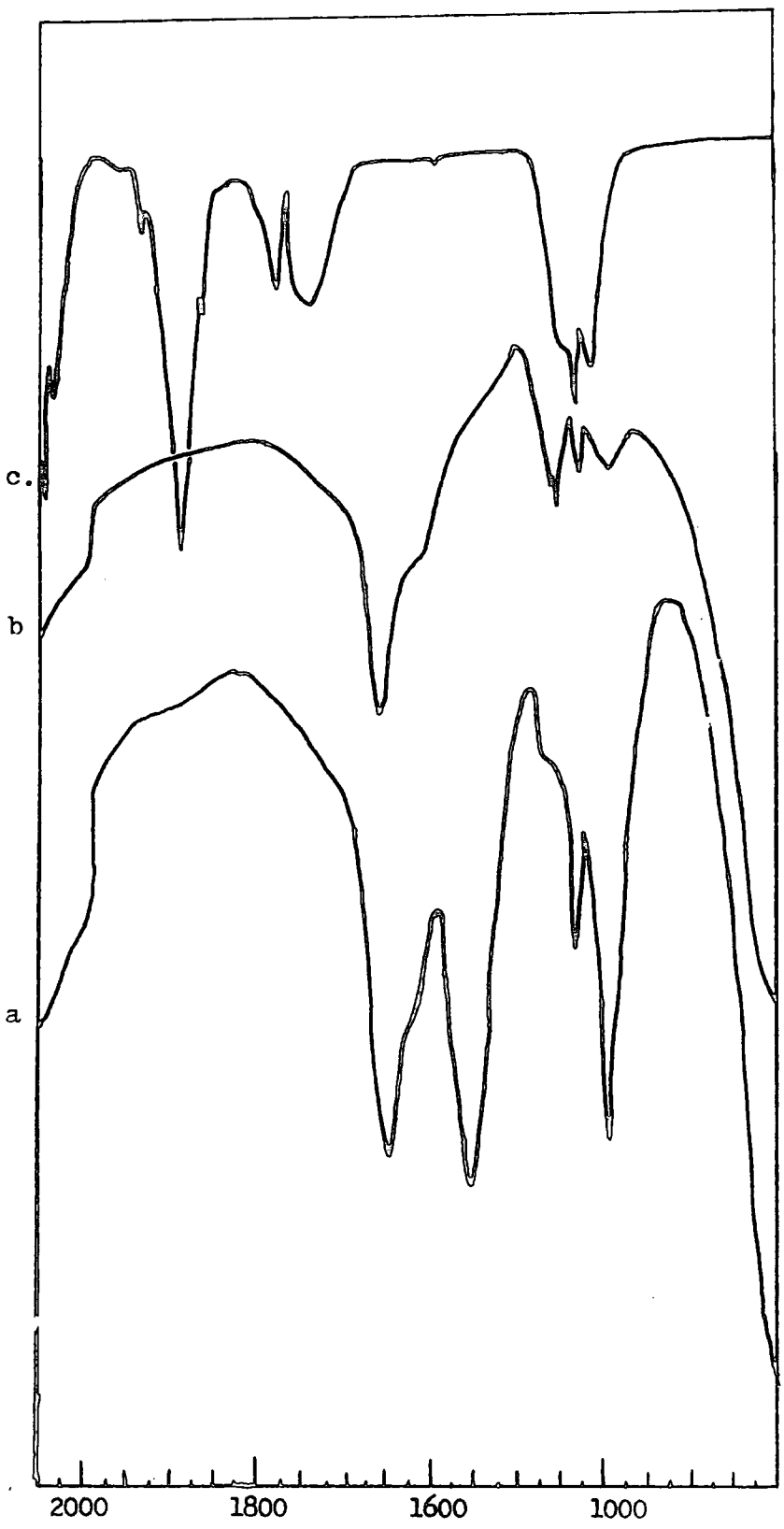

Fig.5 a. Mn-4A-C_3H_6 at 293K
b. Co-4A-C_3H_6 at 293K
c. C_3H_6 gas

Table 4: The symmetry classes and selection rules for adsorbed C_3H_6 molecules (C_{3v})

Symmetry class	No.of fundamental vibrations in classes	Raman	Infrared
A_1	5	active	active
A_2	3	inactive	inactive
E	8	active	active

Table 5: Resolution of D_{3h} into C_{3v} (17)

D_{3h}		C_{3v}
A_1'	→	A_1
A_1''	→	A_2
A_2'	↗	
A_2''	→	A_1
E'	→	E
E''	↗	

The 1456cm^{-1} band has not been observed with Mn-4A zeolite and this is because of the complexity of the spectra of Mn-4A zeolite compared with Co-4A zeolite in the 1600-1300cm^{-1} region. The band at 1430cm^{-1} which was observed in the spectra of Co-4A zeolite and 1435cm^{-1} in the spectra of Mn-4A zeolite may be assigned to $\nu_9(E)$, of the adsorbed C_3H_6.

The interaction between cyclopropane and the zeolites can be described as Miller (18) discussed it using Hallmann-Feynman arguments and ring bending strain energies and they calculated a 'negative pole' in cyclopropane to be 2.88 e . This negative pole or πcloud would be polarized by the field of the Co(II) or Mn(II) ions to form the bond between the cyclopropane and the transition metal ions. It has been found that cyclopropane is adsorbed by partially Ni(II)-exchanged zeolite A complexes (19). Ni(II) was found to be bonded to the centre of the ring, which involve π interaction.

4. Conclusion

From chapters 5 and 6 we can see that there are considerable differences in behaviour between partially exchanged Co-4A and Mn-4A zeolites. These differences include:

1. Mn-4A zeolite can form a hydronium ion when water vapour is adsorbed on the hot zeolite, while Co-4A zeolite does not.

2. Various spectroscopic studies (20) on adsorbed ethylene and cyclopropane on each of Mn-4A and Co-4A zeolites using neutron scattering have also shown the difference in behaviour between the zeolites.

These show that the Mn complexes are stronger than the Co complexes. Since Mn and Co are close together in the periodical table, one would expect their interactions with ligands to be fairly similar but in fact it is now known that this is not the case.

These differences between the Mn and Co zeolites once again illustrate the way in which zeolite properties can be influenced by subtle changes in the zeolite composition.

References

1. Bassett, D.W., and Habgood, H.W., J.Phys.Chem. 64, 769 (1960).

2. Roberts, R.M., J.Phys.Chem. 63, 1400 (1959).

3. Habgood, H.W., and George, Z.M., Proc.Soc.Chem.Ind. Conf.Mol. Sieves, London 130 (1968).

4. Bartley, B.H., Habgood, H.W., and George, Z.M., J.Phys.Chem. 72, 1689 (1968).

5. George, Z.M., and Habgood, H.W., J.Phys.Chem., 74, 1502 (1970).

6. Liengme, B.V., and Hall, W.K., Trans.Faraday Soc. 62 (11),3229 (1966).

7. Hightower, J.W., and Hall, W.K., J.Am.Chem.Soc. 90 (4) 851 (1968).

8. Hightower, J.W., and Hall, W.K., J.Phys.Chem. 72 (13) 4555 (1968).

9. Larson, J.G., Gerberichtt, R., and Hall, W.K., J.Am.Chem.Soc. 87 (9) 1880 (1965).

10. Lishka, H., and Kohler, H.J., J.Am.Chem.Soc. 100 (17) 5297 (1978).

11. Tam, N.T., Cooney, R.P., and Carthoys, G., J.Catal., 44, 81 (1976).

12. Fejes, P., Hannus, I., Kiricsi, I., and Varga, K., Acta.Phys.Chem. 24, 119 (1978).

13. Hannus, I., Magyar Kemikuok Lapja, 32, 594 (1977).

14. Kiricsi, I., Hannus, I., Varca, K., and Fejes, P., J.Catal., 63, 501 (1980).

15. Cruz, W.L., Lenng, P.C., and Seff, K., J.Am.Chem.Soc. 100 (22) 6997 (1978).

16. Linnett, J.W., J.Chem.Phys. 6, 693 (1938).

17. Herzberg, G., IR and Raman spectra, Van Nostrand Reinhold Company, London (1945).

18. Miller, I.J., Tetrahedron, 25, 1349 (1969).

19. Klier, K., and Ralek, M., J.Phys.Chem.Solids, 29, 951 (1968).

20. Howard, J. Private Communication.

Chapter 7

Conclusions and suggestions for future work

In chapter 4, a study of the relation between coke formation and hydroxyl groups which act as active sites was reported. This work was an attempt to repeat some work published earlier but which was unsuccessful because in our samples the band due to the relevant hydroxyl groups were not present at high temperature. Coke formation was, however, observed. Various studies on coke formation using different zeolites could be done to clarify whether or not there is an effect of any particular hydroxyl groups on coke formation.

The exchange of D_2O for H_2O by stirring the liquid with zeolite A has been shown to be very difficult. A comparison study could be achieved by exchanging D_2O for H_2O on a different type of zeolite to find a suitable way of exchanging D_2O inside zeolite A.

Mn-4A zeolite gives different infrared bands when ion exchanged to different degrees and this makes it a complicated and interesting material. The same thing could be done with higher degrees of Mn-exchange as well as on Co-4A zeolite since they show a different behaviour in many respects.

Zeolites can form novel chemical species since stable organometallic complexes of C_3H_6 or N_3H_3 have not been observed outside a zeolite cage, N_3H_3 in fact does not exist in the pure form. These studies are worth doing on different zeolites to observe the conditions under which these species could be formed.

Also of importance is the study of hydronium ions which, as we have seen, forms with Mn-4A zeolite but does not form with Co-4A zeolite. The degree of the Mn-exchange also effects the presence of the hydronium ion. A similar study could be done on a variety of cations and different zeolites to try to understand the conditions under which the hydronium ion is formed.